

**ACTIVE SITE INTERACTIONS IN PROTEOLYTIC ENZYMES**

**By**

**ERNEST ASANTE-APPIAH, M.Sc**

**A Thesis**

**Submitted to the School of Graduate Studies**

**in Partial Fulfillment of the Requirements**

**for the Degree**

**Doctor of Philosophy**

**McMaster University**

ACTIVE SITE INTERACTIONS IN PROTEOLYTIC ENZYMES

Doctor of Philosophy (1994)

McMaster University

Biochemistry

Hamilton, Ontario

Title: Active Site Interactions in Proteolytic Enzymes

Author: Ernest Asante-Appiah, B.Sc (University of Science and Technology, Ghana)

M.Sc (University of London, U.K.)

Supervisor: Dr. William W-C. Chan

Number of pages: xiii, 147

## ABSTRACT

The HIV-1 virus encodes a protease essential for the processing of polyprotein precursors into mature viral proteins. This enzyme is a primary target for drug design against AIDS. Concurrent effects of inhibitors targeted to defined regions of the extended active site were investigated using Yonetani-Theorell kinetics to understand its complex specificity requirements. Kinetic data revealed that the simultaneous presence of two specific inhibitors may increase their binding affinity for the enzyme. A 100-fold enhancement in binding affinity was observed in certain instances. Results from this work showed a correlation between inhibitor synergism and substrate specificity thus implicating subsite interactions in enzyme catalysis.

To facilitate the analysis of enzyme-inhibitor interactions an improved graphical method, the combination plot, was developed as an alternative to the Yonetani-Theorell plot. The method generates a single straight line rather than a family of lines which is the traditional approach in such kinetic studies. The slope of the plot,  $1/\alpha$ , quantitatively measures the extent and nature of interaction between two inhibitors on their target enzyme. The approach was easily extended to analyze, for the first time, the interaction between three competitive inhibitors on an enzyme. The combination approach potentially has broad applications for kinetic analysis.

Combination plots were used in the discovery of *gem*-dialkyl succinic acid derivatives as a new class of unusually potent reversible inhibitors of carboxypeptidases A and B. 2-Ethyl-2-methylsuccinic acid binds to carboxypeptidases A and B with dissociation constants of  $1.1 \times 10^{-7}$  M and  $3.4 \times 10^{-6}$  M respectively. The low dissociation constants



of the inhibitors for the zinc proteases can be attributed primarily to the *gem*-dialkyl groups which presumably make very important hydrophobic contacts within the active site. The inhibitors may also act as zinc ligands while possessing sufficient affinity for the carboxyl-recognition site in the enzymes.

## ACKNOWLEDGEMENTS

I wish to express sincere thanks to the following members of Dr. Chan's laboratory who in various ways helped make my research enjoyable and fulfilling: Naomi Laing, Mrs Jutta Kaiser, Suneel Uphadye and Richard Pfuetzner. Special thanks and appreciation also go to Mrs Barbara Sweet who on several occasions helped to type manuscripts.

I wish to acknowledge the help of Drs. Don Hughes and Richard Smith for their assistance in collecting NMR and mass spectroscopy spectra.

I would also like to express my gratitude to the members of my supervisory committee: Dr. Ananthanarayanan, Dr. Yang and Dr. McCarry for their guidance and invaluable advice.

I would like to say special thanks to Dr. Chan whose insight, support, guidance and encouragement made it all very worthwhile and possible.

Lastly, I would like to express my deepest thanks to my wife, Harriet and family for their love and support. Thanks for all the phone calls.

## TABLE OF CONTENTS

	Page
ABSTRACT	iii
ACKNOWLEDGEMENTS	v
ABBREVIATIONS	x
LIST OF FIGURES	xi
LIST OF TABLES	xiii
1. INTRODUCTION	1
1.1 Enzymes as biological catalysts	1
1.2 Proteolytic enzymes	5
1.2.1 HIV-1 protease	9
1.2.2 Carboxypeptidases A and B	13
1.3 Rational drug design	15
1.4 Active site interactions	17
1.5 Survey and design of research	20
1.5.1 Inhibitor synergism in HIV-1 protease	20
1.5.2 Combination plots	20
1.5.3 <i>Gem</i> -dialkyl succinic acid derivatives	21
2. MATERIALS AND METHODS	22
2.1 Materials	22
2.1.1 Synthetic Reagents	22
2.1.2 Other Chemicals	22
2.1.3 Inhibitors	23
2.1.4 Enzymes and Substrates	23
2.2 Methods	25
2.2.1 Enzyme assays	25
2.2.1.1 HIV-1 protease	25
2.2.1.2 AMV protease	27
2.2.1.3 Pepsin	28
2.2.1.4 Chymotrypsin	28

2.2.1.5	Papain	29
2.2.1.6	Thermolysin	29
2.2.1.7	Carboxypeptidase A	30
2.2.1.8	Carboxypeptidase B	30
2.2.2	Yonetani-Theorell kinetics	31
2.2.3	Determination of Inhibition constants	35
2.2.3.1	Combination plots	35
2.2.3.2	Dixon plot	38
2.2.4	TLC Detection Methods	40
2.2.4.1	Sulfonamides	40
2.2.4.2	Amino acids	40
2.2.4.3	Organic Compounds	40
2.2.5	General Synthetic procedures	40
2.2.5.1	Synthesis of N,N' Bis Phenylalanine ethyl ester Sulfonamide	40
2.2.5.2	Hydrolysis of N,N' Bis Phenylalanine ethyl ester Sulfonamide	41
2.2.5.3	Coupling of Amino Acids	41
2.2.6	Synthesis of Sulfonamides	42
2.2.6.1	N,N' Bis Phe-Val methyl ester sulfonamide	43
2.2.6.2	N,N' Bis Phe-Ile methyl ester sulfonamide	43
2.2.6.3	N,N' Bis Phe-Ala methyl ester sulfonamide	43
2.2.6.4	N,N' Bis Phe-Leu methyl ester sulfonamide	44
2.2.7	Synthesis of Cbz-aminoacyl-aminoalcohols	44
2.2.7.1	Cbz-valyl-phenylalaninol	45
2.2.7.2	Cbz-isoleucyl-phenylalaninol	45
2.2.7.3	Cbz-leucyl-phenylalaninol	45
2.2.7.4	Cbz-glutaminy-phenylalaninol	46
2.2.7.5	Cbz-asparaginy-phenylalaninol	46
2.2.7.6	Cbz-valyl-leucinol	46
2.2.8	Synthesis of Cbz-aminoacyl-isoamylamide derivatives	47
2.2.8.1	Cbz-alanyl-isoamylamide	47
2.2.8.2	Cbz-valyl-isoamylamide	48
2.2.8.3	Cbz-isoleucyl-isoamylamide	48
2.2.8.4	Cbz-leucyl-isoamylamide	48
2.2.8.5	Cbz-asparaginy-isoamylamide	49

2.2.8.6	Cbz-glutaminyl-isoamylamide	49
2.2.8.7	Cbz-glycyl-isoamylamide	49
2.2.8.8	Succinamyl-isoamylamide	50
2.2.9	Synthesis of other Cbz-aminoacyl-alkylamides	50
2.2.9.1	Cbz-asparaginyl-methylamide	50
2.2.9.2	Cbz-valyl-phenethylamide	51
2.2.9.3	Cbz-valyl-benzylamide	51
2.2.9.4	Cbz-glutaminyl-phenethylamide	51
<b>3.</b>	<b>INTERACTIONS OF INHIBITORS WITH ASPARTIC PROTEASES</b>	<b>53</b>
3.1	Results	53
3.1.1	Enzyme assays	53
3.1.2	Sulfonamide inhibitors of HIV-1 protease	54
3.1.3	Detection of Synergism in HIV-1 protease	56
3.1.3.1	Design of active site probes	56
3.1.3.2	Effect of residues at the P <sub>2</sub> ' subsite	60
3.1.3.3	Effect of residues at the P <sub>2</sub> subsite	62
3.1.4	Inhibitor Synergism in Pepsin	64
3.1.4.1	Design of active site probes	64
3.1.4.2	Effect of urea	67
3.1.4.3	Effect of ethylene glycol	68
3.2.	Discussion	69
3.2.1	Sulfonamide Inhibitors	69
3.2.2	Inhibitor Binding Synergism in HIV-1 Protease	70
3.2.3	Inhibitor Binding Synergism in Pepsin	74
3.2.4	Significance and Potential Applications	76
<b>4.</b>	<b>COMBINATION PLOTS: A NEW APPROACH FOR THE ANALYSIS OF ENZYME - INHIBITOR INTERACTIONS</b>	<b>79</b>
4.1	Results	79
4.1.1	Theoretical Analysis	81
4.1.1.1	Interaction between Two Competitive inhibitors	81
4.1.1.1.1	Alternative combination plots	84
4.1.1.2	Interaction between Two Noncompetitive Inhibitors	85
4.1.1.3	Interaction between a Competitive and a Noncompetitive inhibitor	86
4.1.1.4	Interaction between Three Competitive Inhibitors	89

4.1.2	Application of Theoretical Treatment	91
4.1.2.1	Two Competitive Inhibitors	91
4.1.2.2	Three Competitive Inhibitors	104
4.2	Discussion	107
5.	INHIBITORS OF CARBOXYPEPTIDASES A AND B	113
5.1	Results	113
5.1.1	Carboxylic Acid Inhibitors of Carboxypeptidase B	113
5.1.2	Concurrent Effect of Two Inhibitors on Carboxypeptidase B	118
5.1.3	Concurrent Effect of Three Inhibitors on Carboxypeptidase B	124
5.2	Discussion	125
6.	APPENDICES	131
6.1	Appendix I: Kinetic Equation for Three Competitive inhibitors.	131
6.2	Appendix II: Definition of $\phi$ .	133
6.3	Appendix III: Ionization Constants for Dicarboxylic Acid inhibitors of Carboxypeptidase B	134
7.	REFERENCES	135

## ABBREVIATIONS

AIDS	Acquired Immune Deficiency Syndrome
AMV	Avian Myeloblastosis Virus
Cbz	Carbobenzyloxy
DCC	Dicyclohexylcarbodiimide
DMSO	Dimethylsulfoxide
EDTA	N,N,N'N'Ethylenediaminetetraacetic acid
EPNP	1,2-epoxy-(4-nitrophenoxypropane)
<sup>1</sup> H NMR	Proton Nuclear Magnetic Resonance
HOBT	1-Hydroxybenzotriazole
HIV-1	Human Immunodeficiency Virus type 1
HPLC	High Pressure Liquid Chromatography
Iva	Isovaleryl
kD	kilodalton
MES	2-[N-Morpholino]ethanesulfonic acid
RSV	Rous Sarcoma Virus
Sta	Statine: (4-amino-3-hydroxy-6-methylheptanoic acid)
TLC	Thin Layer Chromatography
Tris	Tris-(hydroxymethyl)aminomethane

## LIST OF FIGURES

		page
1.	Gibbs free energy - reaction co-ordinate profile.	2
2.	A schematic representation of the different amino acids observed at $P_4 - P_4'$ subsites in the HIV-1 protease substrates <i>gag</i> and <i>gag-pol</i> polyprotein precursors.	12
3.	Yonetani-Theorell plot for the interaction between Cbz-glutaminyloamylamide and Cbz-isoleucyl-phenylalaninol on HIV-1 protease.	33
4.	A secondary replot of the interaction between Cbz-glutaminyloamylamide and Cbz-isoleucyl-phenylalaninol on HIV-1 protease.	34
5.	Dissociation constant for 2-ethyl-2-methylsuccinic acid on carboxypeptidase B via the method of Hunter and Downs (1945)	36
6.	Dissociation constant for 2-ethyl-2-methylsuccinic acid on carboxypeptidase B via the method of Chan (1994)	37
7.	Dixon plot for 2-ethyl-2-methylsuccinic acid on carboxypeptidase B	39
8.	Structure of A74704, derivative active site probes and expected binding mode in HIV-1 protease.	57
9.	Structure of Iva-Val-Sta-Ala-isoamylamide and derived active site probes.	65
10.	An illustration of the concept of synergism-assisted inactivation.	78
11.	Cube diagram of interaction of three competitive inhibitors.	88
12.	Yonetani-Theorell plot for the synergistic interaction between succinic acid and methylguanidine on carboxypeptidase B.	93
13.	Combination plot for concurrent effect of succinic acid and methylguanidine on carboxypeptidase B.	94
14.	Combination plot for concurrent effect of succinic acid and methylguanidine on carboxypeptidase B at different substrate concentrations.	96



15.	Alternative combination plot (I) for effect of succinic acid and methylguanidine on carboxypeptidase B at different substrate concentrations.	97
16.	Alternative combination plot (II) for effect of succinic acid and methylguanidine on carboxypeptidase B at different substrate concentrations.	98
17.	Combination plot of retrieved data on effect of ortho-phenanthroline and ADP on horse liver alcohol dehydrogenase.	100
18.	Combination plot of retrieved data on effect of ADP-ribose and ADP on horse liver alcohol dehydrogenase.	101
19.	Combination plot illustrating the concurrent effects of different pairs of inhibitors on carboxypeptidase B.	103
20.	An extended combination plot for the concurrent effect of three inhibitors of carboxypeptidase B.	105

## LIST OF TABLES

	Page
I. Effect of pseudosymmetric sulfonamide inhibitors on HIV-1 and AMV proteases.	55
II. Effects of varying the alkylamide fragment on its synergism with Cbz-Val-phenylalaninol on HIV-1 protease.	59
III. Effects of the putative P <sub>2</sub> ' residue in the alkylamide fragment on its synergism with Cbz-Val-phenylalaninol on HIV-1 protease.	61
IV. Effects of varying the P <sub>2</sub> residue in the hydroxyl fragment on its synergism with Cbz-Gln-isoamylamide on HIV-1 protease.	63
V. Concurrent effects of Cbz-Val-leucinol and second inhibitor on porcine pepsin.	66
VI. Summary of equations, slopes and intercepts of combination plots for competitive inhibitors.	106
VII. Carboxylic acid inhibitors of carboxypeptidase B.	114
VIII. Dissociation constants for dicarboxylic acid inhibitors on carboxypeptidase A.	117
IX. Zn ligands and Guanidine inhibitors of Carboxypeptidase B.	119
X. Concurrent effects of Dicarboxylic acids and Guanidine homologues on Carboxypeptidase B.	120
XI. Synergistic factors ( $1/\alpha$ ) for interaction between Formohydroxamic acid and Guanidine homologues on Carboxypeptidase B.	122
XII. Synergistic factors ( $1/\alpha$ ) for interaction between zinc ligands and Dicarboxylic acids on Carboxypeptidase B.	123

## 1. INTRODUCTION

### ENZYMES AS BIOLOGICAL CATALYSTS

Understanding the processes which define life invariably entails an in-depth knowledge of biochemical pathways and the mechanisms of the enzymes involved. While ensuring cellular processes remain highly controlled, enzymes also enhance their rates. Without enzymes most reactions would not proceed fast enough to sustain life. As catalysts, enzymes generally enhance reaction rates by an order of  $10^9$  -  $10^{12}$  over the nonenzymatic reactions (Fersht, 1977). Such remarkable rate accelerations are achieved by virtue of their (enzymes') ability to stabilize the transition state, the highest energetic species on the reaction co-ordinate (Pauling, 1948). This is made possible through suitably placed functional groups at the active site which leads to a reduction of the free energy of activation (Figure 1).

Another hallmark of enzyme-catalyzed reactions is their specificity. Enzymes generally catalyze specific or very closely related chemical reactions (Walsh, 1979). The notion of specificity, however, may be used both to reflect the type of reaction an enzyme catalyzes or the breadth of substrates it utilizes (Stryer, 1988). Thus an enzyme may display broad specificity with respect to its spectrum of substrates, although the type of reaction catalyzed essentially remains the same. For example, alcohol dehydrogenase specifically catalyzes the oxidation of an alcohol to an aldehyde and *vice versa*. Although several alcohols serve as substrates for the enzyme, the primary reaction remains the regiospecific removal of a hydrogen atom to generate the corresponding aldehyde in the forward reaction

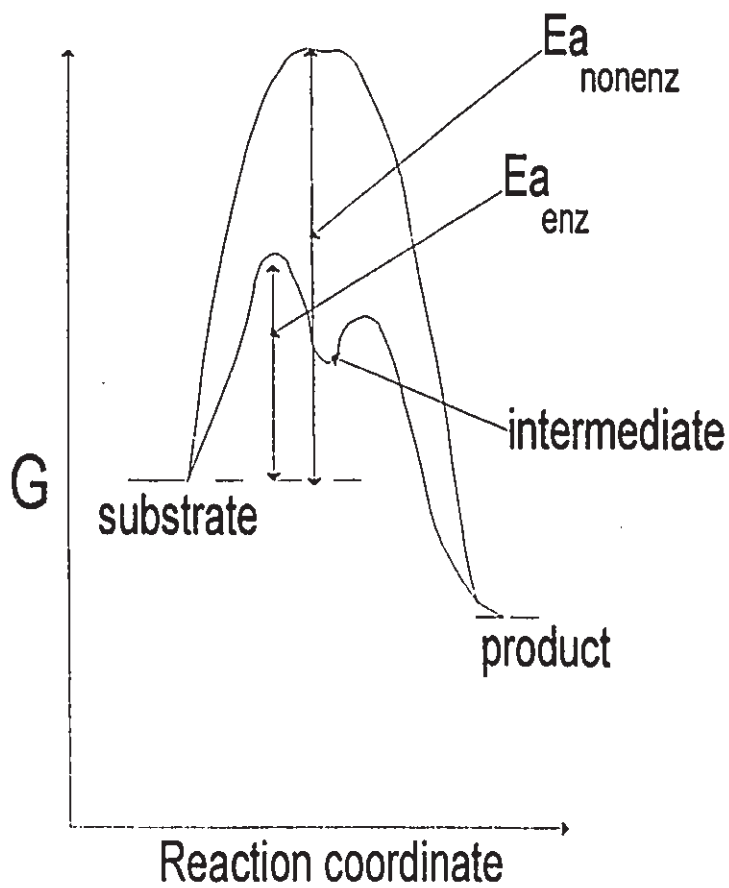


**Figure 1.** Reaction co-ordinate profile of an enzyme-catalyzed versus non-catalyzed reaction.  $Ea_{enz}$  - activation energy of enzyme-catalyzed reaction;  $Ea_{nonenz}$  - activation energy of nonenzymatic reaction; G - Gibbs free energy. (Reproduced from Fersht, 1977 with modifications.)

(Loewus *et al.*, 1953).

Since their discovery in the 1800's, enzymes have been extensively studied in order to assess their role in intermediary metabolism and other cellular processes (Stryer, 1988). Another aspect of enzymology, arguably more academic than practical in many cases, have been efforts aimed at unravelling the origins of the remarkable rate accelerations and high specificities (Pauling, 1948; Koshland, 1958; Jencks, 1975; Burbaum *et al.*, 1989). The enormous potential of applying enzymes in industry and medicine coupled to the possibility of engineering "new" enzymes through molecular biological technology has, however, added renewed impetus in this endeavor (Gacesa and Hubble, 1987). In this thesis, significant information is presented concerning the mode of action of two enzymes and a general method is described for analyzing certain types of enzyme behavior.

Understanding the mechanism of an enzyme entails a detailed examination of both kinetic and chemical mechanisms as well as the structural basis of its action. Kinetic approaches reveal information regarding rates of individual steps on the reaction pathway and thereby indicate which of the physical or chemical steps limits the overall reaction (Segel, 1975). A classic example is the pioneering work of Hartley and Kilby (1954) who applied burst kinetics (an approach where an initial burst of product formation precedes a steady reaction rate) to elucidate the rate-determining step in the catalytic reaction of chymotrypsin, a proteolytic enzyme. The various chemical intermediates generated in the course of a single turnover from substrate to product is described by the chemical mechanism of an enzyme. Through the application of rules from organic chemistry and ingenious methods of trapping reaction intermediates, the transition state which is stabilized

to promote the reaction can be described (Walsh, 1979). To fully appreciate how the binding of a substrate at the active site of an enzyme results in catalysis requires the determination of the three-dimensional structure of the enzyme and the essential residues of the catalytic machinery (Blow and Steitz, 1970). Ultimately, the chemical and structural mechanism of an enzyme-catalyzed reaction must corroborate the kinetic model.

Enzyme inhibitors, compounds that bind and slow down an enzyme reaction, have been powerful tools for the analysis of enzyme action particularly transition-state analogues (inhibitors that resemble the transition state of the reaction) (Lolis and Petsko, 1990). Inhibitors can be broadly grouped into reversible, those which do not react chemically with the target enzyme and irreversible, those which do. Reversible inhibitors are further subclassified into competitive, noncompetitive and uncompetitive on the basis of how they influence the kinetic parameters with respect to the substrate of the enzyme (Segel, 1975). Competitive inhibitors essentially compete with the substrate for binding thereby raising the substrate's  $K_m$  (the substrate concentration that gives half the maximum rate,  $V_{max}$ ). Noncompetitive inhibitors do not influence  $K_m$  but reduces  $V_{max}$ . The binding of uncompetitive inhibitors depend on the presence of the substrate and therefore affect both  $K_m$  and  $V_{max}$ . There are other classification criteria; for example, inhibitors may be grouped based on their rate of association with the enzyme and tightness of binding (Morrison and Walsh, 1988). Generally, because competitive inhibitors similarly bind at the active site they serve as useful diagnostic probes for establishing the mechanism of enzyme-catalyzed reactions (Lolis and Petsko, 1990). Thus, the application of inhibitors contributed greatly to the understanding of the mechanism of chymotrypsin, arguably the most understood

enzyme in biochemistry (Blow and Steitz, 1970; Kraut, 1977).

Another aspect of studies involving enzyme inhibitors is their potential application as drugs against target enzymes in disease states. The use of inhibitors in enzymology has been demonstrated most extensively for proteolytic enzymes as they generally permit variations in substrate structure and therefore their analogues (Aoyagi *et al.*, 1972; Bendall *et al.*, 1977; Smith *et al.*, 1988; Szelke *et al.*, 1982; Rich and Sun, 1980; Byers and Wolfenden, 1972,1973; Ondetti *et al.*, 1979; Roberts *et al.*, 1990; Hanson *et al.*, 1989; Schoellman and Shaw, 1963; Cushman *et al.*, 1977; Lam *et al.*, 1994). Furthermore, proteolytic enzymes have been, historically, the most studied and better understood group of enzymes and have thus served as models for a general understanding of enzyme action. The proteolytic enzymes carboxypeptidases A and B and HIV-1 protease have been studied as model enzymes in this thesis. Based on previous knowledge of the structures and potency of certain inhibitors, studies have been performed which may further contribute to the discovery of new inhibitors and to our understanding of enzyme action.

## PROTEOLYTIC ENZYMES

These enzymes which catalyze the hydrolysis of peptide bonds are also referred to as peptidases, proteinases or proteases. Since proteolytic enzymes are proteins, they may themselves serve as substrates and undergo self-hydrolysis if the particular bonds they hydrolyze are exposed. Consequently, the digestive enzymes, for example, are synthesized in the form of inactive zymogens and undergo activation at their sites of action (Stroud *et al.*, 1977). Pepsin, for example, is synthesized in the form of the zymogen, pepsinogen, in

the pancreas and undergoes activation in the presence of the low pH conditions within the stomach. The mechanism of activation involves an intramolecular cleavage of the N-terminal 44 amino acid residues of the zymogen which block entry of potential substrates to the active site in the precursor (James and Sielecki, 1986). A survey of proteolytic enzymes reveal diverse physiological roles in different cells and tissues (Barrett, 1977). Several lysosomal proteases, for instance, are involved in the degradation of proteins released into that organelle (Barrett, 1977) while other proteases like signal peptidase in the endoplasmic reticulum function to aid in the targeting and trafficking of newly synthesized proteins (Pfeffer and Rothman, 1987). The matrix metalloproteases, including stromelysins and matrilysin are involved in tumour invasiveness (Matrisian, 1992) while several others like the clotting factors act in defense of the host (Walsh, 1975). Industrially, proteases similarly have wide applications including their use in meat tenderization, cheese making and in the brewing industry for removal of beer haze (Gacesa and Hubble, 1987). It is therefore not surprising that they were among the first enzymes to be purified, characterized and three dimensional structures solved (Blow and Steitz, 1970).

Proteolytic enzymes can be broadly classified into two groups depending on the position of the scissile bond (the susceptible peptide bond) relative to the termini of the protein or peptide (Walsh, 1975). Exopeptidases describe those enzymes which cleave the terminal amino acid of the peptide or protein substrate while endopeptidases refer to those enzymes whose cleavage sites occur within the substrate. Exopeptidases are further subdivided into aminopeptidases which cleave the N-terminal residue and carboxypeptidases which cleave the C-terminal amino acid. On the basis of their mechanism of action and the



catalytically essential residue, the family of proteolytic enzymes fall into four major classes: serine, cysteine, aspartic and metalloproteases (Hartley, 1960). Owing to their identical catalytic mechanisms each class is specifically inhibited by characteristic compounds; for instance, aspartic proteases are exclusively inhibited by the antibiotic, pepstatin (Iva-Val-Val-Sta-Ala-Sta) (Umezawa *et al.*, 1970). In addition to sharing a similar catalytic mechanism, members of each class also maintain significant sequence homology and fold into distinct tertiary structures (Fersht, 1977). Surprisingly, though, some members of a class exhibit no sequence homology and do not fold into the defining architecture of the majority of the members, however, they maintain a similar catalytic mechanism. For example, the bacterial serine protease subtilisin versus the mammalian serine proteases. Such effects have been attributed to a convergent evolutionary process where different tertiary folds end up with the same catalytic mechanism (Fersht, 1977).

Proteolytic enzymes ultimately accomplish the same task, hydrolysis of peptide bonds, but through different mechanisms. The differences in mechanism result from the essential amino acid residues employed and their spatial arrangement within the active site (Blow and Steitz, 1970; Kraut, 1977; Lipscomb, 1983). The serine proteases possess a catalytically essential serine residue (Ser-195 in Chymotrypsin) as a member of a catalytic triad necessary for nucleophilic catalysis. The other members of the catalytic triad a histidine and an aspartic acid serve to potentiate the nucleophilicity of the essential serine residue in catalysis (Blow *et al.*, 1969). Mutating or covalently modifying the equivalent of the triad in all members of this class results in a loss of catalytic activity. The thiol or cysteine proteases like the serine proteases catalyze their reactions through the formation of a

covalent intermediate involving the substrate and the catalytically essential cysteine (Cys-25 in papain). However, a charge-relay mechanism involving three catalytically essential residues as found in the serine proteases is absent (Lowe, 1976).

As their name suggests, aspartic or acid proteases like pepsin and HIV protease contain catalytically important aspartic acid residues and are generally active under low pH conditions. In this class of enzymes, catalysis proceeds through a general-base/general-acid mechanism involving a pair of aspartic acid residues and does not involve a covalent intermediate (Polgar, 1987; Pearl, 1987; James and Sielecki, 1986). Although the residue acting as the general base or acid is not clear, Asp-32 and Asp-215 serve this role in pepsin, the archetype of this class (Tang, 1970; Hartsuck and Tang, 1972). The essential aspartic acid residues occur twice in a consensus sequence of Asp-Thr/Ser-Gly in the primary amino acid sequence of monomeric members and once in each subunit of the homodimeric members of the group, like the retroviral proteases from HIV and RSV (Fitzgerald and Springer, 1991; Davies, 1990). Because the retroviral proteases possess less than half the number of residues found in their monomeric group members and are active as homodimers, it is therefore generally believed that the monomeric members of the class must have arisen from a gene duplication during evolution (Pearl and Taylor, 1989).

The fourth class of proteolytic enzymes, the metalloproteases, employ a divalent cation in catalysis (Lipscomb, 1983). Zinc is the metal most commonly used in these enzymes (Auld and Vallee, 1987) and it is tightly held by side chains of three active site residues with water as the fourth ligand (Rees *et al.*, 1983). Substitution of the zinc with other divalent metals in carboxypeptidase A, for example, results in a catalytically active

enzyme of altered properties in certain cases, the apoenzyme (an enzyme without the essential metal cation at the active site), however, is catalytically inactive (Coleman and Vallee, 1960). Catalysis in these enzymes involves the polarization of the carbonyl carbon of the susceptible amide bond by the catalytically essential zinc cation acting as a Lewis acid (Christianson and Lipscomb, 1989). The digestive enzymes, carboxypeptidases A and B are examples of this class of proteases.

#### TARGET ENZYMES.

##### *HIV-1 protease*

The protease from human immunodeficiency virus type 1 (HIV-1) plays a very important role in the life cycle of the virus. Like other retroviruses, HIV translates its proteins in the form of polyprotein precursors, 55 kD *gag*, 165 kD *gag-pol* and 160 kD *env*, which are posttranslationally processed into mature structural proteins and enzymes by the virally encoded protease (Kohl *et al.*, 1988; Seelmeier *et al.*, 1988). The protease does not exhibit activity towards the *env* gene product and its cleavage is believed to be catalyzed by a host protease (Darke *et al.*, 1988). Interestingly, the HIV-1 protease autocatalyzes its excision from the *gag-pol* polyprotein precursor (Kramer *et al.*, 1986; Debouck *et al.*, 1987) therefore deleterious mutations in the *pol* gene which abolishes the activity of the protease leads to an accumulation of polyprotein precursors. Furthermore, virions which result from such disruptions are non-infectious and show deformities in their morphology (Kohl *et al.*, 1988). Biochemically, inhibitors to the HIV-1 protease also lead to a build up of polyprotein precursors (McQuade *et al.*, 1990). Such studies have

established HIV-1 protease as a potential candidate for the design of drugs against AIDS. Thus, there has been an intensive research program on the enzyme in an attempt to develop highly specific and potent inhibitors (recently reviewed by Wlodawer and Erickson, 1993). Such efforts have been facilitated by the vast knowledge accumulated previously on other aspartyl proteases (Szelke *et al.*, 1982; Boger *et al.*, 1983) emphasizing the importance of studies on model enzyme systems.

HIV-1 protease is a 99 amino acid protein with a native molecular weight of about 22,000 kD and is catalytically active as a homodimer (Graves *et al.*, 1988; Meek *et al.*, 1988). The enzyme has been conclusively characterized as an aspartyl protease based on its primary amino acid sequence (Yasunaga *et al.*, 1986), mutational analysis (Kohl *et al.*, 1988; Seelmeier *et al.*, 1988), kinetic properties (Meek *et al.*, 1988; Hansen *et al.*, 1988; Hyland *et al.*, 1991(a); 1991(b)) and three-dimensional structure (Navia *et al.*, 1989; Wlodawer *et al.*, 1989). The tertiary structure of the enzyme revealed the distinctive fold of aspartic proteases with some differences (Wlodawer *et al.*, 1989). Dimerization of the enzyme results in the creation of a  $C_2$  symmetry at the active site; which is formed at the interface of both subunits. Unlike monomeric aspartic proteases which have a single "flap", HIV-1 protease possesses two "flaps" which act as lids over the active site upon substrate binding. The residues of the N and C termini rather than being free and distorted are involved in a four stranded anti-parallel  $\beta$ -sheet (Wlodawer *et al.*, 1989) which stabilize the dimeric structure suggesting activation does not proceed via an intramolecular cleavage as occurs in pepsinogen (James and Sielecki, 1986). The mechanism of activation is presently not clearly understood but it appears to involve an intermolecular rather than an

intramolecular cleavage of the precursor (Wlodawer *et al.*, 1989).

With respect to substrate specificity, a comparison of the cleavage sites of natural and synthetic substrates of HIV-1 protease (Figure 2) indicates that the primary amino acid sequence alone cannot govern the specificity of the enzyme. A more subtle mechanism involving the interplay of subsites could therefore be in operation in view of the extended nature of the enzyme's active site. Subsite effects on inhibitor binding have been previously observed in several metalloproteases (Chan and Pfuetzner, 1993; DiGregorio *et al.*, 1988; Pfuetzner and Chan, 1988; 1993). Such effects have therefore been investigated in HIV-1 protease with interesting implications.

In view of the pharmacological importance of this enzyme several inhibitors have been screened or synthesized with the most potent being the substrate and transition-state analogues with hydroxyethylene, hydroxyethylamine and aminomethylene as non-hydrolyzable scissile bond replacements. Inhibitors containing these groups exhibit dissociation constants ( $K_i$ ) in the  $\mu\text{M}$  - nM range (McQuade *et al.*, 1990; Tomasselli *et al.*, 1990; Richards *et al.*, 1989; Rich *et al.*, 1990; Roberts *et al.*, 1990; Rich *et al.*, 1991). Other scissile bond surrogates include phosphinic acid isosteres (Dreyer *et al.*, 1989; Grobelny *et al.*, 1990), statines (Tomasselli *et al.*, 1990; Billich *et al.*, 1988; Hui *et al.*, 1991), hydroxyethylureas (Getman *et al.*, 1993) and difluoroketones (Dreyer *et al.*, 1989; Sham *et al.*, 1991). The  $C_2$  symmetry of HIV-1 protease has also been exploited in the design of very potent and specific inhibitors including A74704 (see Figure 8; Kempf *et al.*, 1990) which served as the parent compound in the synergistic studies on HIV-1 protease reported in this thesis. Dimerization preventive inhibitors (Schramm *et al.*, 1991; 1993) and




---

1.	P17   P24	SER-GLN-ASN-TYR   PRO-ILE-VAL-GLN
2.	P24   F	ALA-ARG-VAL-LEU   ALA-GLU-ALA-MET
3.	F   P7	ALA-THR-ILE-MET   MET-GLN-ARG-GLY
4.	P7   P6	PRO-GLY-ASN-PHE   LEU-GLN-SER-ARG
5.	F   PR	SER-PHE-ASN-PHE   PRO-GLN-ILE-THR
6.	PR   RT	THR-LEU-ASN-PHE   PRO-ILE-SER-PRO
7.	RT51   RNase H	ALA-GLU-THR-PHE   TYR-VAL- ASP-GLY
8.	RT   IN	ARG-LYS-ILE-LEU   PHE-LEU-ASP-GLY

---

**Figure 2.** Cleavage sites in the *gag* and *gag-pol* polyprotein precursor substrates of HIV-1 protease. Scissile bonds are indicated by |. Reproduced from Debouck (1992) with modifications. F refers to a free terminus which does not delimit a functional protein.

naturally occurring inhibitors have been also pursued (Lingham *et al.*, 1992; Blumenstein *et al.*, 1989).

### *Carboxypeptidases A and B*

These exopeptidases are synthesized as zymogens by the acinar cells of the pancreas and undergo activation by trypsin in the duodenum where they function as digestive enzymes (Stryer, 1988). Both enzymes are similar with respect to their presumed catalytic mechanism (Zisapel and Sokolovsky, 1975), amino acid sequence (Titani *et al.*, 1975) and three dimensional structure (Schmid and Herriott, 1976); they, however, differ in specificity. The suffix A and B of the enzymes relates to their specificity; the A enzyme prefers aromatic amino acids while the B enzymes is specific for basic ones. Bovine carboxypeptidase A (Vallee and Neureth, 1954) and porcine carboxypeptidase B (Folk *et al.*, 1960) are among some of the most extensively studied proteases; they have served as useful models for enzyme structure and function (Blow and Steitz, 1970; Lipscomb, 1983; Auld and Vallee, 1987) and have been used as such in this thesis.

The active sites of both enzymes are fully formed in the inactive zymogen but access is physically blocked by the presence of an N-terminal domain which acts as a latch over the cavity (Guasch *et al.*, 1992). Limited proteolysis by trypsin removes this domain of 95 amino acids to activate the enzymes. An active site extending over five amino acid residues ( $S_4 - S_1'$ ) is indicative of kinetic studies (Abramovitz *et al.*, 1967) and structural data (Lipscomb, 1983). In addition to their proteolytic activity, carboxypeptidases A and B also possess esterase activity (the ability to hydrolyze ester bonds) (Auld and Vallee, 1987)

which appears to proceed via a different mechanism. Breslow and Wernick (1977) have postulated that the general-base and covalent catalysis suggested by available kinetic and structural data reflects the dual activities of carboxypeptidase A. Thus, peptides are primarily hydrolyzed by a general-base mechanism while esters would undergo covalent catalysis owing to the weaker affinity of the ester carbonyl for the catalytically essential zinc atom thereby necessitating the alternate anhydride-intermediate mechanism involving Glu-270.

X-ray crystallographical analysis of the carboxypeptidases has played a major role in understanding the activation and mechanism of action of these enzymes. That the zinc is sequestered at the active site by two histidines and a glutamic acid (His-69, His-196 and Glu-72 in carboxypeptidase A) with water as a fourth ligand has been firmly established in both enzymes (Rees *et al.*, 1983; Schmid and Herriot, 1976). A site specific for the terminal carboxyl group of peptides (primarily Arg-145 in carboxypeptidase A) also confirmed earlier studies using covalent modification approaches (Riordan, 1973). The roles of other amino acids, for example, Tyr-248 and Arg-127 which also participate in catalysis have been elucidated (Christianson and Lipscomb, 1989). The basis of the distinct specificities of the enzymes: the existence of a hydrophobic pocket in carboxypeptidase A and the presence of Asp-255 at the base of the substrate binding pocket in the B enzyme has been resolved (Rees *et al.*, 1983; Schmid and Herriot, 1976).

Several inhibitors of the carboxypeptidases have been synthesized with the view to understanding the catalytic mechanism of the enzymes and also to provide tools for the development of more potent inhibitors of other zinc proteases. For example, Byers and



Wolfenden (1973) successfully synthesized a bi-product analogue, L-benzylsuccinic acid, which showed tight binding ( $K_i$   $4.5 \times 10^{-7}$  M) to carboxypeptidase A and competitively inhibited both ester and peptide hydrolysis. Analysis of the effect of L-benzylsuccinic acid showed it also bound the B enzyme although with a decreased affinity (Zisapel *et al.*, 1973). Similar design approaches were taken by McKay and Plummer (1978) in the synthesis of the potent inhibitor, guanidinoethylmercaptosuccinic acid ( $K_i$   $4 \times 10^{-6}$  M) for carboxypeptidase B. The transition-state concept (Wolfenden, 1972) has been most successful in the design of inhibitors against the carboxypeptidases, for example, Kaplan and Bartlett, (1991) impressively synthesized the phosphonate tripeptide analogue, Cbz-Phe-Val<sup>P</sup>-(O)-Phe, ( $K_i$   $11 \times 10^{-15}$  M) against carboxypeptidase A. In this thesis, a potentially new approach in the design of inhibitors against zinc proteases is presented using carboxypeptidases A and B as model enzymes.

## RATIONAL DRUG DESIGN

The important physiological roles of proteolytic enzymes in metabolism including their involvement in digestion and protein turnover, cell defense mechanisms, production of bioactive peptides, cellular invasiveness, for instance, have spurred on a great deal of research on their mechanism of action. Pharmacologically, the inactivity or superactivity of proteolytic enzymes in several disease states has received a great deal of attention. For example, the search for inhibitors against renin which is an aspartic protease and angiotensin-converting enzyme, a metalloprotease, involved in the modulation of blood pressure has been an on-going research project in several pharmaceutical institutions for

many years (reviewed by Cushman and Ondetti, 1982). Although the serendipitous search for agents against several diseases continues, the increasing knowledge of the mechanism of enzyme action coupled with the availability of high resolution three-dimensional structures has shifted the emphasis toward rational drug design and development.

The transition state theory of enzyme catalysis (Pauling, 1948) suggests that an enzyme displays its highest affinity not for the substrate nor the product (the ground state) but for the transition state on the reaction co-ordinate. Because the transition state occurs only fleetingly during catalysis, it would be expected therefore that a more stable structure resembling that species should bind the enzyme with a higher affinity than a simple substrate or product analogue (Wolfenden, 1972; Leinhard, 1973). On the assumption that a transition state species is in thermodynamic equilibrium with the ground state and irrespective of whether bound to an enzyme or occurring free in solution it decomposes with a vibrational frequency equivalent to that of a chemical bond being formed or broken, the following relationship holds (Wolfenden, 1972):

$$\frac{K_{nonenz}}{K_{enz}} = \frac{K_{TS}}{K_S} = 10^{-8} - 10^{-14}$$

(where transmission coefficients is taken as unity for both reactions)

Since  $K_S$  for a typical substrate occur in the range of  $10^{-3}$  -  $10^{-6}$  M, it follows that  $K_{TS}$ , will be expected to be in the range of  $10^{-11}$  -  $10^{-20}$  M. Thus, a good transition-state analogue would be expected to have a dissociation constant in the above range. Originally postulated by Pauling (1948) and expounded by Wolfenden (1972), this approach towards drug design has been generally exploited for the development of several potent inhibitors including

captopril (D-3-mercapto-2-methylpropanoyl-L-proline) for the metalloprotease, angiotensin-converting enzyme (Cushman *et al.*, 1977).

Since the application of the transition-state concept in drug design is based on mimicking the presumed transition-state of a reaction, it becomes imperative that the mechanism of action of the particular enzyme be known in sufficient detail because the species cannot be physically isolated and characterized. Obtaining an X-ray crystal structure of the enzyme/transition-state analogue complex, in many cases, serve as a diagnostic tool to biophysically highlight the nature of interaction between the lead compound (inhibitor) and the target enzyme (Lolis and Petsko, 1990). From the crystal structure improvements can then be made on the lead structure by including suitable functional groups to enhance potency and presumably solubility. The iterative cycle of design, evaluation and X-ray structure determination of the enzyme-inhibitor complex is pursued rationally until a potent inhibitor of the enzyme is obtained.

#### ACTIVE SITE INTERACTIONS

From the fore-going, it is evident that an insight into how a potential inhibitor interacts at the active site of an enzyme could contribute tremendously towards rational drug design. The active site of several proteases are extended and capable of binding several amino acids (Schechter and Berger, 1967). HIV-1 protease, for example, binds three amino acid residues of its substrate to either side of the scissile bond (Schneider and Kent, 1988; Moore *et al.*, 1988). Such extensive interactions can, no doubt, be harnessed in developing more potent inhibitors against this enzyme for instance. Furthermore, subsite interactions

leading to increased inhibitor potency through the phenomenon of synergism has been documented in some zinc proteases. In angiotensin-converting enzyme, for instance, the simultaneous presence of a zinc ligand, acetohydroxamic acid, and acetyl-proline, an affinity probe, improves their affinity for the enzyme by a factor of 150 (Pfuetzner and Chan, 1988). A similar phenomenon has also been observed in other zinc proteases including microsomal aminopeptidase (DiGregorio *et al.*, 1988), thermolysin (Pfuetzner and Chan, 1993) and carboxypeptidases A and B (Chan and Pfuetzner, 1993).

Even though the role of inhibitor synergism in drug design has not been totally defined the potential clearly exists. The approach can provide invaluable information regarding the topographical architecture of an enzyme's active site. Traditionally, the concurrent effect of pairs of inhibitors at an enzyme's active site has been analyzed primarily by the method of Yonetani and Theorell (1964). On the assumption that the inhibitors do not react chemically but bind reversibly, the method yields an interaction constant,  $\alpha$ , which quantitatively describes the nature and extent of interaction between two inhibitors on the enzyme. When the measured interaction constant is less than 1 ( $\alpha < 1$ ), it indicates that the inhibitors interact synergistically. In this thesis, the reciprocal of the value of  $\alpha$  which gives directly the quantitative measure of the fold-increase in affinity ie. the synergistic factor of the inhibitors for the enzyme will be used. Thus,  $1/\alpha$  of 10 ie. an  $\alpha$  of 0.1 indicates a 10-fold increase in affinity of the inhibitors for their target enzyme. When  $\alpha = 1$ , it signifies that the inhibitors bind independent of each other. In other words, two independent, non-interacting subsites exist for the inhibitors within the active site. The binding of one inhibitor interferes with the other when the value of  $1/\alpha < 1$ . A situation

where the binding of one inhibitor does not physically prevent the binding of the other directly but induces a conformational change in the enzyme which masks the binding site of the second inhibitor would also yield  $1/\alpha < 1$ . These two forms of antagonism cannot be distinguished on the basis of the kinetic approach. In the extreme case where the binding of one inhibitor totally excludes the other  $1/\alpha \sim 0$  ie.  $\alpha \sim \infty$ .

The Yonetani-Theorell approach (1964) of analyzing inhibitor synergism follows an established tradition in enzymology where the interception point of a family of lines is used to evaluate some kinetic parameter (Segel, 1975). Following the formulation of the rate equation of enzymes by Michaelis and Menten (1913), several plots have been suggested to facilitate the determination of kinetic constants ( $K_m$  and  $k_{cat}$ ) of which the most commonly used is that of Lineweaver and Burk (1934). By using a family of lines representing effects at different substrate concentrations, the double reciprocal Lineweaver-Burk method (where the reciprocal of the reaction rate,  $1/v$ , is plotted against the reciprocal of the substrate concentration,  $1/[s]$ ) could also be employed for determination of inhibition constants where the point of interception of the lines reveals the constant. The work of Dixon (1952) adopted "the family of lines" approach and introduced the secondary replot for a direct determination of the inhibition constant graphically. Presently, the determination of virtually all kinetic constants where a variation of a dependent parameter is employed relies on the use of a family of lines (Segel, 1975); for example, the determination of binding order of multi substrates of an enzyme reaction and the determination of inactivation rates at different temperatures. In this thesis, a different approach is presented which departs from this long-standing tradition of determining kinetic constants. In the

approach presented, an equation unifying the primary and secondary plots is derived and plotted as a single line to directly determine the desired kinetic parameter from the intercepts and slope.

## DESIGN AND SURVEY OF RESEARCH

### *Interactions of inhibitors with aspartic proteases*

The first part of this thesis is aimed at understanding ligand interactions in HIV-1 protease. To investigate the potential involvement of subsite interactions in the catalytic mechanism of HIV-1 protease, the possible existence of synergistic interactions among inhibitors targeted to defined regions of the active site is examined. Following the detection of inhibitor binding synergism in HIV-1 protease, the generality of the phenomenon in aspartic proteases, is assessed by examining pepsin, the archetype of the class, for similar effects.

### *Combination plots: An alternative approach to the analysis of enzyme-inhibitor interactions*

This part of the thesis deals with the development of an improved graphical method, the combination plot, for the analysis of enzyme-inhibitor interactions. The utility of the combination plots is illustrated with carboxypeptidase B, an enzyme which was previously shown to exhibit inhibitor synergism with easily obtainable inhibitors (Chan and Pfuetzner, 1993). The merits of the approach in relation to other methods are discussed.

*Gem-dialkyl succinic acids inhibitors of carboxypeptidases A and B*

*Gem*-dialkyl succinic acid derivatives were discovered as unusually potent inhibitors of both carboxypeptidases A and B. This part of the thesis pertains to studies performed on this new class of reversible inhibitors of the carboxypeptidases. The work explores the origins of the remarkable inhibitory potency and attempts to characterize the inhibitors which cannot be strictly classified as either transition-state or substrate/product analogues.

## 2. MATERIALS AND METHODS

### 2.1 Materials

#### 2.1.1 *Synthetic reagents*

N-carbobenzyloxy(Cbz)-L-amino acids, amino acid derivatives, 1,1'-carbonyldiimidazole, dicyclohexylcarbodiimide (DCC) and  $\beta$ -phenethylamine were purchased from Sigma Chemical Co. (St. Louis, MO). Sodium hydrogen carbonate, magnesium sulphate, dimethylformamide (DMF), methylene chloride, chloroform, cyclohexane, hexane and ethylacetate were products of British Drug House (BDH) (Toronto, ONT). Hydrochloric acid (HCl), formic acid and absolute ethanol were obtained from Fisher Scientific Chemical Co. (Toronto, ONT). Isoamylamine, diisopropylethylamine, methylamine, benzylamine and 1-hydroxybenzotriazole (HOBT), were bought from Aldrich Chemicals Co. (Milwaukee, WI).

#### 2.1.2 *Other chemicals*

Tris(hydroxyethyl)aminomethane (TRIS), ethylenediaminetetraacetic acid (EDTA), dithiothreitol (DTT), ninhydrin, 2,4,6-collidine, tetramethylsilane, citric acid, MOPS and 2-[N-Morpholino]ethanesulfonic acid (MES) were obtained from Sigma (St. Louis, MO). Dimethylsulfoxide (DMSO), acetic acid, methanol, pyridine and HPLC grade acetonitrile were purchased from Fisher Scientific Chemical Co. (Toronto, ONT). Glycerol, 1-phenyl-3-methyl-2-pyrazolin-5-one and isobutyric acid were purchased from Aldrich (Milwaukee, WI). Ethylene glycol was bought from British Drug House (BDH) (Toronto, ONT). Ultra



pure urea was obtained from Canada Scientific Products (Toronto, ONT). All deuterated solvents for NMR were products of MSD isotopes.

Silica gel TLC plates were obtained from Analtech (Toronto, ONT). Silica gel (35-70 microns) for column chromatography was purchased from Digital Specialty Chemicals (Mississauga, ONT).

### 2.1.3 *Inhibitors*

Methylsuccinic acid, 2-ethyl-2-methylsuccinic acid, 2,2-dimethylsuccinic acid, meso-2,3-dimethylsuccinic acid and  $\beta$ -mercaptoethanol were products of Aldrich Chemical Co. (Milwaukee, WI). Succinic acid, succinamic acid, Pepstatin, pivalic acid, methylguanidine and acetohydroxamic acid were purchased from Sigma Chemical Co. (St. Louis, MO). Ultra pure guanidine was obtained from Schwarz/Mann Chemical Co. (Orangeman, NJ). Butyric acid and propionic acid were purchased from Fisher Scientific Chemical Co. (Toronto, ONT). Formohydroxamic acid and ethylguanidine were synthesized by Richard Pfuetzner (Chan and Pfuetzner, 1993). N,N' bis phenylalanine ethyl ester sulfonamide was synthesized by Mrs J. Kaiser.

### 2.1.4 *Enzymes and substrates*

The affinity purified recombinant HIV-1 protease (EC 3.4.23) was obtained from Bachem (Philadelphia, PA). The HIV-1 protease substrate, acetyl-SQNYPVV-amide and the hydrolytic product, acetyl-SQNY, were custom synthesized by Pharmacia (Toronto, ONT).

A crude preparation of AMV protease (EC 3.4.23) was obtained from the virus by modifying the procedure of Johnson *et al.*, (1983). 500 mg of virus was solubilized in 25 mL of 0.1 M NaCl and extracted with 52.5 mL of chloroform:methanol (2:1) (v/v) mixture. The aqueous and organic phases were separated by centrifugation. The protease was obtained from the aqueous phase by dialyzing against 10 mM  $\beta$ -mercaptoethanol for 4 hrs at 4°C with two changes of buffer. The dialysate was lyophilized overnight and stored at -70° C until required. (Purification was largely carried out by Mrs. J. Kaiser).

Specific activity of the lyophilized enzyme extract was 0.61 U/mg of protein. A unit of activity is defined as nanomoles of TFQAYPLREA hydrolyzed per min per mg of protein. AMV virus was purchased from Life Sciences Inc. (St. Petersburg, FL). The decapeptide substrate, TFQAYPLREA, of AMV protease which spans the cleavage site between reverse transcriptase and integrase in the polyprotein precursor together with the peptapeptide hydrolytic product, TFQAY, were custom synthesized by Multiple Peptide Systems (San Diego, CA).

Porcine carboxypeptidase B (EC 3.4.17.2), bovine carboxypeptidase A (EC 3.4.17.1),  $\alpha$ -chymotrypsin (EC 3.4.21.1), papain (EC 3.4.22.2), thermolysin (EC 3.4.24.4) and their respective substrates Furyl[acryloyl]-Ala-Lys, Furyl[acryloyl]Phe-Phe, Succinyl-Ala-Ala-Pro-Phe-*p*-nitroanilide, Benzoyl-Ala-*p*-nitroanilide and Furyl[acryloyl]Gly-Leu-amide were obtained from Sigma Chemical Co. (St. Louis, MO). Porcine pepsin (EC 3.4.23.1) was also a product of Sigma.

## 2.2 Methods

### *Nomenclature*

E - free enzyme

$E_T$  - total enzyme

S - substrate

i - inhibitor

$V_{max}$  - maximum rate

$K_m$  - Michaelis constant

$K_i$  - dissociation constant of inhibitor

$IC_{50}$  - inhibitor concentration that gives half the control rate

v - control rate in the absence of inhibitor

$v_i$  - rate in the presence of inhibitor

### 2.2.1 *Enzyme assays*

#### 2.2.1.1 *HIV-1 protease*

The method of Darke and co-workers (1988) was modified in assaying the activity of HIV-1 protease. A 50  $\mu$ L reaction volume containing 0.3 mM substrate (acetyl-SQNYPVV-amide), 50 mM MES buffer pH 6.0, 1 mM EDTA, 1 mM DTT, 100 mM NaCl, 20 % glycerol, and 0.8 ng/ $\mu$ L enzyme was incubated at 37°C for 20 min. 5% DMSO was included in assays to facilitate solubility of inhibitors. The assay temperature was maintained constant with the aid of a circulating water bath. Under these conditions, less than 10% of the substrate was utilized. The reaction was quenched by the addition of 75

$\mu\text{L}$  of 12 % acetic acid and 100  $\mu\text{L}$  of the quenched reaction analyzed by reverse phase HPLC. The activity of the enzyme was computed from integrated peaks corresponding to the N-terminal cleavage product, acetyl-SQNY, by interpolating peak areas on a standard curve constructed under identical experimental conditions using highly purified acetyl-SQNY.

Cleavage products were separated on either a Beckman 421 HPLC system or on a Beckman System Gold<sup>TM</sup>. Hydrolytic products were detected by monitoring their elution at a dual wavelength of 205 and 230 nm. The HPLC solvent system consisted of 0.1% TFA in water (solvent A) and acetonitrile (solvent B). To separate cleavage products, 5% acetonitrile was maintained for 10 min followed by a linear gradient of 5 - 30% acetonitrile in 20 min on a C-18 Separon (Fisher) column at a flow rate of 1 mL/min. Under these conditions, the retention times for the cleavage product (acetyl-SQNY) and substrate (acetyl-SQNYPVV-amide) were  $19.5 \pm .5$  and  $28 \pm .5$  min respectively. As previously observed (Darke *et al.*, 1988), the C-terminal cleavage product (PVV-amide) is not detected.

The potencies of inhibitors on the activity of HIV-1 protease were examined by either determining their  $\text{IC}_{50}$  values at a single substrate concentration of 0.3 mM by employing the median-effect method of Chou and Talalay (1981) or via Dixon plots (Dixon, 1952) using three or four different substrate concentrations (0.3 - 1.2 mM). In either case, four or five different concentrations of the inhibitor were assayed.

The concurrent effects of pairs of inhibitors were analyzed by employing Yonetani-Theorell kinetics (Yonetani and Theorell, 1964). Three or four different concentrations of

one inhibitor were assayed at four or five different fixed concentrations of the second inhibitor.

#### 2.2.1.2 *AMV protease*

The activity of AMV protease was routinely assayed by following the modified method of Kotler and co-workers (1989). A 50  $\mu$ L reaction mixture containing 0.5 mM substrate (TFQAYPLREA), 0.1 M sodium citrate pH 5.5, 0.1 M NaCl, 5% DMSO and 0.1 mg/mL of AMV protease (crude preparation) was incubated for 20 min. The assay temperature was maintained at 37°C with the aid of a circulating water bath. To stop the reaction, 75  $\mu$ L of 12% acetic acid containing 0.05M isobutyric acid as an internal standard was added to the reaction mixture. 100  $\mu$ L of the quenched reaction was analyzed by reverse phase HPLC.

HPLC analysis was performed on either a Beckman 421 HPLC system or on a Beckman System Gold™. A linear gradient of 15 - 65% acetonitrile in 20 min at a flow rate of 1 mL/min was used (Solvent system A: 0.1% TFA in water; Solvent system B: acetonitrile). Separation of hydrolytic products was carried out on a C-18 Separon (Fisher) column. The activity of AMV protease was computed from integrated peak areas which corresponded to the N-terminal cleavage product, TFQAY, by interpolating on a standard curve established for highly purified TFQAY under identical conditions of reverse phase HPLC separation. Under these conditions the retention times for the cleavage product, TFQAY, and substrate, TFQAYPLREA were  $10 \pm .5$  and  $18.5 \pm .5$  respectively.

The determination of  $K_i$ s and  $IC_{50}$ s of inhibitors on the activity of AMV protease

were by the methods of Dixon (1952) or Chou and Talalay (1981) respectively. The effect of four or five different concentrations of the inhibitor at three or four fixed concentration of the substrate were (0.5 - 2.0 mM) used in the Dixon plots.

#### 2.2.1.3 *Pepsin*

A modified version of the method of Kotler and co-workers (1989) was followed in assaying the proteolytic activity of pepsin. Reactions were performed in 0.1 M sodium citrate buffer at pH 4.0 containing 100 mM NaCl, 5% DMSO, 0.5 mM substrate (TFQAYPLREA) and 0.1 mg/mL of pepsin. A final reaction volume of 50  $\mu$ L was incubated for 20 min at 37°C. Reactions were terminated by heating in a boiling water bath for 3 min. Quenched reactions were diluted into 75  $\mu$ L of 12% acetic acid and analyzed by reverse phase HPLC.

HPLC analysis were exactly as described for the AMV protease assay (see 2.2.1.2. above).

Dixon plots (Dixon, 1952) were used to determine the dissociation constants of all inhibitors on pepsin. The effect of four or five different concentrations of the inhibitor at three or four fixed concentrations of the substrate were (0.5 - 2.0 mM) used in the determinations.

The interaction constants of pairs of inhibitors were analyzed by the method of Yonetani and Theorell (1964).

#### 2.2.1.4 *Chymotrypsin*

Kinetic assays were performed at 25°C in 0.1 M Tris.HCl pH 7.8, containing 160 mM NaCl, 0.1 mM substrate, Succ-Ala-Ala-Pro-Phe-*p*-nitroanilide (DelMar *et al.*, 1979) and 0.1 µg/mL enzyme. The release of *p*-nitroanilide was monitored continuously at 410 nm in a Gilford spectrophotometer. The effect of pseudosymmetrical sulfonamide inhibitors on chymotrypsin was assessed by determining their IC<sub>50</sub> values by the method of Chou and Talalay (1981).

#### 2.2.1.5 *Papain*

To determine the activity of the enzyme, a reaction mixture containing 100 mM Bis-Tris pH 6.5, 1 mM EDTA, 5 mM DTT, 180 mM NaCl and 0.4 mM substrate, Benzoyl-Ala-*p*-nitroanilide was initiated by the addition of papain to a final concentration of 0.1 µg/mL. The increase in absorbance at 410 nm was followed spectrophotometrically following hydrolysis of the substrate. IC<sub>50</sub>s of inhibitors were determined following the method of Chou and Talalay (1981).

#### 2.2.1.6 *Thermolysin*

The activity of thermolysin was determined spectrophotometrically by monitoring the continuous decrease in absorbance for 5 min at 345 nm following hydrolysis of the substrate, furyl[acryloyl]Gly-Leu-amide (Feder, 1968). The assay was carried out in 0.1M MES pH 6.5, 10 mM CaCl<sub>2</sub> and 100 mM NaCl at 25°C. The potency of inhibitors on thermolysin was ascertained by determining IC<sub>50</sub>s (Chou and Talalay, 1981) under the above-stated experimental conditions.

### 2.2.1.7 *Carboxypeptidase A*

The activity of carboxypeptidase A was measured by monitoring the decrease in absorbance at 335 nm following hydrolysis of the substrate, (N-(3-[2-Furyl]Acryloyl)-Phe-Phe (Peterson *et al.*, 1982) for 2 min in 0.1M Tris.HCl pH 7.5 containing 0.3 M NaCl at 25°C. For the determination of  $K_s$ , (Dixon, 1952; Hunter and Downs, 1945; Chan, 1994) substrate concentration was varied between 0.05 - 0.25 mM. A fixed enzyme concentration of  $5.9 \times 10^{-10}$  M was used in all assays.

### 2.2.1.8 *Carboxypeptidase B*

The activity of carboxypeptidase B was assayed in 100 mM Tris.HCl pH 7.5 containing 0.5 M NaCl and substrate (N-(3-[2-Furyl]Acryloyl)-Ala-Lys) (Plummer and Kimmel, 1980) at 25°C. An enzyme concentration of  $1.17 \times 10^{-8}$  M was used in all assays. The rate of substrate hydrolysis was continuously monitored by following the decrease in absorbance at 345 nm for 2 min in a Gilford (Response) spectrophotometer. The dissociation constants of inhibitors on carboxypeptidase-B were determined by Dixon (Dixon, 1952) or combination plots (Hunter and Downs, 1945; Chan, 1994). The concurrent effect of pairs of inhibitors on this enzyme was examined by either Yonetani-Theorell (1964) plots or by combination plots (see chapter 5, section 5.1.1). The concurrent effect of triplets of inhibitors on carboxypeptidase-B was examined by an extended combination plot (see chapter 4, section 4.1.1.4).



### 2.2.2 Yonetani-Theorell kinetics

This approach which can yield a quantitative measure of the extent and nature of interaction between inhibitors on an enzyme was employed for the analysis of concurrent effect of pairs of inhibitor as indicated above 2.2.1. The plot is based on the following equation:

$$\frac{1}{v_1} = \frac{1}{V_m} + \frac{K_m}{[s]V_m} \left(1 + \frac{[i_2]}{K_{i_2}}\right) + \frac{K_m}{[s]V_m K_{i_1}} \left(1 + \frac{[i_2]}{\alpha K_{i_2}}\right) [i_1]$$

where  $[i_1]$ , and  $[i_2]$  are the concentrations of inhibitor-1 and inhibitor -2 respectively.  $K_{i_1}$  and  $K_{i_2}$  represent inhibition constants for the enzyme-inhibitor complexes  $Ei_1$ ,  $Ei_2$ , and  $\alpha$  is the interaction constant between the inhibitors in the  $Ei_1i_2$  complex. Hence, a plot of  $1/v_1$  against the  $[i_1]$  at fixed different concentrations of  $[i_2]$  yields a family of curves with slopes equivalent to  $K_m(1 + [i_2]/\alpha K_{i_2})/[s]V_m K_{i_1}$ . Since  $[i_2]$  is kept constant for the varying concentrations of  $i_1$ , the point of interception of the resulting family of curves can be extrapolated onto the abscissa to obtain the apparent dissociation constant ( $\alpha K_{i_1}$ ) of the inhibitor plotted on that axis,  $[i_1]$ ; where  $\alpha$  represents the interaction constant for the inhibitors on the enzyme.  $\alpha$  therefore is inversely proportional to the extent of interaction between two inhibitors as it influences the numerical value of  $K_{i_1}$ . Thus, when  $\alpha < 1$ , the inhibitors interact synergistically and when  $\alpha > 1$  the inhibitors are antagonistic. It follows then that  $\alpha$  is unity when the inhibitors bind independent of each other and in the extreme case where the binding of one inhibitor excludes the other,  $\alpha \approx \infty$ . An example of the plot illustrating the synergistic interaction between Cbz-Gln-isoamylamide and Cbz-Ile-phenylalaninol on HIV-1 protease is given in figure 3. Figure 12 shows another example

where the interaction between succinic acid and methylguanidine is presented. The two examples, figures 3 and 12, show cases where a high and low synergistic interaction (respectively) between pairs of inhibitors have been examined.

In certain cases, the point of interception cannot be unequivocally determined from the Yonetani-Theorell plot as previously observed by Pfuetzner and Chan (1988) owing to experimental errors. In such instances, the slopes from the Yonetani-Theorell plot are replotted against the concentration of the second inhibitor to obtain the  $(\alpha K_i)$  value for that inhibitor. The slopes obtained from figure 3 have been replotted in figure 4 against the concentration of the second inhibitor, Cbz-Val-phenylalaninol, to illustrate this point. Final errors in the determination of interaction constants,  $\alpha$ , were products of errors in the determination of either of the inhibition constants ( $K_{i1}$  and  $K_{i2}$ ) and errors associated with either the Yonetani-Theorell or combination plots. Standard errors were determined using the software package, *Enzfitter* (Leatherbarrow, 1987).

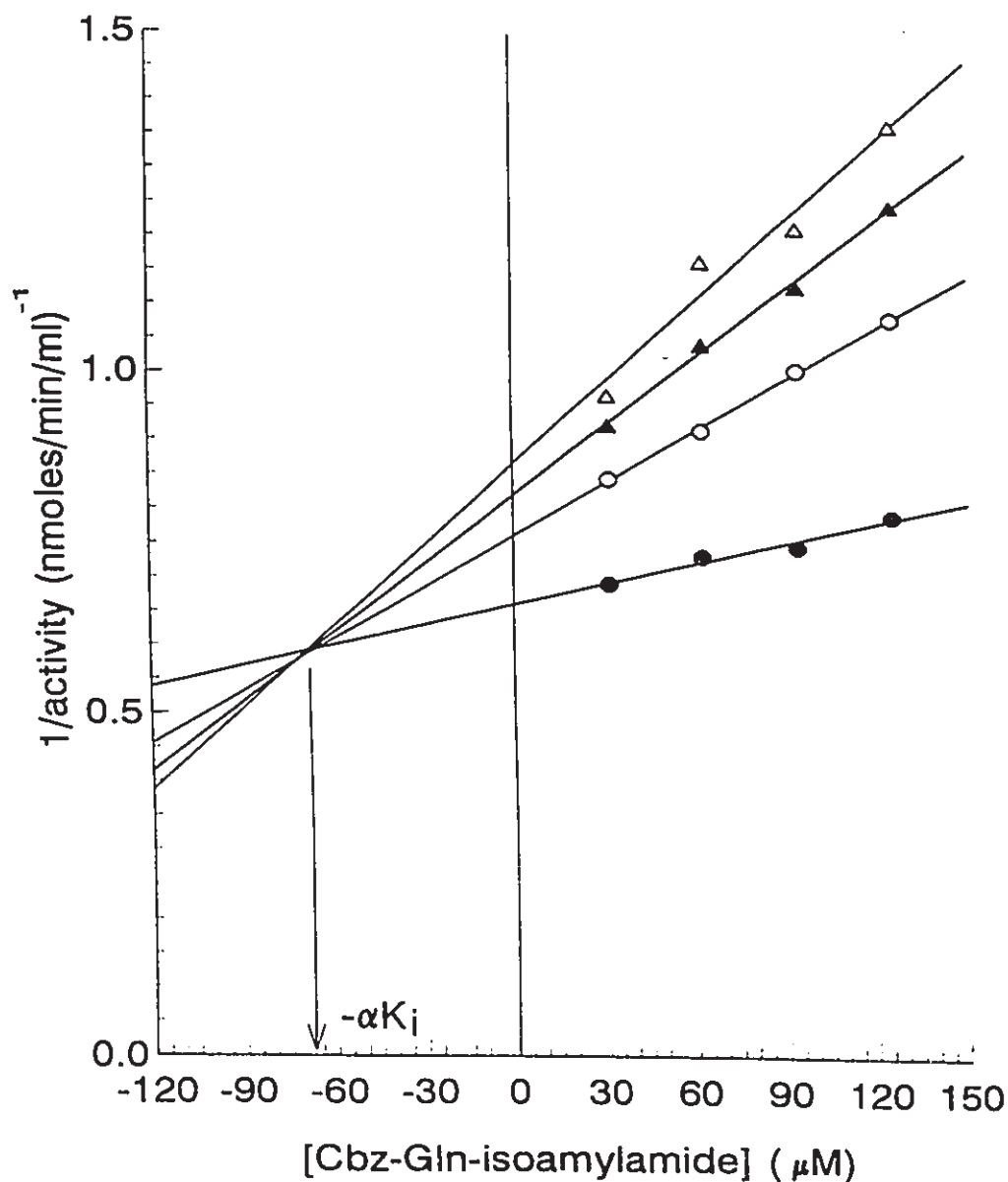


**Figure 3.** Analysis of the inhibition data by the method of Yonetani-Theorell (1964). The reciprocal of enzyme activity is plotted against the concentration of one inhibitor (Cbz-Gln-isoamylamide in this case). The various lines represent different concentrations of the second inhibitor (Cbz-Ile-phenylalaninol): ●, 7.5  $\mu\text{M}$ ; ○, 15  $\mu\text{M}$ ; ▲, 22.5  $\mu\text{M}$ ; and △, 30  $\mu\text{M}$ . Note that the concentration ranges selected for both inhibitors were much lower than the  $K_i$  values (8.9 mM and 0.29 mM) because of the unusually high value of  $1/\alpha$  in this case (125, see Table 4). The synergistic factor ( $1/\alpha$ ) was calculated from the intersection point which corresponds to an inhibitor concentration equal to  $-\alpha K_i$ . For assay conditions, see Materials and methods 2.2.1.

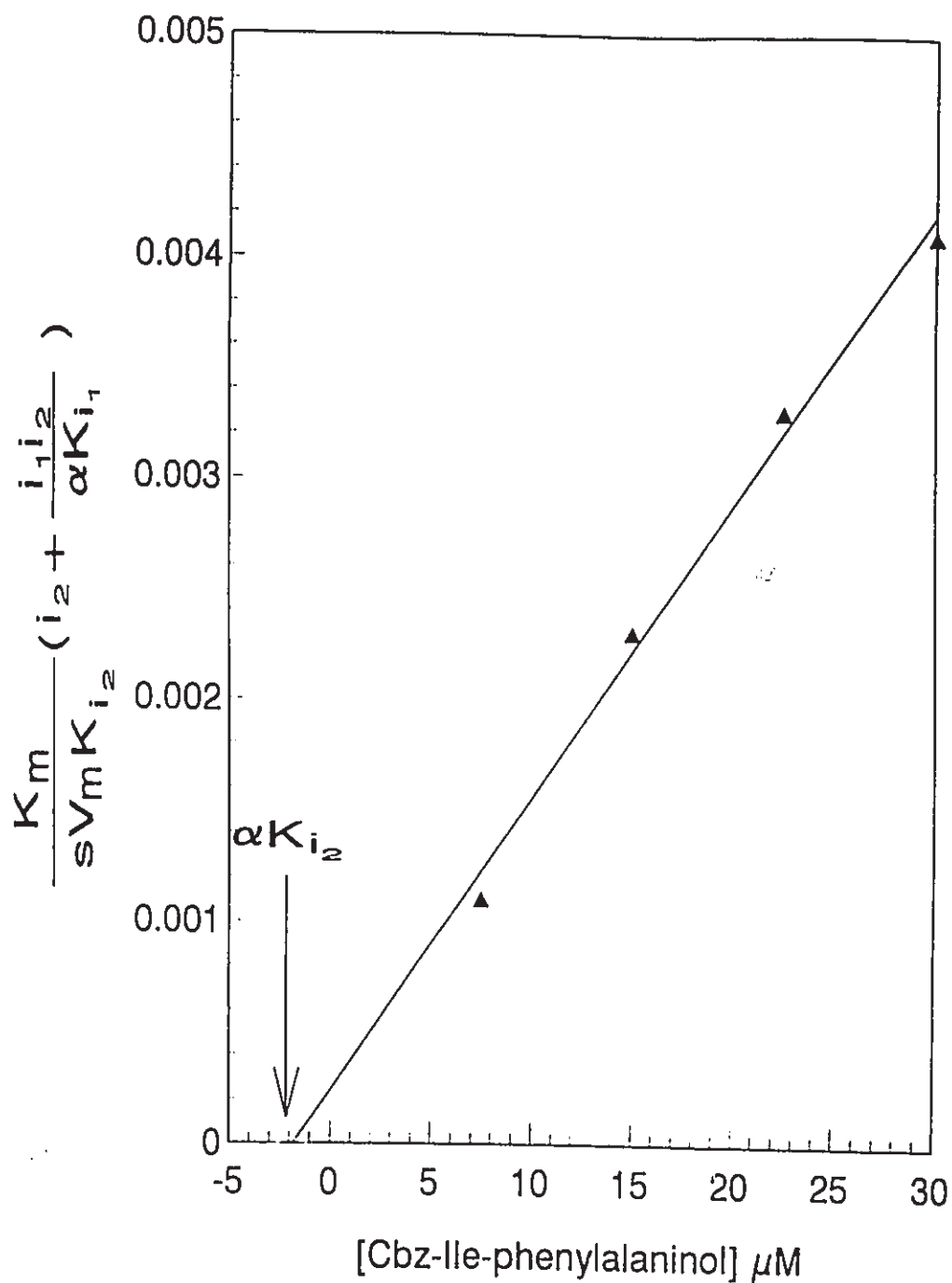


**Figure 4.** A secondary replot of the interaction between Cbz-glutaminyloamylamide and Cbz-isoleucyl-phenylalaninol on HIV-1 protease. Slopes from the Yonetani-Theorell plot (figure 3) are replotted against the concentration of Cbz-isoleucyl-phenylalaninol.

### 2.2.3 Determination of inhibition constants

#### 2.2.3.1. Combination plots.

The dissociation constants ( $K_i$ ) of inhibitors were determined in a 10-point assay via the method of Hunter and Downs (1945), a form of combination plot. Five assays without inhibitor were performed to obtain the  $K_m$  and  $V_{max}$  while another five assays contained inhibitor varied in the same proportion as the concentration of substrate to determine the  $K_i$ . The plot is based on the following equation :

$$[i] \left( \frac{v_i}{v-v_i} \right) = K_i \left( 1 + \frac{[s]}{K_m} \right)$$

For a competitive inhibitor, a plot of  $[i] \cdot (v_i/v-v_i)$  against  $[s]$  gives a straight line with an intercept on the ordinate equivalent to the  $K_i$  of the inhibitor (Figure 5). The intercept on the abscissa represents the  $K_m$  of the substrate under the assay conditions. A line parallel to the abscissa is obtained for a non-competitive inhibitor. Uncompetitive inhibitors give linear plots only when the abscissa is plotted as  $1/[s]$ .

The combination plot of Chan (1994) was also used (Figure 6) for competitive inhibitors. The rationale for this plot is the following equation:

$$[s] \left( \frac{V_m - v_i}{v_i} \right) = k_m \left( 1 + \frac{[i]}{K_i} \right)$$

Hence a plot of  $[s](V_m - v_i/v_i)$  against  $[i]$  gives a straight line with an ordinate intercept equivalent to  $K_m$  and an intercept on the abscissa equivalent to  $K_i$ . The experimental setup was identical to the previous plot.

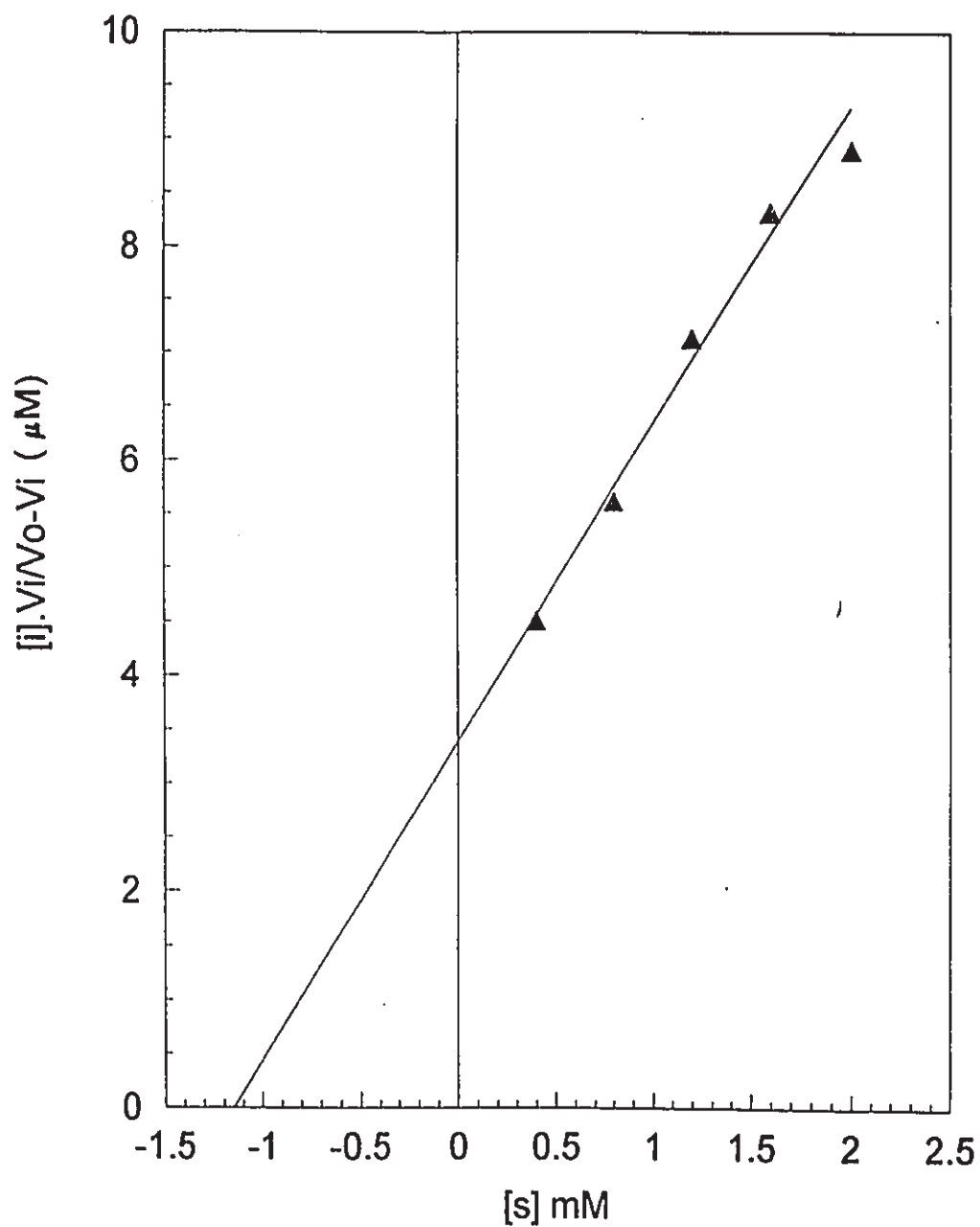


**Figure 5.** Determination of dissociation constant for 2-ethyl-2-methylsuccinic acid on carboxypeptidase B by the method of Hunter and Downs (1945). The intercept on the ordinate gives the  $K_i$  of the inhibitor on carboxypeptidase B under the assay conditions (see 2.2.1.8).

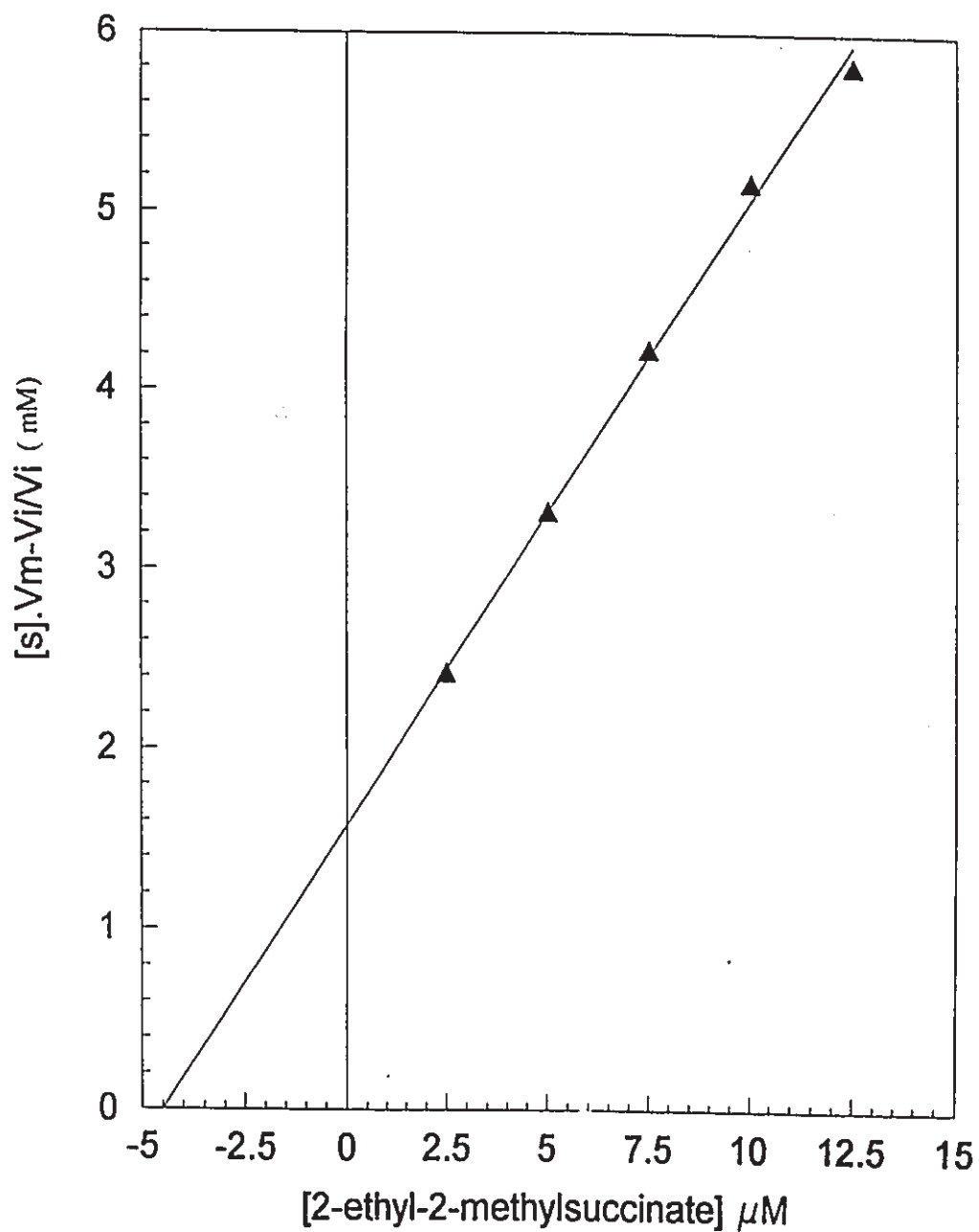


**Figure 6.** An alternative plot for determination of inhibition constants (Chan, 1994). The data from figure 5 is replotted to confirm the competitiveness of the inhibitor. The intercept on the abscissa is equivalent to the  $K_i$  of 2-ethyl-2-methylsuccinic acid on carboxypeptidase B.

### 2.2.3.2 *Dixon plot*

The method of Dixon (1952) was also used for the determination of inhibition constants. Four or five different concentrations of the inhibitor at three or four different fixed concentrations of the appropriate substrate was used. Figure 7 shows a Dixon plot for the determination of the inhibition constant of 2,2-dimethylsuccinic acid on carboxypeptidase B.

The combination plots therefore convert the family of lines that are normally obtained in such kinetic analysis into a single straight line.



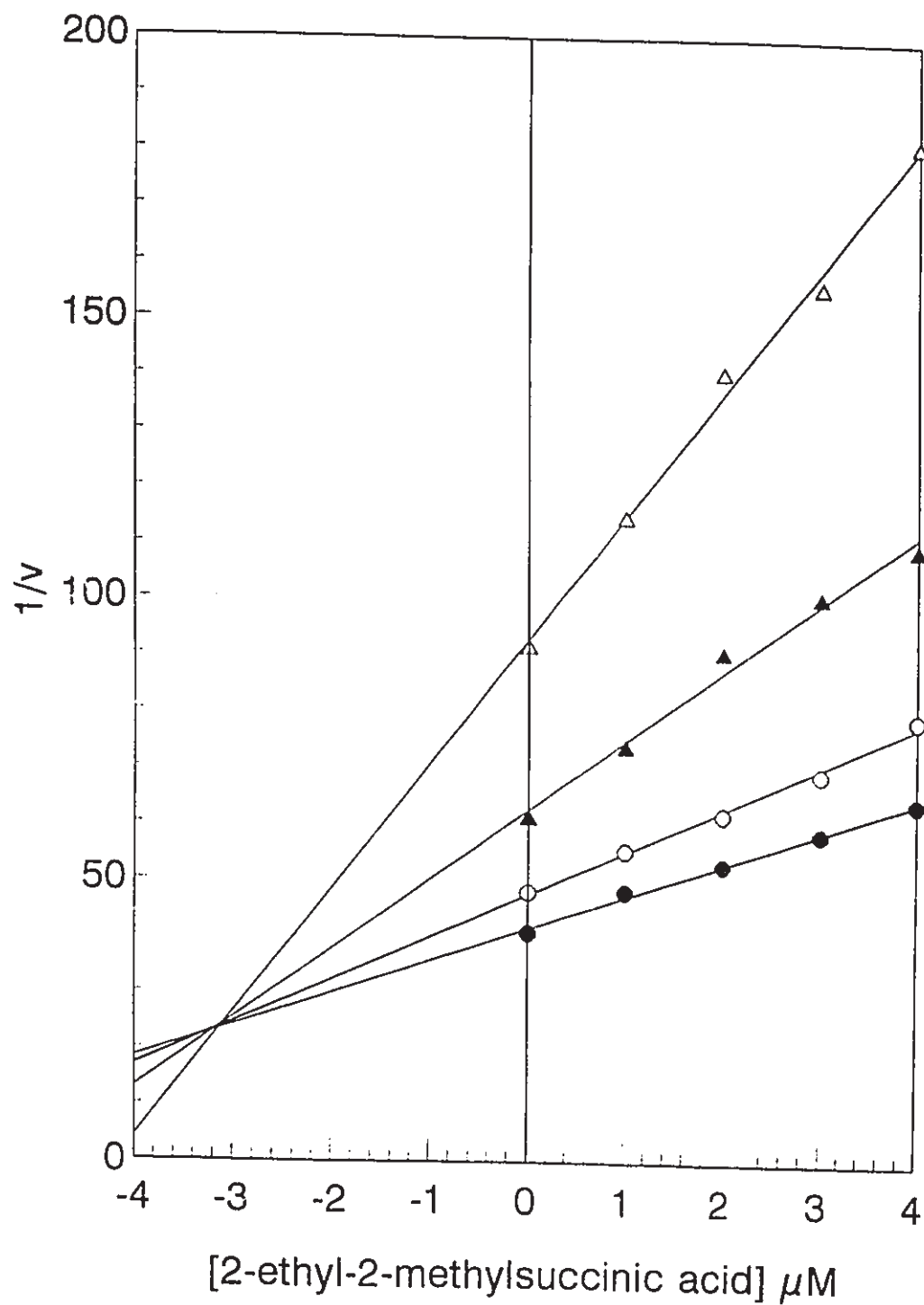


**Figure 7.** Determination of dissociation constant for 2-ethyl-2-methylsuccinic acid on carboxypeptidase B by the method of Dixon (1952).

#### 2.2.4 *TLC detection methods*

##### 2.2.4.1 *Sulfonamide derivatives*

Sulfonamide derivatives were detected by following an established procedure (Stahl, 1969). After separation of reaction products, TLC plates were initially chlorinated with the aid of potassium permanganate and 25% hydrochloric acid. After drying, plates were subsequently sprayed with a 1:1 mixture of 0.2 M 1-phenyl-3-methyl-2-pyrazolin-5-one in pyridine and 1 N aqueous potassium cyanide. Positive spots appeared bright red and subsequently turned purple.

##### 2.2.4.2 *Amino acids*

A ninhydrin detection system was used in detecting the presence of amino acids (Stahl, 1969). The spray reagent consisted of a solution of 0.2 g ninhydrin in 100 mL of isopropyl alcohol to which is added 100  $\mu$ L of 2,4,6-collidine. TLC plates were heated after spraying until full color development.

##### 2.2.4.3 *Organic compounds*

An iodine chamber was generally used to follow synthetic reactions and also detect the presence of organic contaminants in products.

#### 2.2.5 *General synthetic procedures*

##### 2.2.5.1 *Synthesis of N, N' Bis phenylalanine ethyl ester sulphonamide*

0.2 mmole of phenylalanine ethyl ester was dissolved in 4 mL of a mixture of

methylene chloride and pyridine (2.5:1). The reaction temperature was brought to 0°C after which 0.1 mmole of sulfonyl chloride was added dropwise and stirred. After the reaction was complete (as determined by TLC), the products were extracted several times with 12% phosphoric acid. The organic layer was dried over magnesium sulphate, filtered and rotary evaporated. The product was recrystallized from carbon tetrachloride and hexane.  $C_{22}H_{28}N_2O_6S$ . Mol. wt. 448. Melting point 76 - 78°C. (500 MHz,  $CDCl_3$ )  $\delta$  7.92-7.11 (m, 10H, ArH), 4.89 (d,  $J = 9.21$ , 2H, NH), 4.19 (m, 2H, CH), 4.11 (q,  $J = 7.15$ , 4H,  $CH_2$ ), 3.00 (m, 4H,  $CH_2$ ), 1.20 (t,  $J = 7.21$ , 6H,  $CH_3$ ). (Synthesis was carried out by Mrs. J. Kaiser.)

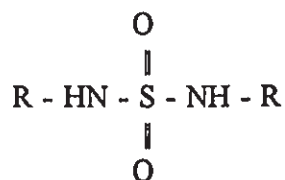
#### 2.2.5.2 Hydrolysis of *N,N'* Bis phenylalanine ethyl ester sulfonamide

0.5 mmole of the above compound was dissolved in ethanol and 20 equivalents of sodium hydroxide added. The resulting solution was stirred overnight. The mixture was subsequently neutralized and then partitioned into ethyl acetate and water. The organic phase was dried over magnesium sulphate, filtered and rotary evaporated. The free acid was triturated under ether. An 85 - 95% yield was normally obtained. The progress of the reaction was followed by monitoring the disappearance of the starting material in an iodine chamber. The presence of a sulfonamide was confirmed by a positive detection method (see 2.2.2.1.). (Product: *N,N'* Bis phenylalanine sulfonamide).

#### 2.2.5.3 General method for coupling of amino acids (Sheehan and Hess, 1955; Konig and Geiger, 1970)

To 0.1 mmole solution of the N-blocked amino acid in a 1:1 (v/v) mixture of ethyl acetate and acetonitrile (4 mL) or dimethylformamide (4 mL) was added 0.1 mmole of the amino acid methyl ester, 0.1 mmole diisopropylethylamine and 0.1 mmole 1-hydroxybenzotriazole. The resulting solution was brought to 0°C and DCC (0.12 mmole) added. After 1 hr at 0°C, the suspension was stirred for an additional 3 hr at room temperature. Dicyclohexylurea was then filtered and the solvent removed *in vacuo*. The residue was dissolved in ethyl acetate and washed in succession with 0.1 M sodium hydrogen carbonate, 0.1 N HCl and three times with water. The organic layer was dried (MgSO<sub>4</sub>), filtered and rotary evaporated. The dipeptide derivative was then recrystallized. The progress of the reaction was monitored by following the disappearance of the free amino acid as detected with ninhydrin (2.2.2.3.). A 65-75% yield of product was normally obtained.

#### 2.2.6 *Synthesis of pseudosymmetric bis-sulfonamides*



The synthesis of sulfonamide derivatives was monitored with the aid of a positive detection system (see 2.2.3.1). A solvent system of 5% methanol, 95% dichloromethane was used for TLC and column chromatography.

### 2.2.6.1 *Synthesis of N, N' Bis phenylalanyl valine methyl ester sulfonamide*

To the hydrolytic product, bis N,N' phenylalanine sulfonamide (see 2.2.4.1.), was coupled valine methyl ester by employing the general coupling method (see 2.2.5.3). The product was recrystallized from ethanol/hexane.  $C_{30}H_{42}N_4O_8S$ . Mol. wt. 618. Melting point 122 - 125°C. (500 MHz,  $CDCl_3$ )  $\delta$  7.29-7.16 (m, 10H, ArH), 6.81 (d, J = 8.58, 2H, NH), 5.17 (d, J = 6.42, 2H, NH), 4.47 (dd, J = 5.51, 5.1, 2H, CH), 4.22 (q, J = 7.17, 2H, CH), 3.71 (s, 6H,  $CH_3$ ), 2.99 (m, 4H,  $CH_2$ ), 2.11 (m, 2H, CH), 0.89 (d, J = 7.27, 6H,  $CH_3$ ), 0.85 (d, J = 6.86, 6H,  $CH_3$ ).  $R_f = 0.54$ .

### 2.2.6.2 *Synthesis of N, N' Bis phenylalanyl isoleucine methyl ester sulfonamide*

The above product was synthesized by coupling isoleucine methyl ester to N,N' phenylalanine sulfonamide via the general coupling method (2.2.5.3). The product was recrystallized from ethanol/hexane.  $C_{32}H_{46}N_4O_8S$ . Mol. wt. 646. Melting point 120-123°C. (500 MHz  $CDCl_3$ )  $\delta$  7.29-7.17 (m, 10H, ArH), 5.16 (d, J = 7.62, 2H, NH), 4.50 (dd, J=5.55, 2.90, 2H, CH), 4.21 (q, J = 7.18, 2H, CH), 3.71 (s, 6H,  $CH_3$ ), 3.00 (d, J = 6.81, 4H,  $CH_2$ ), 1.91 (m, 2H, CH), 1.11 (m, 4H,  $CH_2$ ), 0.89 (t, J = 7.39, 6H,  $CH_3$ ), 0.85 (d, J = 6.85, 6H,  $CH_3$ ).  $R_f = 0.60$ .

### 2.2.6.3 *Synthesis of N, N' Bis phenylalanyl alanine methyl ester sulfonamide*

Synthesis of this compound was achieved by coupling alanine methyl ester to N,N' phenylalanine sulfonamide via the general coupling method (2.2.5.3). An ethanol/hexane mixture was used for recrystallization.  $C_{26}H_{34}N_4O_8S$ . Mol. wt. 562. Melting point 143-

147°C. (500 MHz CDCl<sub>3</sub>) δ 7.30-7.17 (m, 10H, ArH), 6.99 (d, J = 7.6, 2H, NH), 5.39 (d, J = 7.34, 2H, NH), 4.51 (m, 2H, CH), 4.19 (q, J = 6.92, 2H, CH), 3.72 (s, 6H, CH<sub>3</sub>), 3.00 (m, 4H, CH<sub>2</sub>), 1.36 (d, J = 7.27, 6H, CH<sub>3</sub>). R<sub>f</sub> = 0.51.

#### 2.2.6.4 *Synthesis of N, N' Bis phenylalanyl leucine methyl ester sulfonamide*

By coupling N,N' bis phenylalanine sulfonamide to leucine methyl ester using the DCC/HOBT coupling procedure (2.2.5.3) the above compound was synthesized. The product was recrystallized from ethanol/hexane. C<sub>32</sub>H<sub>46</sub>N<sub>4</sub>O<sub>8</sub>S. Mol. wt. 646. Melting point 136-139°C. (500 MHz CDCl<sub>3</sub>) δ 7.30-7.18 (m, 10H, ArH), 7.00 (d, J = 8.25, 2H, NH), 5.43 (d, J = 7.36, 2H, NH), 4.55 (m, 2H, CH), 4.24 (q, J = 7.3, 2H, CH), 3.69 (s, 6H, CH<sub>3</sub>), 3.00 (d, J = 6.81, 4H, CH<sub>2</sub>), 1.58 (m, 2H, CH, CH<sub>2</sub>), 0.91 (t, J = 6.05, 12H, CH<sub>3</sub>). R<sub>f</sub> = 0.58.

#### 2.2.7 *Synthesis of Cbz-aminoacyl-phenylalaninols*

These inhibitors were all synthesized by coupling the appropriate Cbz-amino acid to phenylalaninol or leucinol (2.2.6.6) via the general coupling method discussed above (2.2.5.3). Work up included further purification via column chromatography on silica gel (35-70 microns). In all cases, a solvent system of methanol/dichloromethane (5:95, v/v) served as the mobile phase. The compounds were recrystallized from methanol/water unless otherwise stated. TLC solvent systems **A**: 5% methanol, 95% dichloromethane; **B**: 1% formic acid, 15% ethanol, 84% dichloromethane. Molecular weight determination was via chemical ionization mass spectrometry. The fragmentation pattern were all consistent with

the structures.

#### 2.2.7.1 *Cbz-valyl-phenylalaninol*

$C_{22}H_{28}N_2O_4$ . Mol. wt. 384. Melting point 148-151°C.  $^1H$  NMR (500 MHz,  $CDCl_3$ ),  $\delta$  7.37-7.18 (m, 10H, ArH), 6.14 (d,  $J = 7.82$ , 1H, NH), 5.20 (b, 1H, NH), 5.11 (s, 2H,  $CH_2$ ), 4.18 (m, 1H, CH), 3.90 (dd,  $J = 5.92, 2.32$ , 1H, CH), 3.65 (b, 1H,  $CH_2(a)$ ), 3.57 (b, 1H,  $CH_2(b)$ ), 2.87 (m, 2H  $CH_2$ ), 2.11 (m, 1H, CH), 0.92 (d,  $J = 6.81$ , 3H,  $CH_3$ ), 0.82 (d,  $J = 5.99$ , 3H,  $CH_3$ ). MS  $m/z$  402(4)( $M^+ + 18$ ), 385 ( $M^+ + 1$ )(100), 277(50), 251(15), 108(9), 91(4), 72(4). TLC:  $R_f = 0.43$  in A;  $R_f = 0.60$  in B. HPLC  $t_R = 5.91$  min.

#### 2.2.7.2 *Cbz-isoleucyl-phenylalaninol*

$C_{23}H_{30}N_2O_4$ . Mol. wt. 398. Melting point 155-158°C.  $^1H$  NMR (500 MHz,  $CDCl_3$ ),  $\delta$  7.39-7.17 (m, 10H, ArH), 6.17 (d,  $J = 19.3$ , 1H, NH), 5.18 (b, 1H, NH), 5.11 (s, 2H,  $CH_2$ ), 4.19 (m, 1H, CH), 3.95 (dd,  $J = 6.60, 2.17$ , 1H, CH), 3.64 (m, 2H,  $CH_2$ ), 2.85 (dd,  $J = 7.87, 2H, CH_2$ ), 1.85 (m, 1H, CH), 1.35 (b, 2H,  $CH_2$ ), 0.86 (m, 6H,  $CH_3$ ). MS  $m/z$  416(4) ( $M^+ + 18$ ), 399 ( $M^+ + 1$ )(100), 291(20), 264(14), 108(12), 91(6), 86(5). TLC:  $R_f = 0.42$  in A;  $R_f = 0.88$  in B. HPLC  $t_R = 5.85$  min.

#### 2.2.7.3 *Cbz-leucyl-phenylalaninol*

$C_{23}H_{30}N_2O_4$ . Mol. wt. 398. Melting point 109-112°C.  $^1H$  NMR (200 MHz,  $CDCl_3$ ),  $\delta$  7.37-7.17 (m, 10H, ArH), 6.26 (d,  $J = 7.77$ , 1H, NH), 5.10 (s, 2H,  $CH_2$ ), 4.99 (b, 1H, NH), 4.12 (m, 1H, CH), 3.75 (m, 1H, CH), 3.68 (m, 2H,  $CH_2$ ), 2.84 (d,  $J = 7.31$ , 2H,

CH<sub>2</sub>), 1.65 - 1.59 (m, 3H, CH<sub>2</sub>, CH), 0.90 (d, J = 6.11, 6H, CH<sub>3</sub>). MS m/z 399(50) (M<sup>+</sup> + 1), 381(70), 291(100), 273(48), 247(7), 108(10), 91(6). TLC: R<sub>f</sub> = 0.45 in A; R<sub>f</sub> = 0.75 in B. HPLC t<sub>R</sub> = 5.88 min.

#### 2.2.7.4 *Cbz-glutaminy-phenylalaninol*

C<sub>22</sub>H<sub>27</sub>N<sub>3</sub>O<sub>5</sub>. Mol. wt. 413. Melting point 187-189°C. <sup>1</sup>H NMR (500 MHz, DMSO-D<sub>6</sub>) δ 7.65 (d, J = 8.36, 1H, NH), 7.35 - 7.14 (m, 10H, ArH), 6.71 (δ, 2H, NH), 5.01 (s, 2H, CH<sub>2</sub>), 4.76 (s, 1H, NH), 3.95 - 3.87 (m, 2H, CH), 3.29 (m, 2H, CH<sub>2</sub>), 2.80 (dd, J = 5.85, 5.77, 1H, CH<sub>2</sub>(a)), 2.63 (dd, J = 7.86, 5.74, 1H, CH<sub>2</sub>(b)), 2.06 - 1.98 (m, 2H, CH<sub>2</sub>), 1.79 (m, 1H, CH<sub>2</sub>), 1.65 (m, 1H, CH<sub>2</sub>). MS m/z 414(32) (M<sup>+</sup> + 1), 396(36), 323(6), 306(100), 288(31), 245(6), 172(6), 108(7), 91(6). TLC: R<sub>f</sub> = 0.07 in A; R<sub>f</sub> = 0.33 in B. HPLC t<sub>R</sub> = 5.87 min.

#### 2.2.7.5 *Cbz-asparaginy-phenylalaninol*

C<sub>21</sub>H<sub>25</sub>N<sub>3</sub>O<sub>5</sub>. Mol. wt. 399. Melting point 202-204°C. <sup>1</sup>H NMR (200 MHz, DMSO-D<sub>6</sub>) δ 7.63 (d, J = 8.32, 1H, NH), 7.24 (m, 10H, ArH), 6.89 (δ, 2H, NH), 5.02 (s, 2H, CH<sub>2</sub>), 4.76 (t, J = 5.67, 1H, NH), 4.29 (m, 1H, CH), 3.84 (m, 1H, CH), 2.79 (dd, J = 7.86, 5.59, 1H, CH<sub>2</sub>(a)), 2.63 (dd, J = 7.58, 5.94, 1H, CH<sub>2</sub>(b)), 2.51 - 2.25 (m, 4H, CH<sub>2</sub>). MS m/z 400(100) (M<sup>+</sup> + 1), 309(20), 292(27), 266(52), 152(17), 108(18), 91(6), 87(9). TLC: R<sub>f</sub> = 0.07 in A; R<sub>f</sub> = 0.44 in B. HPLC t<sub>R</sub> = 5.88 min.

#### 2.2.7.6 *Cbz-valyl-leucinol*



This compound was recrystallized from dichloromethane/hexane.  $C_{19}H_{30}N_2O_4$ . Mol. wt. 350. Melting point 117-119°C.  $^1H$  NMR (500 MHz,  $CDCl_3$ )  $\delta$  7.35 - 7.24 (m, 5H, ArH), 5.91 (d,  $J = 8.12$ , 1H, NH), 5.28 (b, 1H, NH), 5.10 (s, 2H,  $CH_2$ ), 4.02 - 4.00 (m, 1H, CH), 3.91 (dd,  $J = 6.23$ , 2.00, 1H, CH), 3.64 (b, 1H,  $CH_2(a)$ ), 3.51 - 3.47 (m, 1H,  $CH_2(b)$ ), 2.15 - 2.11 (m, 2H, CH). 1.70 - 1.56 (m, 3H, CH/ $CH_2$ ), 0.97 - 0.87 (m, 12H,  $CH_3$ ). MS  $m/z$  351(4) ( $M^+ + 1$ ), 243(100), 108(4), 81(4). TLC:  $R_f = 0.35$  in A. HPLC  $t_R = 5.85$  min.

## 2.2.8 Synthesis of isoamylamide derivatives

These inhibitors were synthesized by coupling the appropriate carboxylic acid (Cbz-amino acid or succinamic acid) to isoamylamine by following the general coupling method (see 2.2.4.2). Recrystallization was accomplished with methanol/water unless otherwise stated. TLC solvent systems A: 5% methanol, 95% dichloromethane; B: 1% formic acid, 15% ethanol, 84% dichloromethane.

### 2.2.8.1 Cbz-alanyl-isoamylamide

$C_{16}H_{24}N_2O_3$ . Mol. wt. 292. Melting point 102-104°C.  $^1H$  NMR (500 MHz,  $CDCl_3$ )  $\delta$  7.35 - 7.23 (m, 5H, ArH), 5.86 (b, 1H, NH), 5.22 (b, 1H, NH), 5.09 (s, 2H,  $CH_2$ ), 4.16 - 4.13 (m, 1H, CH), 3.23 (q,  $J = 6.55$ , 2H,  $CH_2$ ), 1.58 - 1.53 (m, 3H, CH/ $CH_2$ ), 1.35 (d,  $J = 7.03$ , 3H,  $CH_3$ ), 0.88 (d,  $J = 6.62$ , 6H,  $CH_3$ ). MS  $m/z$  310(3) ( $M^+ + 18$ ), 293 (100)( $M^+ + 1$ ), 202(33), 185(32), 159(12), 108(7), 81(3). TLC:  $R_f = 0.58$  in A. HPLC  $t_R = 5.85$  min.

#### 2.2.8.2 *Cbz-valyl-isoamylamide*

$C_{18}H_{28}N_2O_3$ . Mol. wt. 320. Melting point 138-141°C.  $^1H$  NMR (200 MHz,  $CDCl_3$ ),  $\delta$  7.37 - 7.30 (m, 5H, ArH), 5.78 (b, 1H, NH), 5.30 (b, 1H, NH), 5.11 (s, 2H,  $CH_2$ ), 3.89 (dd,  $J = 6.34, 2.45$ , 1H, CH), 3.27 (m, 2H,  $CH_2$ ), 2.12 (m, 2H,  $CH_2$ ), 1.60 (m, 1H, CH), 0.92 (m, 12H,  $CH_3$ ). MS  $m/z$  321(100) ( $M^+ + 1$ ), 225(11), 162(7), 108(6), 91(5), 72(4). TLC:  $R_f = 0.61$  in A;  $R_f = 0.82$  in B. HPLC  $t_R = 6.10$  min.

#### 2.2.8.3 *Cbz-isoleucyl-isoamylamide*

$C_{19}H_{30}N_2O_3$ . Mol. wt. 334. Melting point 124-126°C.  $^1H$  NMR (500 MHz,  $CDCl_3$ ),  $\delta$  7.36 - 7.24 (m, 5H, ArH), 5.71 (b, 1H, NH), 5.28 (b, 1H, NH), 5.08 (s, 2H,  $CH_2$ ), 3.90 (dd,  $J = 6.68, 2.08$ , 1H, CH), 3.27 - 3.21 (m, 2H,  $CH_2$ ), 1.85 (b, 1H,  $CH_2$ ), 1.58 - 1.53 (m, 3H, CH/ $CH_2$ ), 1.36 (q,  $J = 7.21$ , 2H,  $CH_2$ ), 0.92 (m, 12H,  $CH_3$ ). MS  $m/z$  335(100) ( $M^+ + 1$ ), 227(14), 201(6), 176(10), 108(8), 91(7), 86(5). TLC:  $R_f = 0.70$  in A;  $R_f = 0.82$  in B. HPLC  $t_R = 6.08$  min.

#### 2.2.8.4 *Cbz-leucyl-isoamylamide*

$C_{19}H_{30}N_2O_3$ . Mol. wt. 334. Melting point 92-93°C.  $^1H$  NMR (200 MHz,  $CDCl_3$ )  $\delta$  7.36 - 7.30 (m, 5H, ArH), 5.94 (b, 1H, NH), 5.15 (b, 1H, NH), 5.10 (s, 2H,  $CH_2$ ), 4.10 (m, 1H, CH), 3.24 (q,  $J = 6.33$ , 2H,  $CH_2$ ), 1.70 - 1.31 (m, 6H, CH/ $CH_2$ ), 0.92 (m, 12H,  $CH_3$ ). MS  $m/z$  335(58) ( $M^+ + 1$ ), 244(11), 227(100), 201(6), 176(5), 108(6), 91(4). TLC:  $R_f = 0.68$  in A;  $R_f = 0.79$  in B. HPLC  $t_R = 6.02$  min.

#### 2.2.8.5 *Cbz-asparaginyloxyisoamylamide*

The compound was recrystallized from acetonitrile.  $C_{17}H_{25}N_3O_4$ . Mol. wt. 335. Melting point 176-179°C.  $^1H$  NMR (200 MHz, DMSO- $D_6$ )  $\delta$  7.76 (b, 1H, NH), 7.35 - 7.30 (m, 5H, Ar), 6.88 (s, 1H, NH), 5.58 (d,  $J = 7.89$ , 1H, NH), 5.02 (s, 2H,  $CH_2$ ), 4.26 (m, 1H, CH), 3.03 (m, 2H,  $CH_2$ ), 2.40 (m, 2H,  $CH_2$ ), 1.54 (m, 1H, CH), 1.25 (m, 2H,  $CH_2$ ), 0.84 (d,  $J = 6.55$ , 6H,  $CH_3$ ). MS  $m/z$  336(100) ( $M^+ + 1$ ), 292(5), 245(19), 228(26), 202(17), 108(8), 91(3), 87(8). TLC:  $R_f = 0.17$  in A;  $R_f = 0.49$  in B. HPLC  $t_R = 6.13$  min.

#### 2.2.8.6 *Cbz-glutaminyloxyisoamylamide*

$C_{18}H_{27}N_3O_4$ . Mol. wt. 349. Melting point 203-205°C.  $^1H$  NMR (500 MHz, DMSO- $D_6$ )  $\delta$  7.76 (t,  $J = 5.55$ , 1H, NH), 7.36 - 7.23 (m, 5H, ArH), 6.71 (s, 1H, NH), 5.01 (s, 2H,  $CH_2$ ), 3.89 (m, 1H, CH), 3.05 (m, 2H,  $CH_2$ ), 2.06 (m, 2H,  $CH_2$ ), 1.81 (m, 1H, CH), 1.68 (m, 1H,  $CH_2$ ), 1.54 (m, 1H,  $CH_2$ ), 1.27 (m, 2H,  $CH_2$ ), 0.85 (d,  $J = 6.61$ , 6H,  $CH_3$ ). MS  $m/z$  350(58) ( $M^+ + 1$ ), 332(3), 289(3), 259(8), 242(100), 224(5), 198(8), 108(5), 91(4). TLC:  $R_f = 0.15$  in A;  $R_f = 0.52$  in B. HPLC  $t_R = 5.92$  min.

#### 2.2.8.7 *Cbz-glycylisoamylamide*

The compound was recrystallized from chloroform/hexane.  $C_{15}H_{22}N_2O_3$ . Mol. wt. 278. Melting point 77-78°C.  $^1H$  NMR (500 MHz,  $CDCl_3$ )  $\delta$  7.38 - 7.30 (m, 5H, ArH), 5.97 (b, 1H, NH), 5.45 (b, 1H, NH), 5.13 (s, 2H,  $CH_2$ ), 3.83 (d,  $J = 5.63$ , 2H,  $CH_2$ ), 3.27 (q,  $J = 6.23$ , 2H,  $CH_2$ ), 1.59 (m, 1H, CH), 1.37 (m, 2H,  $CH_2$ ), 0.90 (d,  $J = 6.61$  Hz, 6H,  $CH_3$ ). MS  $m/z$  557(8) ( $2M^+ + 1$ ), 296(11) ( $M^+ + 18$ ), 279(100) ( $M^+ + 1$ ), 188(14), 171(56),

147(6), 108(4), 91(2). TLC:  $R_f = 0.46$  in A;  $R_f = 0.72$  in B. HPLC  $t_R = 5.98$  min.

#### 2.2.8.8 *Succinamyl-isoamylamide*

The compound was recrystallized from chloroform/methanol/hexane.  $C_9H_{18}N_2O_2$ . Mol. wt. 186. Melting point 187-190°C.  $^1H$  NMR (500 MHz, DMSO-D6),  $\delta$  7.69 (t, 1H, NH), 7.22 (s, 1H, NH), 6.67 (s, 1H, NH), 3.02 (m, 2H,  $CH_2(a)$ ), 2.24 (m, 4H,  $CH_2(b,c)$ ), 1.54 (m, 1H, CH), 1.95 (q,  $J = 7.47$ , 2H,  $CH_2$ ), 0.84 (m, 6H,  $CH_3$ ). MS  $m/z$  187(100) ( $M^+ + 1$ ), 169(19), 100(3). TLC:  $R_f = 0.09$  in A;  $R_f = 0.36$  in B. HPLC  $t_R = 5.21$  min.

#### 2.2.9 Synthesis of other Cbz-amino acyl-alkylamides

These inhibitors were synthesized by coupling the corresponding Cbz-amino acids to the appropriate alkylamines. The DCC/HOBT coupling procedure (see 2.2.5.3) was followed. Column chromatography was used to purify the compounds with methanol/dichloromethane (5:95,  $v/v$ ) as the mobile solvent system. TLC solvent systems A: 5% methanol, 95% dichloromethane; B: 1% formic acid, 15% ethanol, 84% dichloromethane.

##### 2.2.9.1 *Cbz-asparaginy-methylamide*

The compound was recrystallized from acetonitrile.  $C_{13}H_{17}N_3O_4$ . Mol. wt. 279. Melting point 200-205°C.  $^1H$  NMR (500 MHz, DMSO-D6)  $\delta$  7.75 (d,  $J = 4.18$ , 1H, NH), 7.37 - 7.24 (m, 5H, ArH), 6.83 (s, 1H, NH), 5.00 (dd,  $J = 12.60, 6.52$ , 2H,  $CH_2$ ), 4.27 (m, 1H, CH), 2.56 (d,  $J = 4.45$ , 3H,  $CH_3$ ), 2.45 (dd,  $J = 5.25, 9.97$ , 1H,  $CH_2$ ), 2.35 (dd,  $J =$

8.45, 6.76, 1H, CH<sub>2</sub>). MS m/z 280(9)(M<sup>+</sup> + 1), 263(3), 189(28), 172(100), 146(3), 126(4), 108(7), 91(3), 75(5), 60(3). TLC: R<sub>f</sub> = 0.09 in A; R<sub>f</sub> = 0.71 in B. HPLC t<sub>R</sub> = 5.44 min.

#### 2.2.9.2 *Cbz-valyl-phenethylamide*

Recrystallization of this compound was from methanol/water. C<sub>21</sub>H<sub>26</sub>N<sub>2</sub>O<sub>3</sub>. Mol. wt. 354. Melting point 158-160°C. <sup>1</sup>H NMR (500 MHz, CDCl<sub>3</sub>) δ 7.35 - 7.16 (m, 10H, ArH), 5.89 (b, 1H, NH), 5.3, (b, 1H, NH), 5.09 (dd, J = 12.30, 1.94, 2H, CH<sub>2</sub>), 3.87 (dd, J = 6.22, 2.58, 1H, CH), 3.58 (m, 1H, CH<sub>2</sub>), 3.48 (m, 1H, CH<sub>2</sub>), 2.80 (t, J = 6.76, 2H, CH<sub>2</sub>), 2.08 (q, J = 6.57, 1H, CH), 0.90 (d, J = 6.79, 3H, CH<sub>3</sub>), 0.86 (d, J = 6.80, 3H, CH<sub>3</sub>). MS m/z 372(3) (M<sup>+</sup> + 18), 355(100) (M<sup>+</sup> + 1), 311(2), 264(15), 247(96), 225(10), 162(6), 108(9), 104(14), 91(7). TLC: R<sub>f</sub> = 0.67 in A; R<sub>f</sub> = 0.81 in B. HPLC t<sub>R</sub> = 6.10 min.

#### 2.2.9.3 *Cbz-valyl-benzylamide*

The purified compound was recrystallized from methanol/water. C<sub>20</sub>H<sub>24</sub>N<sub>2</sub>O<sub>3</sub>. Mol. wt. 340. Melting point 162-164°C. <sup>1</sup>H NMR (500 MHz, CDCl<sub>3</sub>) δ 7.37 - 7.24 (m, 10H, ArH), 6.15 (s, 1H, NH), 5.30 (d, J = 7.5, 1H, NH), 5.09 (s, 2H, CH<sub>2</sub>), 4.43 (m, 2H, CH<sub>2</sub>), 3.98 (dd, J = 6.30, 2.43, 1H, CH), 2.17 (m, 1H, CH), 0.97 (d, J = 6.79, 3H, CH<sub>3</sub>), 0.92 (d, J = 6.84, 3H, CH<sub>3</sub>). MS m/z 358(9) (M<sup>+</sup> + 18), 341(84) (M<sup>+</sup> + 1), 250(31), 233(100), 207(6), 162(6), 108(15), 91(12). TLC: R<sub>f</sub> = 0.63 in A; R<sub>f</sub> = 0.81 in B. HPLC t<sub>R</sub> = 5.90 min.

#### 2.2.9.4 *Cbz-glutaminy-phenethylamide*

The purified compound was recrystallized from acetonitrile.  $C_{21}H_{25}N_3O_4$ . Mol. wt. 383. Melting point 198-201°C.  $^1H$  NMR (500 MHz, DMSO- $D_6$ )  $\delta$  7.90 (t, 1H, NH), 7.35 - 7.16 (m, 10H, ArH), 6.71 (s, 1H, NH), 5.01 (s, 2H,  $CH_2$ ), 3.90 (m, 1H, CH), 3.15 (t, J = 5.24, 2H,  $CH_2$ ), 2.69 (t, J = 7.38, 2H,  $CH_2$ ), 2.10 (m, 2H,  $CH_2$ ), 1.81 (m, 1H,  $CH_2(a)$ ), 1.67 (m, 1H,  $CH_2(a)$ ). MS m/z 384(29) ( $M^+ + 1$ ), 293(15), 276(100), 232(9), 108(4), 104(10), 91(4). TLC:  $R_f$  = 0.18 in A;  $R_f$  = 0.77 in B. HPLC  $t_R$  = 6.03 min.

Melting points were determined on a Fisher-Johns melting point apparatus and are uncorrected.  $^1H$  NMR spectra were recorded on either a 200 or 500 MHz Bruker spectrometer and are referenced to internal tetramethylsilane. Desorption chemical ionization (DCI) were generated on a VG Analytical ZAB-E double focussing mass spectrometer.

The purity of compounds was assessed by TLC and HPLC. The purity of compounds was >95% as determined by HPLC analysis. HPLC retention times for all compounds were obtained under isocratic conditions with methanol as solvent on a separon C-18 column (Fisher) at a flow rate of 0.5 mL/min. Absorbance at a dual wavelength of 205 nm and 280 nm was read. TLC revealed single spots for all compounds.

### 3. INTERACTIONS OF INHIBITORS WITH ASPARTIC PROTEASES

#### 3.1 RESULTS

##### 3.1.1 Enzyme assays

The initial objective of establishing a dependable and reproducible assay for HIV-1 protease culminated in an HPLC-based non-continuous sampling assay. Development and optimization of HPLC separation methods was achieved by maximizing the resolution of cleavage products through the monitoring of selectivity factors, an indicator of eluent resolution. This was primarily achieved by adjusting flow rates, time of separation and solvent composition including the use of ion-pairing agents.

In establishing a kinetic assay for HIV-1 protease, several cosolvents were also explored in an attempt to improve solubility of hydrophobic peptides and peptide analogues. All solvents investigated showed nonlinear characteristics on the enzyme's proteolytic activity reminiscent of protein denaturation effects. Dimethylsulfoxide (DMSO) was the most effective cosolvent. Under the conditions of the assay which included 5 % (v/v) DMSO, a 30-minute incubation at 37°C resulted in an 8 - 10 % utilization of the substrate; peptide hydrolysis, however, remained linear for at least 80 minutes. In order to compare results obtained under the newly established assay parameters to previously published values, kinetic parameters for HIV-1 protease were determined. The  $K_m$  of  $6.5 \pm .5$  mM and  $V_{max}$  of  $24 \pm 4$  nmoles/min/ $\mu$ g determined were comparable to previously reported values for the same substrate under similar assay conditions (Moore *et al.*, 1989).

### 3.1.2 Sulfonamide Inhibitors of HIV-1 protease.

Owing to the  $C_2$  symmetry of the active site of HIV-1 protease, an attempt was made at synthesizing symmetric sulfonamide peptide analogues as potential inhibitors for the enzyme. Symmetrical inhibitors were generated by replacing the  $P_1$ - $P_1'$  scissile bond with a non-hydrolyzable sulfonamide group to potentially mimic the geometry of the tetrahedral transition-state species during catalysis.

Table I shows the effect of these pseudosymmetrical sulfonamide inhibitors on the activity of HIV-1 and AMV (nonhomogenous preparation) proteases. These inhibitors acted competitively on the enzymes with  $N,N'$  bis phenylalanyl-isoleucyl methyl ester sulfonamide being the most potent with an  $IC_{50}$  of 28  $\mu$ M on HIV-1 protease. Although the potencies of the pseudosymmetrical sulfonamide derivatives were generally low, they appeared to be fairly specific to the retroviral proteases as they showed no detectable affinity towards pepsin. With the exception of  $N,N'$  bis phenylalanyl-isoleucyl methyl ester sulfonamide which showed some detectable inhibitory effect on the thiol protease, papain ( $IC_{50}$  197  $\mu$ M), these compounds were virtually inert to the non-aspartic proteases assessed viz. chymotrypsin, thermolysin and papain.



Table I. Effect of pseudosymmetric sulfonamide inhibitors on HIV-1 and AMV proteases<sup>a</sup>.

Inhibitor	IC <sub>50</sub> , $\mu$ M	
	HIV-1 protease	AMV protease
N,N' bis phenylalanine ethyl ester sulfonamide	>500 <sup>b</sup>	>500 <sup>c</sup>
N,N' bis phenylalanyl-alanine methyl ester sulfonamide	83	>200 <sup>c</sup>
N,N' bis phenylalanyl-valine methyl ester sulfonamide	51	139
N,N' bis phenylalanyl-leucine methyl ester sulfonamide	62	85
N,N' bis phenylalanyl-isoleucine methyl ester sulfonamide	28	77

<sup>a</sup> Assay conditions described under materials and methods (see 2.2.1) were followed. <sup>b</sup>15 % inhibition (% of control) was obtained at this concentration. <sup>c</sup>The enzyme's activity was inhibited to 15 % of the control reaction.

### 3.1.3 Detection of synergism in HIV-1 protease.

#### 3.1.3.1 Design of active site probes.

To investigate structure-activity relationship between inhibitors and HIV-1 protease, the concurrent effects of pairs of inhibitors on the enzyme were examined. Since the approach requires that two inhibitors bind simultaneously within the extended active site of HIV-1 protease, fragments of a known potent symmetrical inhibitor of the enzyme were synthesized. The inhibitor, A74704, originally designed and synthesized by Kempf and co-workers (1990) had been shown to be very potent against the HIV-1 protease with an inhibition constant of 4.5 nM. Furthermore, the X-ray crystal structure of the inhibitor complexed to the enzyme had been solved (Erickson *et al.*, 1990). To obtain active site probes for HIV-1 protease A74704 was conceptually split asymmetrically into two fragments potentially capable of independent and simultaneous inhibition of the enzyme (see Figure 8). As indicated in table II, both the hydroxyl and alkylamide fragments synthesized retain sufficient structural features from the parent compound to competitively inhibit the enzyme as indicated by their independently measured dissociation constants ( $K_i$ ). More interestingly, when both inhibitors were assayed together by the application of Yonetani-Theorell kinetics (Yonetani-Theorell, 1964), the enzyme exhibited synergistic behavior (Table II). Since the influence of one inhibitor on the other is reciprocal, the interaction constant reflects their mutual effect on the enzyme and *vice versa*. The affinity of the inhibitors for the enzyme, as measured by their apparent dissociation constant ( $\alpha K_i$ ), therefore increased by a factor of 10 ( $1/\alpha$ ). The fairly high standard deviations of the

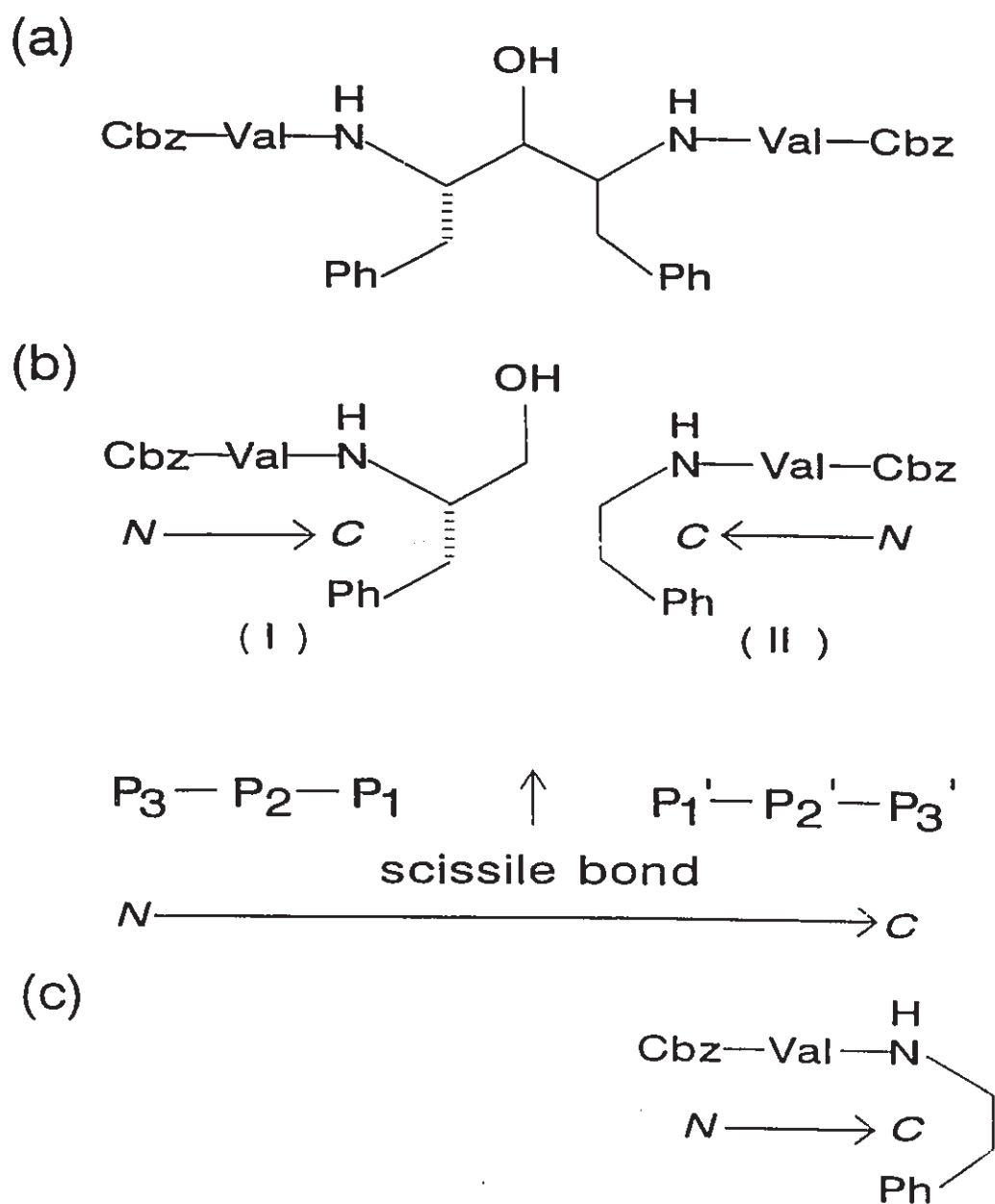


**Figure 8.** Structures of inhibitors and expected binding modes. (a) The symmetrical inhibitor A74704 (Kempf *et al.*, 1990). (b) The hydroxyl fragment (I, Cbz-Val-phenylalaninol) and the alkylamide fragment (II, Cbz-Val-phenethylamide) aligned in the same way as the intact inhibitor above. For comparison, the corresponding positions of the scissile bond and various residues of the substrate are shown below the structures. The direction of the backbone is indicated as  $N - C$ . (c) An alternative binding mode for the alkylamide fragment.

synergistic factors resulted from the propagated errors from the determination of either dissociation constant coupled with errors associated with the Yonetani-Theorell plots.

To understand the synergistic phenomenon, homologues of both the "hydroxyl" ((I) in Figure 8) and "alkylamide" fragments (Figure 8(II)) were synthesized and examined for their ability to interact synergistically with HIV-1 protease (Table II). A reduction of the hydrophobic character of the P<sub>1</sub>' residue to isoamylamide reflected in a reduction in both potency and synergism. The presence of a benzyl moiety at the P<sub>1</sub>' position, resulted in a complete loss of the synergistic effect with the same hydroxyl fragment, Cbz-valyl-phenylalaninol.

The high preference for glutamine by HIV-1 protease at the P<sub>2</sub>' subsite had been noted in the literature (Poorman *et al.*, 1991), the influence of this amino acid on the synergistic phenomenon was therefore assessed. Although, the enzyme displayed a weaker affinity for the glutamine alkylamide derivative (K<sub>i</sub>, 2.3mM) compared to Cbz-Val-phenethylamide (K<sub>i</sub>, 0.07mM), both inhibitors interacted synergistically with Cbz-valyl-phenylalaninol to about the same extent. Unlike the scenario observed for the valine derivative (Table II), substituting an isoamyl group for the phenethyl moiety with glutamine at the P<sub>2</sub>' subsite of the inhibitor led to a ten-fold increase in synergism. It is interesting that the affinity of the enzyme for Cbz-Gln-isoamylamide alone was, however, decreased by a factor of four compared to the phenethyl-containing inhibitor. Thus, flanking groups exerted considerable influence in the observed inhibitor synergism.

Table II. Effects of varying the alkylamide fragment on its synergism with Cbz-Val-phenylalaninol<sup>a</sup>.

Alkylamide fragment	$K_i$ (mM)	Synergistic factor ( $1/\alpha$ )
Cbz-Val-phenethylamide	$0.07 \pm 0.03$	10 $\pm$ 10
Cbz-Val-isoamylamide	$0.20 \pm 0.05$	2.5 $\pm$ 1.2
Cbz-Val-benzylamide	$0.05 \pm 0.02$	1.1 $\pm$ 0.2
Cbz-Gln-phenethylamide	$2.3 \pm 0.6$	7.7 $\pm$ 2.9
Cbz-Gln-isoamylamide	$8.9 \pm 1.2$	71.4 $\pm$ 25

<sup>a</sup>For consistency in comparing synergistic factors, all values were calculated using the  $K_i$  value ( $0.25 \pm 0.01$  mM) for Cbz-Val-phenylalaninol. Assays were carried out as described under materials and methods ( see 2.2.1.).

### 3.1.3.2. Influence of residues at the $P_2'$ subsite on synergism.

To further investigate the role of flanking residues on synergism, the influence of the residue occupying the  $P_2'$  subsite was examined (Table III). Cbz-Val-phenylalaninol was similarly maintained as the hydroxyl inhibitor. The choice of amino acids was based on their frequency of occurrence in the natural *gag* and *gag-pol* polyprotein precursors (Figure 1; Debouck, 1992). Furthermore, to negate a direct electrostatic effect on the observed phenomenon, amino acids without ionizable side chains were preferentially selected. The isoamylamide group which tended to give the highest synergism (Table II) was maintained at the  $P_1'$  position of the next series of alkylamide inhibitors. As shown in table III, the presence of asparagine at the  $P_2'$  subsite resulted in synergism with a twenty-fold enhancement of affinity with the resident Cbz-Val-phenylalaninol. A glycine residue at the same position completely abolished synergism revealing the importance of side chains at the subsite in eliciting synergism. Increasing the hydrophobic character of the side chain with leucine resulted in only a two-fold improvement in binding affinity ( $1/\alpha = 2.5$ ) of both inhibitors, although the inhibitor's sole affinity for the enzyme increased ( $K_i$ , 0.15 mM). Substituting isoleucine for leucine reduced the dissociation constant of the inhibitor and proportionately improved synergism. Thus, the interaction appeared to be specific differentiating between the two isomers. Succinamyl isoamylamide which lacked the Cbz group but maintained the side chain of the asparagine derivative interacted synergistically with Cbz-Val-phenylalaninol yielding a synergistic factor of 4.8 indicating that the occupation of the  $P_3'$  was not critical under those settings. Cbz-glutaminy-isoamylamide thus gave the highest synergism with Cbz-Val-phenylalaninol (Table II) and reflected the

Table III. Effects of the putative P<sub>2</sub>' residue in the alkylamide fragment on its synergism with Cbz-Val-phenylalaninol<sup>a</sup>.

Alkylamide fragment	K <sub>i</sub> (mM)	Synergistic factor (1/α)
Cbz-Asn-isoamylamide	2.3 ± 0.8	20 ± 4
Cbz-Gly-isoamylamide	4.2 ± 1	0.8 ± 0.2
Cbz-Leu-isoamylamide	0.15 ± 0.06	2.5 ± 1.2
Cbz-Ile-isoamylamide	0.05 ± 0.02	7.7 ± 2.9
Succinamyl-isoamylamide	4.1 ± 0.6	4.8 ± 0.7

<sup>a</sup> Experimental conditions were as described under materials and methods (2.2.1).

known preference of the enzyme for substrates containing glutamine at the  $P_2'$  position (Poorman *et al.*, 1991).

### 3.1.3.3 *Effect of residues at the $P_2$ subsite.*

In view of the symmetrical nature of the active site of HIV-1 protease, it was of interest to investigate whether amino acid preference at the  $P_2$  subsite would reflect those observed at the  $P_2'$  subsite. In these experiments, Cbz-glutaminy-isoamylamide, the alkylamide which gave the highest synergism (section 3.1.3.2) served as the inhibitor probe (Table IV). Substituting for valine with isoleucine did not significantly alter the independent potencies of the inhibitors but increased the observed synergism. The observed synergistic factor of 125 between Cbz-isoleucyl-phenylalaninol and Cbz-glutaminy-isoamylamide was the highest synergism observed in these studies. With leucine replacing isoleucine, a ten-fold drop in synergism resulted similarly implicating specific interactions. Having glutamine in a pseudosymmetrical setting to complement the dyad active site did not elicit a higher inhibitor synergism. An asparagine residue at the  $P_2$  subsite even failed to yield a higher synergistic response compared to the glutamine derivative. This result was unexpected owing to the high preponderance of asparagine residues at this subsite in natural substrates (Figure 2; Debouck, 1992). However, modelling studies by Griffiths and co-workers (1993) suggest asparagine is preferred only when proline occurs at the  $P_1'$  subsite and might account for the lower synergism. The much higher synergistic effects observed for the  $\beta$ -branched amino acids was consistent with known preferences for these residues at this position in substrates (Poorman *et al.*, 1991).



Table IV. Effects of varying the P<sub>2</sub> residue in the hydroxyl fragment on its synergism with Cbz-Gln-isoamylamide<sup>a</sup>.

Hydroxyl fragment	K <sub>i</sub> (mM)	Synergistic factor (1/α)
Cbz-Val-phenylalaninol	0.25 ± 0.01	71.4 ± 25
Cbz-Ile-phenylalaninol	0.29 ± 0.08	125 ± 16
Cbz-Leu-phenylalaninol	0.4 ± 0.2	14.3 ± 4.1
Cbz-Gln-phenylalaninol	0.6 ± 0.6	11.1 ± 2.5
Cbz-Asn-phenylalaninol	0.6 ± 0.1	7.7 ± 1.8

<sup>a</sup> For consistency in comparing synergistic factors, all values were calculated using the K<sub>i</sub> value for Cbz-Gln-isoamylamide (8.9 mM). Other experimental conditions were the same as described under materials and methods (see 2.2.1.).

### 3.1.4 Inhibitor synergism in Pepsin.

#### 3.1.4.1 *Design of active site probes.*

To confirm the generality of inhibitor binding synergism in aspartic proteases the phenomenon was investigated in pepsin. To design two inhibitors which potentially could bind simultaneously to different regions of porcine pepsin's active site, a strategy analogous to that which had previously been employed for the design of probes for HIV-1 protease was used. The structures of several potent inhibitors of pepsin were carefully examined with the effort culminating in the synthesis of two modified fragments derived from the potent pepstatin derivative, Iva-Val-Sta-(3S,4S)-Ala-Isoamylamide ( $K_i = 1.1$  nM) (Rich and Sun, 1980), as illustrated in figure 9. Reflecting on the role of the statine residue in the inhibitor, leucinol was used at the  $P_1$  position of inhibitor(I), the hydroxyl fragment (Figure 9(b)). Leucinol was used rather than statine to prevent possible steric hindrance from the  $P_1'$  residue of the alkylamide fragments and also to eliminate the negatively charged carboxylate moiety from the active site of the aspartic protease. Cbz was substituted for the isovaleryl (Iva) group since it had been reported that this change results in a more potent inhibitor for pepsin (Aoyagi *et al.*, 1972).

Inhibitor (II), the alkylamide fragment, was synthesized by modifying the C-terminal dipeptide of the pepstatin derivative as illustrated in figure 9(b(ii)). To negate the positive charge and improve binding, the dipeptide was N-blocked with a Cbz group in view of pepsin's preference for aromatic moieties at this position (Fruton, 1987).

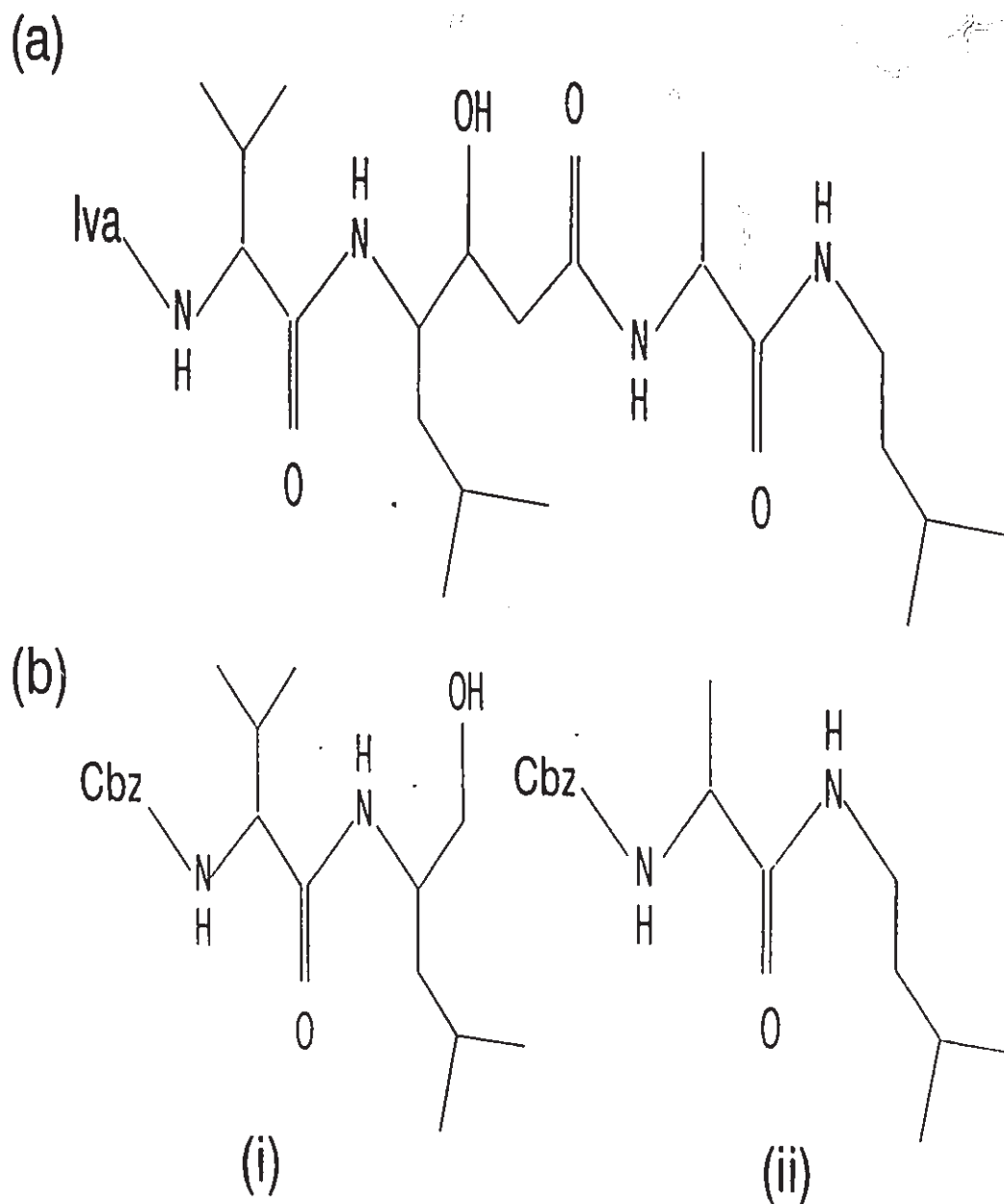


**Figure 9.** Alignment of the N and C-terminal derived fragments and the parent compound. (a) Structure of Iva-Val-Sta-Ala-Isoamylamide (Rich and Sun, 1980). (b)(i) Modified N-terminal fragment, Cbz-Val-leucinol. (ii) Modified C-terminal fragment, Cbz-Ala-Isoamylamide. Basis for modifying the derived fragments is explained in text.

Table V. Concurrent effects of Cbz-Val-leucinol and second inhibitor on porcine pepsin<sup>a</sup>.

second inhibitor	$K_i$ (mM)	synergistic factor ( $1/\alpha$ )
Cbz-Ala-isoamylamide	$3 \pm 0.4$	$2.3 \pm 0.5$
Cbz-Ile-isoamylamide	$0.4 \pm 0.1$	$3.8 \pm 0.8$
Cbz-Asn-isoamylamide	$4 \pm 0.4$	$4.8 \pm 1.4$

<sup>a</sup> Experimental conditions were as described under materials and methods.  $K_i$  for Cbz-Val-leucinol is  $0.15 \pm 0.03$ .

As shown in table V, the two inhibitors acted synergistically on the enzyme with a synergistic factor of 2.3. Substituting the P<sub>2</sub>' residue with either a more hydrophilic asparagine or a hydrophobic isoleucine had very little effect on the observed synergism .

#### 3.4.2 *Effect of Urea.*

In an attempt to explore the origins of inhibitor synergism, the influence of a sub-critical concentration of urea on the ability of Cbz-Ala-isoamylamide and Cbz-Val-leucinol to elicit the phenomenon was investigated. Inhibitor synergism is postulated to reflect a substrate-induced conformational change (Chan and Pfuetzner, 1993) thus the influence of a denaturant such as urea on the phenomenon should be revealing. A urea concentration of 0.5M which resulted in a 25% reduction in the activity of pepsin was employed for this analysis. The choice of concentration was based on several considerations. At this concentration, the dissociation constants for both inhibitors were similar to control values. Thus, although a 25% loss in enzyme activity occurred, the enzyme clearly maintained affinity for the inhibitors. This concentration of urea also had no effect on the inhibitory potency of pepstatin on pepsin. From a technical stand point, 0.5M urea reduced the enzyme's activity to a significant enough level at which cleavage products resulting from further inhibition (as a result of a enhanced synergism) could still be conveniently detected on the HPLC-based assay without modifications to the assay conditions. This therefore avoided the unnecessary introduction of additional variables into the pre-optimised experimental set-up. The synergistic effect of inhibitor binding was completely abolished in 0.5M urea with a synergistic factor of  $0.91 \pm 0.2$  determined for the interaction between

Cbz-Ala-isoamylamide and Cbz-Val-leucinol.

#### 3.1.4.3 *Effect of ethylene glycol.*

A brief study was initiated to explore the probable cause of the observed elimination of synergism in urea by re-assessing the concurrent effect of the same inhibitors in ethylene glycol, a perturbant which presumably stabilizes protein structure (Simpson and Kauzmann, 1953; von Hickel and Wong, 1965; Herskovitz and Laskowski, 1962). A concentration of ethylene glycol (5%, v/v) which also resulted in a 25% reduction in enzyme activity was used. Rather like in urea, the affinity of the enzyme for the inhibitors was essentially preserved under these conditions. In contrast to urea, however, the synergistic interaction between Cbz-Ala-isoamylamide and Cbz-Val-leucinol on pepsin was not abolished in ethylene glycol (5 %, v/v). A synergistic factor of  $3 \pm .5$  not significantly different from the control value of  $2.3 \pm .5$  was obtained.

## 3.2 DISCUSSION

### 3.2.1 Sulfonamide inhibitors

In view of the  $C_2$  symmetry of HIV-1 protease (Wlodawer *et al.*, 1989), pseudosymmetric inhibitors incorporating a nonhydrolyzable sulfonamide scissile bond surrogate, were designed to complement the dyad symmetry of the active site. Although fairly weak inhibitors, these pseudosymmetric inhibitors were pure competitive inhibitors of the enzyme and displayed some affinity for the symmetric retroviral proteases. Assayed against pepsin, a comparatively nonsymmetric aspartic protease, no detectable inhibition was observed for the pseudosymmetric inhibitors. This apparent specificity of the sulfonamide inhibitors was indicated by their undetectable effect on non-aspartic proteases chymotrypsin, thermolysin and papain assayed as representative members of the other three protease classes. Because of the generally hydrophobic nature of the inhibitors, the choice of enzymes was biased towards proteases with specificity for hydrophobic amino acids.

While this work was in progress, Kempf and co-workers (1990) reported the synthesis of highly specific symmetric diaminodiols and pseudosymmetric diaminoalcohols for HIV-1 protease based on a similar strategy. These inhibitors were, however, considerably more potent than the sulfonamides reported here with  $IC_{50}$ s in the nM range. The lower affinity of the sulfonamide inhibitors for the HIV-1 protease may be attributed to their comparatively smaller size among others. The sulfonamides were designed to occupy  $S_2$  through  $S_2'$  while the diaminodiols and diaminoalcohols additionally interacted with  $S_3$  and  $S_3'$  (Erickson *et al.*, 1990). The extra binding energy derived from interactions within the two extra binding sites contributed greatly to their enhanced potency since

smaller inhibitors occupying S<sub>2</sub> through S<sub>2</sub>' showed a thousand-fold weaker affinity (Kempf *et al.*, 1990). Furthermore, the presence of a hydroxyl group in scissile bond replacements (Dreyer *et al.*, 1989; McQuade *et al.*, 1990; Tomasselli *et al.*, 1990; Richards *et al.*, 1989) has been observed to greatly increase inhibitor potency through X-ray crystallographic studies (Jaskolski *et al.*, 1990; Fitzgerald *et al.*, 1990). The sulfonamides are, however, comparable in potency to some reduced amide inhibitors which also lack hydroxyl groups within the scissile bond replacement (Tomasselli *et al.*, 1990; Billich *et al.*, 1988; Moore *et al.*, 1989).

### 3.2.2 Inhibitor binding synergism in HIV-1 protease

A further investigation of the nature of ligand interactions at the active site of HIV-1 protease was pursued by examining inhibitor binding synergism. This approach at structure-activity relationships was pursued after it became clear that the limited resources available to me could not ensure a direct competition against the big pharmaceutical companies. Inhibitors synthesized for this work were rather small and involved modest synthetic protocols thus reducing time-consuming organic synthesis to a minimum. Furthermore, since inhibitors were mixed and matched in the experimental design, the approach was more efficient (Tables II-V). Additionally, because HIV-1 protease generally exhibits specificity towards hydrophobic groups, the synthesis of fragments of a bulky inhibitor circumvented potential solubility problems. Even with this approach, limited solubility in certain cases prevented the analysis of more hydrophobic inhibitors owing to their lower affinities; this in spite of the inclusion of 5 % (v/v) DMSO in assay buffers.



As evident from the results, two mutually non-exclusive inhibitors possessing enough structural characteristics recognizable by HIV-1 protease can interact synergistically increasing their individual affinity for the enzyme. The subsite preferences of inhibitors reflected known specificities of residues in substrates of the enzymes. The binding of the derived fragments cannot, however, be unequivocally established and must be taken into consideration as illustrated in figure 8. On account of the identical alignment of the hydroxyl fragment to the N-terminal portion of a typical substrate of the enzyme, this fragment can be presumed to bind in a fashion identical to the parent fragment as revealed by X-ray crystallography (Erickson *et al.*, 1990). Furthermore, X-ray crystallographic analysis of hydroxyl-containing inhibitors complexed to HIV-1 protease all show similar modes of binding with the hydroxyl group positioned between the essential aspartic acid residues (Jaskolski *et al.*, 1990; Fitzgerald *et al.*, 1990; Erickson *et al.*, 1990; Bone *et al.*, 1991). Because the direction of the peptide bond in the alkylamide fragment is reversed compared to a normal substrate, two possible binding modes can be envisaged. On the one hand, binding could occur analogously to the parent compound (structure II, figure 8(b)). It is also conceivable that the normal N to C direction of the peptide bond is maintained upon binding as illustrated in figure 8(c).

The observed synergistic phenomenon apparently stems from a subtle interaction between separate or overlapping subsites within the active site. For instance, although Cbz-Val-isoamylamide interacted less synergistically with Cbz-Val-phenylalaninol compared to Cbz-Val-phenethylamide, the converse was true when glutamine serves as the putative P<sub>2</sub>' residue in the corresponding alkylamide homologues. The high synergistic effects observed

for glutamine and the  $\beta$ -branched amino acids at the  $P_2'$  and  $P_2$  subsites, respectively, reflect the known preference for these amino acids in natural substrates (Jupp *et al.*, 1990; Konvalinka *et al.*, 1990; Poorman *et al.*, 1992) and thus suggests a potential role for the phenomenon in catalysis. That subsite interaction plays a role in catalysis is also indicated by the abolition of the phenomenon when glycine was used at the  $P_2'$  position. The inability of the protease to cleave its peptide substrate with glycine at the  $P_2'$  position has also been noted previously (Konvalinka *et al.*, 1990).

The significance of the synergistic effects observed devolves into a question of whether the phenomenon is a result of a direct interaction between the inhibitors or an indirect effect on the inhibitors communicated through the enzyme. To account for a direct interaction between inhibitors, it can be postulated that the binding of the first inhibitor excludes some water molecules from the active site and thereby facilitate the binding of the second inhibitor. This interpretation stresses on the exclusion of water molecules from the active site upon inhibitor binding which is known to occur in HIV-1 protease (Miller *et al.*, 1989); and hinges on the preferentially partitioning of inhibitors into the hydrophobic active site with a possible enhancement of affinity from restraints on rotational and translational motions of bound inhibitors (Jencks, 1975). Such a mechanism would, however, be rather non-specific as opposed to the effects observed in this study. That, in certain cases, higher synergistic effects are even observed for the more hydrophilic inhibitors is not consistent with such an interpretation (Tables II & III).

The results appear to implicate the involvement of highly specific interactions that can be only orchestrated by the enzyme. The observed correlation between synergism and

substrate specificity argues strongly in favor of a prominent role for the enzyme in the manifestation of the phenomenon. That different affinities are displayed by the enzyme towards the same inhibitor suggests the conformation of the protein probably changes in the absence of a strictly direct interaction between the inhibitors. The involvement of conformational changes to HIV-1 protease upon ligand binding has previously been observed in the crystal structures of several enzyme-inhibitor complexes (Jaskolski *et al.*, 1990; Fitzgerald *et al.*, 1990; Swain *et al.*, 1990; Erickson *et al.*, 1990; Miller *et al.*, 1989; Bone *et al.*, 1991; Dreyer *et al.*, 1993; Lam *et al.*, 1994). Minimally, a mechanism involving a single conformational change could account for the enhanced affinities observed in inhibitor binding synergism. Binding of the first inhibitor can be postulated to induce a conformational change in the enzyme which then displays an enhanced affinity for the second inhibitor. Such a mechanism has previously been postulated by Chan and Pfuetzner (1993) to account for similar synergistic effects in zinc proteases.

Thus, HIV-1 protease might be postulated to undergo a substrate-induced conformational change during its normal catalytic process. Several subsites could act in concert to influence catalysis in this enzyme analogously to the enhanced binding of the inhibitors. The xerophilic-shift mechanism (Chan and Pfuetzner, 1993) which has been postulated to generally account for the potential role of synergism in catalysis may therefore operate in the enzyme. The authors postulate that an enzyme initially recognizes a key specificity-determining feature of the substrate. Binding of the substrate then induces a conformational change in the enzyme which consequently increases its affinity towards the soon-to-be departing portion of the substrate. Subsequently, when water is excluded from

the active site, a shift in pK of an essential ionizable residue at the active site is postulated to occur which converts the enzyme into the catalytically competent form. The enzyme then reacts with an increased rate towards the substrate.

On the basis of similarities between the catalytic mechanism of aspartic and zinc proteases (James and Sielecki, 1985; Polgar, 1990; Christianson and Lipscomb, 1989), a similar mechanism based on such a substrate-induced conformational change may be invoked for HIV-1 protease to account for the correlation between synergism and substrate specificity. Catalysis in this enzyme may therefore be influenced by subtle subsite interactions as has also been noted by other investigators (Cameron *et al.*, 1993; Griffiths *et al.*, 1992) with the aid of peptide substrates. It is conceivable that subsite interactions via synergism contribute to the choice of substrates and could account to some extent for the lack of a strict primary amino acid sequence dependency (Dunn and Kay, 1992).

These results challenge the notion that subsites are independent and non-interacting within this enzyme. Epps and co-workers (1990) have also reported the lack of independence among subsites in another aspartyl protease, renin. Those results also argue against a direct interaction between inhibitors as being primarily responsible for the observed effects. The non-additivity in the binding of inhibitors to renin was, however, determined through thermodynamic methods thus correlation between the observed effect and catalysis was not directly evident.

### **3.2.3 Inhibitor binding synergism in pepsin**

To establish the generality of inhibitor synergism in aspartic proteases, the

phenomenon was investigated in pepsin, the archetype of this class of enzymes. The phenomenon certainly can be observed in pepsin and thus adds to the mounting evidence that substrate-induced conformational change might represent a general mechanism in enzyme catalysis (Chan and Pfuetzner, 1993). Although not extensively investigated, it is interesting that altering the P<sub>2</sub>' residue did not markedly influence the observed synergism in stark contrast to the situation observed for HIV-1 protease. Presumably, this reflects the stricter emphasis pepsin places on the P<sub>1</sub> and P<sub>1</sub>' residues in the choice of substrates compared to the retroviral HIV-1 protease which appears to rely on the concerted interaction of several residues (Cameron *et al.*, 1993; this study).

It is interesting that while inhibitor binding synergism in pepsin was abolished in the presence of urea, it was preserved in ethylene glycol. Although both perturbants influence protein structure through different mechanisms (Simpson and Kauzmann, 1953; von Hückel and Wong, 1965; Herskovitz and Laskowski, 1962), clearly, there exist different structural requirements for independent inhibitor binding and inhibitor synergism in pepsin. The results indicate that under certain conditions the synergistic effects of inhibitors can be uncoupled from independent binding to the enzyme. Chan and Pfuetzner (1993) have postulated that synergism is a manifestation of a substrate-induced conformational change employed by enzymes to enhance their catalytic rates in a predominantly aqueous environment. Such approaches may therefore be useful in testing the basic tenet of the hypothesis: the enzyme's need to undergo the necessary conformational change(s) which normally accompanies its synergistic inhibition.

### 3.2.4 Significance and potential applications

The significance of this work is that it describes, for the first time, multi-inhibitor interactions in aspartic proteases. The phenomenon was observed in both subgroups of this class; HIV-1 protease representing the homodimeric retroviral enzymes and pepsin a member of the monomeric cellular enzymes. The current evidence does not appear to support a mechanism involving a direct interaction between inhibitors. The phenomenon rather appears to be manifested through a conformational change in the protein. The work further sheds some light on the complex substrate specificity of HIV-1 protease. With respect to rational drug design, this work impacts and cautions on the dogmatic adherence to strict subsite preferences in the optimization of drug potency ie. combinatorial synthesis and stresses on the importance of maintaining a balance between individual subsite preferences and a possible interaction between subsites.

Taking cognisance of the entropic advantage for an enzyme to interact with a single molecule (Jencks, 1981), the pharmacological application of two synergistic fragments of a bulky drug does not appear to be very promising. However, in certain (perhaps limited) cases, it is conceivable that the use of two fragments may circumvent such problems as low solubility, low bioavailability and possibly high resistance to the parent drug, especially if the derivatives of the fragments can be mixed and matched to the same desired effect.

The identification of inhibitor binding synergism in HIV-1 protease suggests the application of synergism-assisted inactivation as a potential therapeutic strategy. Although potentially highly effective, the use of active site-directed reagents as drugs have been limited owing to their generally high dissociation constants compared to their reversible

counterparts. For aspartic proteases, for instance, epoxide-containing compounds for example, EPNP, have been generally used in inactivating these enzymes (Tang, 1971; Takahashi and Chang, 1976). Invariably, the design of such agents is of a configuration such that the reactive group is located to the very end of the molecule and suitably located close to their susceptible essential active site residues. This configurational design necessitates that only one half of the active site is utilized for binding. Thus, the other half of the active site could presumably be bound by a rationally designed artificial synergistic effector to enhance both the binding potency and increase the rate of inactivation of the active site-directed reagent (Figure 10).

A second conceivable application which also stems from this work is the potential design of synergism-dependent self-assembling inhibitors. To this end, once a synergistic pair of competitive inhibitors have been identified, suitable functional groups could then be incorporated onto one or both inhibitors to promote a chemical reaction with the objective of generating a single more potent molecule at the active site. For example, a reaction between an aldehyde and an amino group suitably positioned on both molecules to form a schiff's base can be envisaged. The entropic advantage associated with an enzyme interacting with a single molecule (Jencks, 1980) coupled to the initial synergistic effect between the inhibitors should greatly enhance the potency of such synergism dependent self-assembling inhibitors. The advantages associated with synergism-assisted inactivation can similarly be envisioned in this approach.

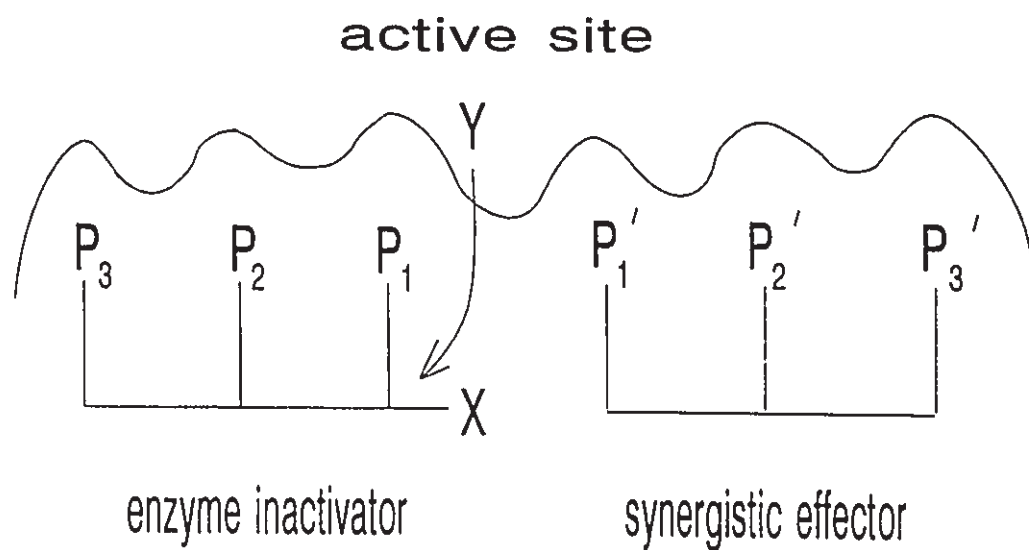


**Figure 10.** The concept of synergism-assisted inactivation. An active site directed-reagent with a functional group,  $X$ , and a synergistic effector bind concurrently at the active site of a target enzyme. The presence of the synergistic effector induces a specific recognition process thereby enhancing the rate of inactivation of the enzyme via covalent modification of the susceptible group  $Y$ .



## 4. COMBINATION PLOTS: AN ALTERNATIVE APPROACH TO THE ANALYSIS OF ENZYME-INHIBITOR INTERACTIONS

### 4.1 RESULTS

In the course of the analysis of synergistic interactions between inhibitors of HIV-1 protease and pepsin, it became apparent that the method of analysis, the Yonetani-Theorell plot (Yonetani and Theorell, 1964), was not particularly suited for routine analysis of enzyme-inhibitor interactions. Although the approach appropriately characterizes the interaction between two chemically nonreacting inhibitors by yielding an interaction constant,  $\alpha$ , a quantitative measure of the extent of interaction, the approach can be laborious involving too many assays. Although there is no dearth of approaches for the analysis of enzyme-inhibitor interactions (Slater and Bonner, 1952; Loewe, 1957; Yagi and Ozawa, 1960; Webb, 1963; Segel, 1975; Chou and Talalay, 1981, 1983; Johnson *et al.*, 1943) none exhibits the overall merits of the Yonetani-Theorell plot.

Commonly used approaches like the fractional inhibition method of Webb (1953) generally only give a qualitative insight into the type of interactions whether synergistic, additive or antagonistic without providing a stringent and reliable quantitative estimate of the magnitude of the interaction between the inhibitors. Without *a priori* knowledge of the kinetic constants and nature of inhibition, the median-effect method of Chou and Talalay (1981), which is widely used in pharmacology, can also provide a description of the interaction between inhibitors whether synergistic, additive or antagonistic. On the other hand, methods that provide a reliable quantitative measure of ligand interactions, like the

method of Yagi and Ozawa (1960), for instance, are restricted to fixed proportions of inhibitor concentrations in the analysis and also requires a secondary replot of the data. In the Yagi and Ozawa plot, synergism is concluded when a plot of  $v/v_i$  against  $(i_1 + i_2)$  is concave in the upward direction. The resulting second order curve is then fitted to an equation describing the kinetic effect of the inhibitors to indirectly obtain the apparent dissociation constant from which the interaction constant is computed.

The method of Yonetani and Theorell (1964) extends this approach by directly yielding an interaction constant which aptly describes the extent and nature of interaction between inhibitors from a family of lines (an example is shown in figures 3 or 12). Although very suitable, the tedium associated with the plot makes it unattractive for routine analysis of enzyme-inhibitor interactions. Invariably, the interaction constant between inhibitors cannot be determined with certainty from the intercepting family of lines necessitating a secondary replot of the data. Furthermore, since the analysis is done at a single substrate concentration discrepancies resulting from substrate and/or inhibitor effects is not readily apparent. An improved method for the analysis of multi-inhibitor interactions in unireactant enzymic systems was therefore pursued. The objective was to devise a plot that was quantitative and yielded an interaction constant between pairs of inhibitors rather like the Yonetani-Theorell plot but without the tedium associated with such approaches.

To achieve the objective of a relatively easy-to-use analytic graphical method, the strategy was to obtain a single linear plot capable of yielding an interaction constant. Traditionally, it has been the practice that kinetic constants are derived from a single interception point from a family of primary plots or in certain cases, secondary replots of

slopes or intercepts obtained from the primary plots (Segel, 1975). Theoretically, an equation which combined the primary and secondary plots should yield the kinetic constant of interest on a single plot circumventing the need for primary and secondary plots. Hence, the objective was to obtain an expression which described the kinetic effect of two or more inhibitors on an enzyme where the interaction constant or synergistic factor would be equivalent to the slope of the plot.

#### 4.1.1 Theoretical analysis.

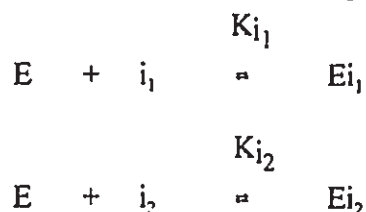
##### *Definition of symbols*

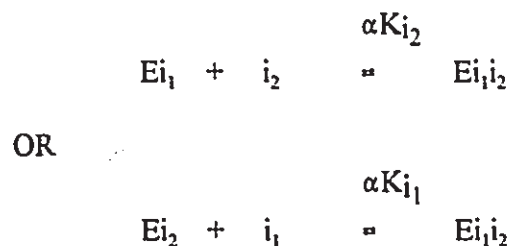
$$\rho = \frac{K_m + [S]}{K_m}$$

$$\phi = \frac{v - v_i}{v_i} = \frac{[i]}{IC_{50}}$$

##### 4.1.1.1 *Interaction between two mutually nonexclusive competitive inhibitors.*

An expression describing the kinetic effect of two competitive inhibitors simultaneously bound to different regions of an enzyme's active site can be derived from the following equilibria where  $Ei_1$ ,  $Ei_2$ , and  $Ei_1i_2$  represent the various enzyme-inhibitor complexes and  $\alpha$  is the interaction constant between the inhibitors.





$\alpha$  is therefore less than 1 when the inhibitors act synergistically and is greater than 1 when they are antagonistic.  $\alpha$  approaches  $\infty$  when the inhibitors are mutually exclusive and when both inhibitors bind independent of each other  $\alpha$  is unity. On the assumption that

- i. both inhibitors,  $i_1$  and  $i_2$ , do not interact chemically
- ii.  $i_1$  and  $i_2$  bind reversibly to the enzyme
- iii.  $[i_1]$ ,  $[i_2]$  and  $[s] \gg [E]$

then the Yonetani-Theorell equation for the system can be derived (Yonetani and Theorell, 1964):

$$\frac{1}{v_i} = \frac{1}{V_m} + \frac{K_m}{[s]V_m} \left(1 + \frac{[i_2]}{K_{i_2}}\right) + \frac{K_m[i_1]}{[s]V_m K_{i_1}} \left(1 + \frac{[i_2]}{\alpha K_{i_2}}\right) \quad (1)$$

$$v = \frac{V_{\max} [s]}{K_m + [s]} \quad (2)$$

From equation (1) and the Michaelis-Menten equation (2) (Michaelis and Menten, 1913)

the combination equation (3) can be derived

$$\left(\frac{v}{v_i} - 1\right) - \left(\frac{K_m}{K_m + [s]}\right) \left(\frac{[i_1]}{K_{i_1}} + \frac{[i_2]}{K_{i_2}}\right) = \frac{[i_1][i_2]}{\alpha K_{i_1} K_{i_2}} \cdot \frac{K_m}{K_m + [s]} \quad (3)$$

where  $v_i$  is the rate in the presence of both inhibitors.

Thus if

$$\left(\frac{v}{v_1} - 1\right) - \left(\frac{K_m}{K_m + [S]}\right) \left(\frac{[i_1]}{K_{i_1}} + \frac{[i_2]}{K_{i_2}}\right)$$

is plotted against

$$\frac{[i_1][i_2]}{K_{i_1}K_{i_2}} \cdot \frac{K_m}{k_m + [S]}$$

a straight line through the origin with a gradient equivalent to the reciprocal of the interaction constant,  $1/\alpha$  is obtained.

Alternatively,

$$\left(\frac{v}{v_1} - 1\right) \left(\frac{K_m + [S]}{K_m}\right) - \left(\frac{[i_1]}{K_{i_1}} + \frac{[i_2]}{K_{i_2}}\right)$$

can be plotted against

$$\left(\frac{[i_1][i_2]}{K_{i_1}K_{i_2}}\right)$$

to give similarly a straight line through the origin with a slope equivalent to  $1/\alpha$ .

Equation (3) can be simplified into the general form of the combination equation (4)

by introducing  $\phi$  and  $\rho$ .

$$\phi_{1,2} - \phi_1 - \phi_2 = \phi_1 \cdot \phi_2 \cdot \rho \cdot \frac{1}{\alpha} \quad (4)$$

where

$$\phi_j = \frac{i_j}{IC_{50_j}} = \frac{i_j}{\rho K_{i_j}} \quad (5)$$

Thus by plotting  $\phi_{1,2}-\phi_1-\phi_2$  against  $\phi_1\phi_2\rho$ , a slope equivalent to  $1/\alpha$  is obtained. Hence, either  $K_i$  or  $IC_{50}$  of inhibitors may be employed to determine their interaction constant.

#### 4.1.1.1.1 *Alternative combination plots*

Alternative forms of the combination plot can be derived through simple mathematical transformations of the general equation (4).

##### **Alternative plot 1:**

$$\frac{\phi_{1,2}-\phi_1-\phi_2}{\phi_1\phi_2} = \frac{1}{\alpha} + \frac{[s]}{K_m} \cdot \frac{1}{\alpha} \quad (6)$$

Hence, a plot of

$$\frac{\phi_{1,2}-\phi_1-\phi_2}{\phi_1\phi_2}$$

against  $[s]/K_m$  yields both an ordinate intercept and slope equivalent to  $1/\alpha$ . The intercept on the abscissa remains a constant, -1.

##### **Alternative plot 2:**

$$\frac{\phi_{1,2}-\phi_1}{\phi_1\phi_2\rho} = \frac{1}{[i_1]} \cdot K_{i_1} + \frac{1}{\alpha} \quad (7)$$

Hence, a plot of

$$\frac{\phi_{1,2}-\phi_1}{\phi_1\phi_2\rho}$$

against  $1/[i_1]$  gives an ordinate intercept of  $1/\alpha$ , a slope of  $K_{i_1}$  and an abscissa intercept of

$1/\alpha K_{i1}$ .

Similarly,

$$\frac{\phi_{1,2} - \phi_2}{\phi_1 \phi_2 \rho}$$

can be plotted against  $1/[i_2]$  to give an ordinate intercept of  $1/\alpha$ , a slope of  $K_{i2}$  and an abscissa intercept of  $1/\alpha K_{i2}$ .

#### 4.1.1.2 Interactions between two noncompetitive inhibitors.

Assumptions made under section 4.1.1.1 similarly apply.

Equation (8) describes the interaction between two noncompetitive inhibitors on their target enzyme (Segel, 1975)

$$v = \frac{V_{\max} [s]}{K_m \left( 1 + \frac{[i_1]}{K_{i1}} + \frac{[i_2]}{K_{i2}} + \frac{[i_1][i_2]}{\alpha K_{i1} k_{i2}} \right) + [s] \left( 1 + \frac{[i_1]}{K_{i1}} + \frac{[i_2]}{K_{i2}} + \frac{[i_1][i_2]}{\alpha K_{i1} k_{i2}} \right)} \quad (8)$$

From equation (2) and equation (8) the combination equation (9) can be obtained.

$$\frac{v - v_i}{v_i} = \frac{[i_1]}{K_{i1}} + \frac{[i_2]}{K_{i2}} + \frac{[i_1][i_2]}{\alpha K_{i1} K_{i2}} \quad (9)$$

Hence by plotting

$$\frac{v - v_i}{v_i} - \frac{[i_1]}{K_{i1}} - \frac{[i_2]}{K_{i2}}$$

against

$$\frac{[i_1]}{K_{i_1}} \cdot \frac{[i_2]}{K_{i_2}} \cdot \rho$$

a straight line through the origin with a slope equivalent to the reciprocal of the interaction constant ( $1/\alpha$ ) between the inhibitors is obtained. Because the binding of substrate and a linear noncompetitive inhibitor are independent of each other  $K_i = IC_{50}$ , a  $\rho$  factor need not be applied to interconvert between these parameters.

Alternative plots can be derived in an analogous fashion as presented for two competitive inhibitors under section 4.1.1.1.1.

#### 4.1.1.3 Interactions between two inhibitors ( $i_1$ , competitive and $i_2$ , noncompetitive).

Based on similar assumptions as stated under 4.1.1.1, the following equation describes the kinetic effect of a competitive inhibitor and a noncompetitive inhibitor acting together on a target enzyme (Segel, 1975).

$$v = \frac{V_{max} [s]}{K_m \left( 1 + \frac{[i_1]}{K_{i_1}} + \frac{[i_2]}{K_{i_2}} + \frac{[i_1][i_2]}{\alpha K_{i_1} K_{i_2}} \right) + [s] \left( 1 + \frac{[i_2]}{K_{i_2}} \right)} \quad (10)$$

From equations (2) and equation (10) the combination format of equation (11) can be derived.

$$\frac{v-v_i}{v_i} \cdot \frac{[i_2]}{K_{i_2}} = \frac{K_m}{K_m + [s]} \cdot \frac{[i_1]}{K_{i_1}} = \frac{K_m}{K_m + [s]} \cdot \frac{[i_1][i_2]}{K_{i_1} K_{i_2}} \cdot \frac{1}{\alpha} \quad (11)$$

Hence, if the left side of equation (11) is plotted against



$$\frac{K_m}{K_m + [S]} + \frac{[i_1][i_2]}{K_{i_1}K_{i_2}}$$

a linear plot through the origin with a slope equivalent to  $1/\alpha$  is obtained. The potency parameter of the competitive inhibitor,  $\phi_1$  can be interconverted between  $K_i$  and  $IC_{50}$  by virtue of the  $p$  factor while for the noncompetitive inhibitor,  $K_i = IC_{50}$ . Alternative plots as derived under section 4.1.1.1 are similarly applicable.

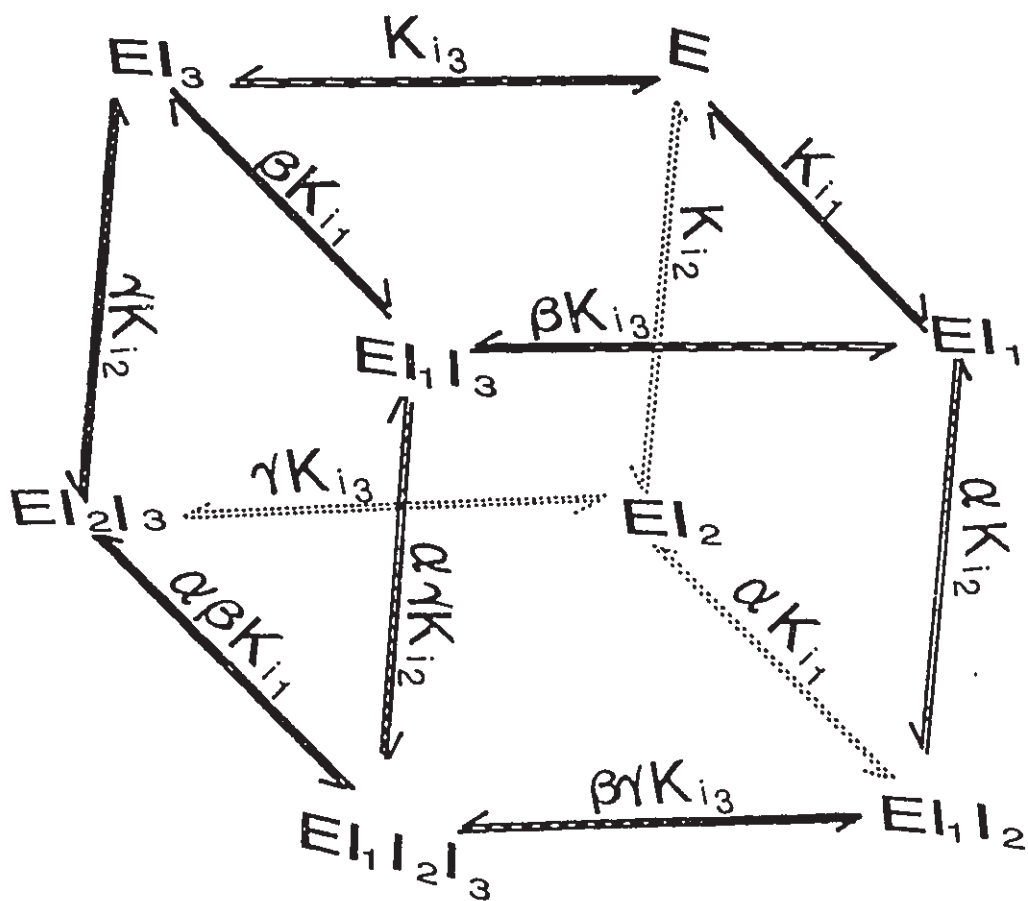


Figure 11. A cube diagram showing the possible complexes and equilibria in a unireactant enzymic system with three linear mutually non-exclusive competitive inhibitors. Broken faint lines represent those at the back of the cube.

#### 4.1.1.4 Interactions between three competitive inhibitors

Unlike previous methods, the present combination approach can be faithfully extended to the analysis of the concurrent effects of three inhibitors on an enzyme. Figure 11 illustrates the possible equilibria between an enzyme and three inhibitors assuming binding is reversible and does not involve the formation of chemical complexes. Michaelis-Menten kinetics is also assumed in deriving the necessary rate equations. Equation 12 then describes the net kinetic effect of having three linear competitive inhibitors act simultaneously on an enzyme (see Appendix I).

$$v_i = \frac{V_{\max} [s]}{K_m \left( 1 + \frac{[i_1]}{K_{i_1}} + \frac{[i_2]}{K_{i_2}} + \frac{[i_3]}{K_{i_3}} + \frac{[i_1][i_2]}{\alpha K_{i_1} K_{i_2}} + \frac{[i_1][i_3]}{\beta K_{i_1} K_{i_3}} + \frac{[i_2][i_3]}{\gamma K_{i_2} K_{i_3}} + \frac{[i_1][i_2][i_3]}{\theta K_{i_1} K_{i_2} K_{i_3}} \right) + [s]} \quad (12)$$

Transforming equation (12) into the combination form results in equation (13)

$$\frac{v-v_i}{v_i} = \frac{[i_1]}{K_{i_1}} + \frac{[i_2]}{K_{i_2}} + \frac{[i_3]}{K_{i_3}} + \frac{[i_1][i_2]}{K_{i_1} K_{i_2}} \cdot \frac{\rho}{\alpha} + \frac{[i_1][i_3]}{K_{i_1} K_{i_3}} \cdot \frac{\rho}{\beta} + \frac{[i_2][i_3]}{K_{i_2} K_{i_3}} \cdot \frac{\rho}{\gamma} + \frac{[i_1][i_2][i_3]}{K_{i_1} K_{i_2} K_{i_3}} \cdot \frac{\rho^2}{\theta} \quad (13)$$

where  $\alpha$  is the interaction constant between inhibitors 1 and 2

$\beta$	"	"	" 1 and 3
$\gamma$	"	"	" 2 and 3
$\theta$	overall	"	" 1, 2 and 3

Equation (13) can be similarly condensed into a form

$$\phi_{123} - \phi_{12} - \phi_{13} - \phi_{23} + \phi_1 + \phi_2 + \phi_3 = \phi_1 \phi_2 \phi_3 \cdot \frac{\rho^2}{\theta} \quad (14)$$

which is expressed as

$$\phi_{123} - \sum_{j=1}^2 \sum_{k=2}^3 \phi_{jk} + \sum_{m=1}^3 \phi_m = \phi_1 \phi_2 \phi_3 \cdot \frac{\rho^2}{\theta} \quad (15)$$

where  $j \neq k$  and

$$\phi_{12} - \phi_1 + \phi_2 + \phi_1 \phi_2 \cdot \frac{\rho}{\alpha}$$

$$\phi_{13} - \phi_1 + \phi_3 + \phi_1 \phi_3 \cdot \frac{\rho}{\beta}$$

$$\phi_{23} - \phi_2 + \phi_3 + \phi_2 \phi_3 \cdot \frac{\rho}{\gamma}$$

The tripartite interaction constant,  $\tau$  is defined as  $\theta/\alpha\beta\gamma$ . Thus when

$\tau = 1$  , synergistic interaction between pairs of ligands is independent of one another

$\tau < 1$  , synergism occurs in a third dimension within the ternary complex

$\tau \rightarrow \infty$  , mutually exclusive

$\infty > \tau > 1$  , antagonism or steric hindrance

Thus for the determination of the tripartite interaction constant,  $\tau$ , between three inhibitors, there is an initial requirement for the extent of interaction between each pair of the triplet to be known.  $\tau$  therefore gives a measure of the enhanced or decreased potency resulting from the quaternary  $Ei_1i_2i_3$  complex.

#### 4.1.2 Application of theoretical treatment: Properties of combination plots

Having obtained the necessary equations, the combination plots have been illustrated by investigating the nature of ligand/inhibitor interactions on carboxypeptidase B. This enzyme was chosen upon several considerations. The enzyme has been extensively studied as a model for zinc enzymes and is well characterized. The crystal structure of the enzyme has been solved and could provide a clearer understanding of the kinetic data. Furthermore, inhibitor synergism had previously been observed in the enzyme (Chan and Pfuetzner, 1993). The continuous spectrophotometric assay for this enzyme was fairly easy compared to the HPLC-based assay for HIV-1 protease thus numerous assays could be routinely performed to illustrate the plots. Finally, the feasibility of potentially demonstrating the concurrent application of three inhibitors were greater for carboxypeptidase B based on its specificity requirements compared to the symmetric HIV-1 protease.

##### 4.1.2.1 *Interactions between two competitive inhibitors*

To verify the derivations and ascertain the integrity of the equations, several experiments were performed and results from the combination method compared to those obtained from the established Yonetani-Theorell plot (Yonetani and Theorell, 1964) using

the same set of experimental data. The concurrent effects of succinic acid and methylguanidine on porcine carboxypeptidase B which had previously been shown to be synergistic was re-analyzed (Chan and Pfuetzner, 1993). As indicated by the Yonetani-Theorell plot (Figure 12), the two inhibitors acted synergistically yielding an interaction constant of 0.04. Figure 13 shows the same experimental data replotted using the combination approach. As expected from equation (4), a straight line through the origin is obtained with a slope of 25, which is equivalent to the reciprocal of the interaction constant determined by the Yonetani-Theorell plot. Both plots therefore yield the same result confirming the integrity of the equations.

Several revealing observations about the combination plot emerge when the two approaches ie figures 12 and 13 are compared. The most obvious observation is how well the two approaches converge at the same result although it is evident that the number of data points defining the slope of the combination plot are rather excessive. In most instances, the same data point is obtained in duplicate; in the extreme case, (the fourth point from the origin, Figure 13) the data point is actually composed of three independent experimental values. Thus, certain independent combination of inhibitor concentrations become redundant when the combination plot is applied. This would be expected if the value of  $\phi$  represents the normalized concentrations of both inhibitors and therefore is independent of the combination of inhibitor concentration used to achieve that value; hence, the same level of inhibition would be similarly observed.

Since the Yonetani-Theorell plot is carried out under a fixed substrate concentration, deviations or anomalous effects which may potentially arise with respect to changes in

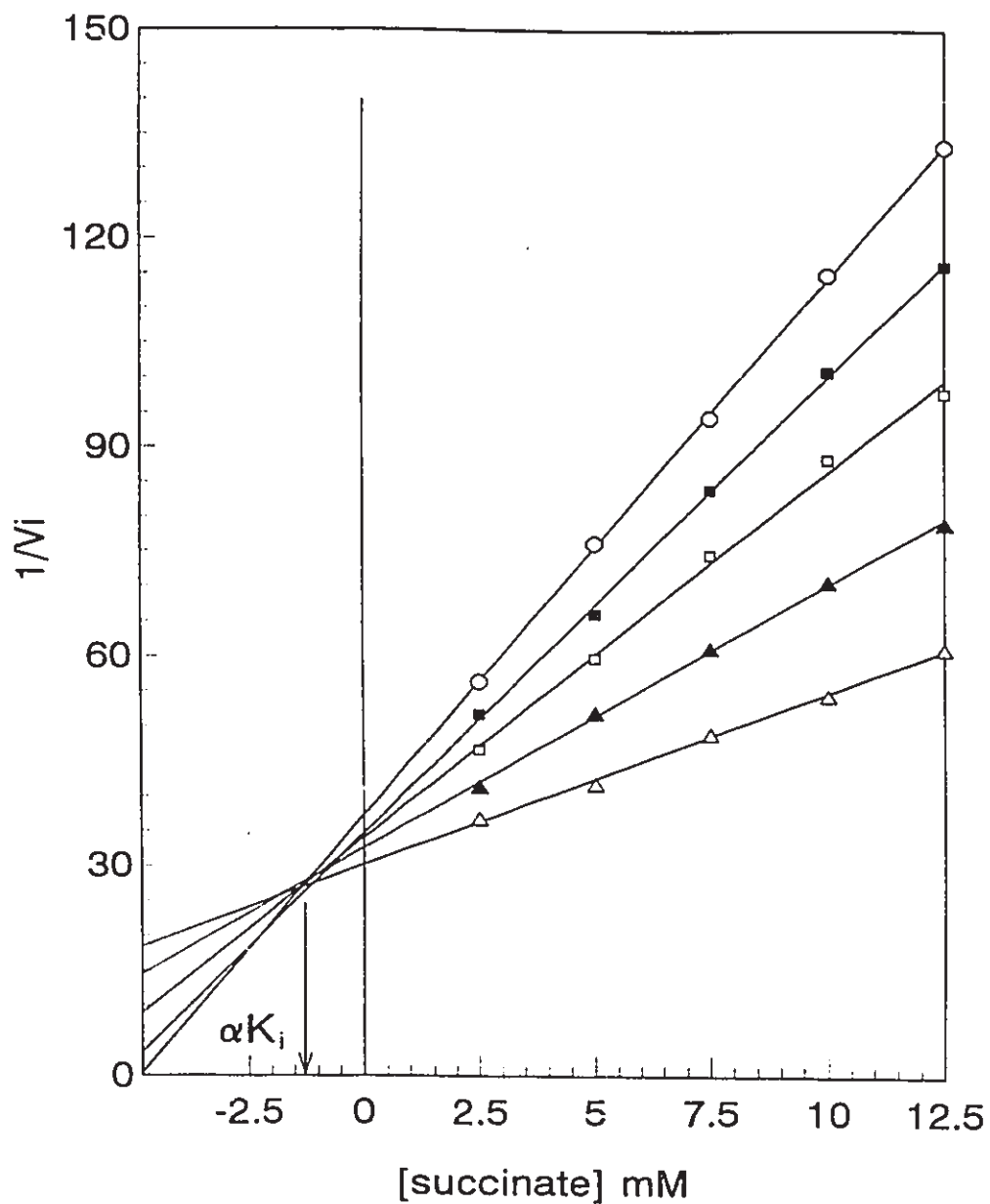


**Figure 12.** Yonetani-Theorell plot for the concurrent effects of succinic acid and methylguanidine on Carboxypeptidase-B. The concentration of succinic acid is as indicated on the abscissa while that of methylguanidine is as follows:  $\Delta$  0.1 mM  $\blacktriangle$  0.2 mM,  $\square$  0.3 mM,  $\blacksquare$  0.4 mM, &  $\circ$  0.5 mM. The  $K_i$  for succinic acid and methylguanidine are 28 and 1.3 mM respectively. An interaction constant of  $0.04 \pm .006$  is obtained from the data.

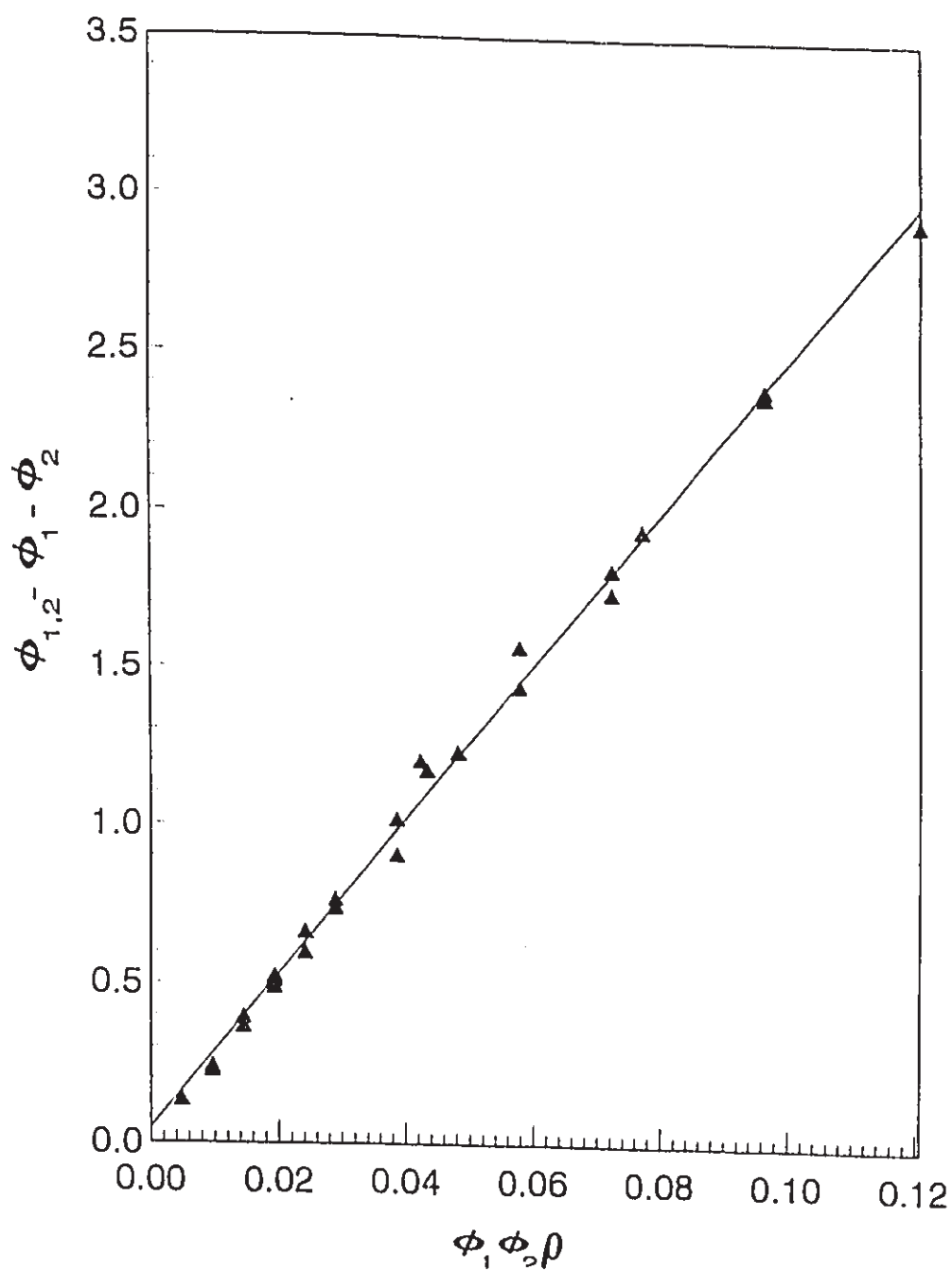


**Figure 13.** Combination plot for the interaction between succinate and methylguanidine. All 25 data points from figure 12 have been replotted. The slope value of  $25 \pm 4$  is equivalent to the  $1/\alpha$ .  $\rho=1.32$  (See text section 4.1.1 for definition of  $\rho$  and  $\alpha$ ).



substrate concentration cannot be observed. Such effects could potentially lead to erroneous deductions as to the nature of inhibitor interaction and possibly the mechanism involved. The combination method, on the other hand, can successfully accommodate varying substrate concentrations within the same experiment setup. The concurrent effect of the same pair of inhibitors (succinic acid and methylguanidine) was therefore re-examined using varying substrate concentrations and also substantially limiting the number of data points to that comparable to a single straight line in a Yonetani-Theorell plot. As shown in figure 14, no deviations are evident, but more importantly, a similar synergistic factor ( $1/\alpha$ ) of 30 is obtained.

Figure 15 shows an alternative plot based on equation (6) (see section 4.1.1.1.1) of the data from figure 14. This plot, in addition to yielding a synergistic factor also serves as a diagnostic; if competitiveness is maintained, the intercept on the abscissa remains at -1. Furthermore, both the slope and ordinate intercept give the synergistic factor,  $1/\alpha$ . A second alternative combination plot derived from equation (7) (see section 4.1.1.1.1) is shown in figure 16. As illustrated, the same experimental values from figure 14 have been similarly used. The slope of this plot is equivalent to the  $K_i$  of the inhibitor being analyzed on the abscissa while the intercept on the ordinate gives the synergistic factor,  $1/\alpha$ . Obviously, the alternative plots are applicable only when varying substrate concentrations are employed in the assay.

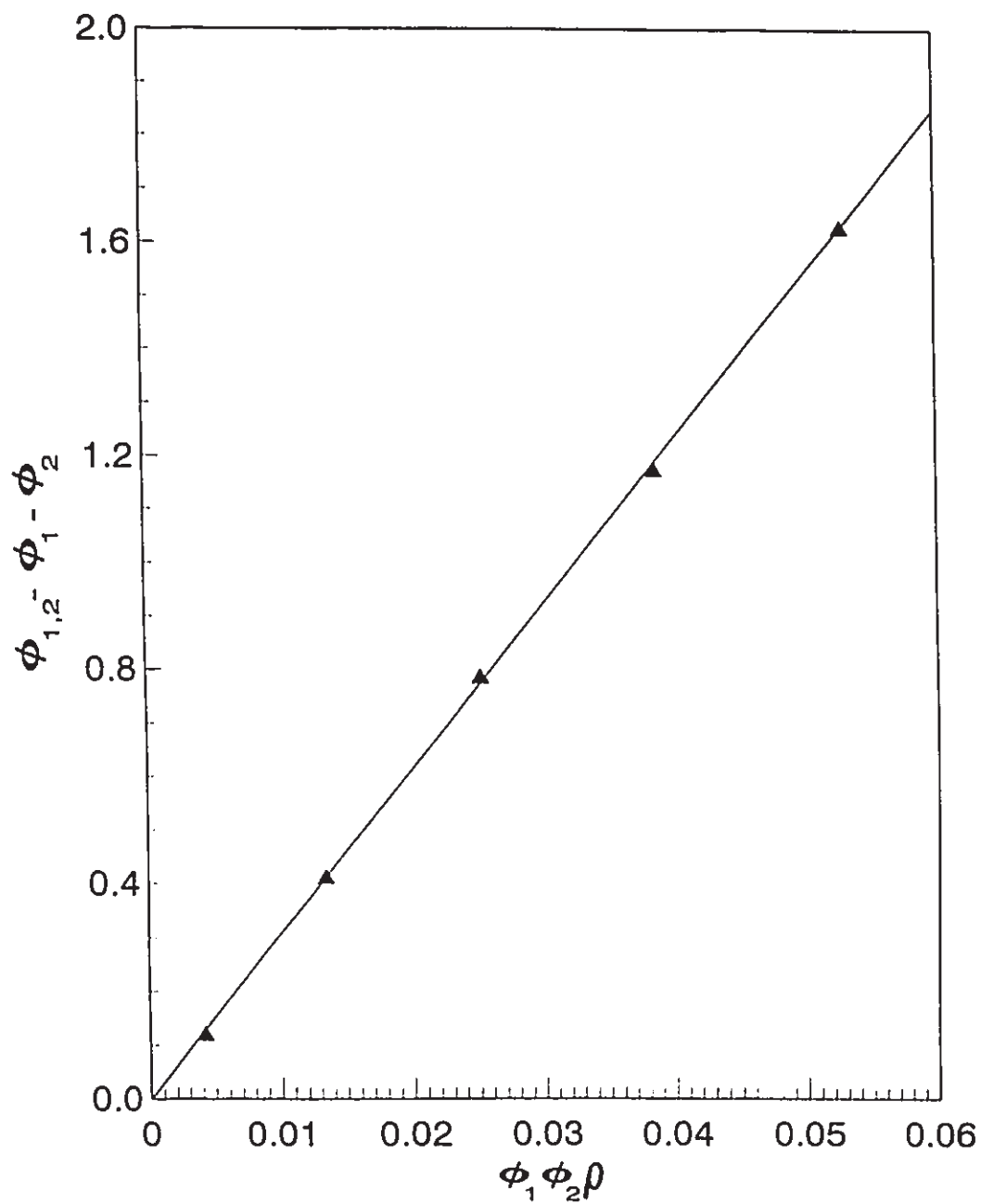


**Figure 14.** Five different substrate concentrations was used to investigate potential deviations from linearity in the interaction between succinic acid and methylguanidine on carboxypeptidase-B. The slope ( $1/\alpha$ ) is  $30 \pm 2$ .

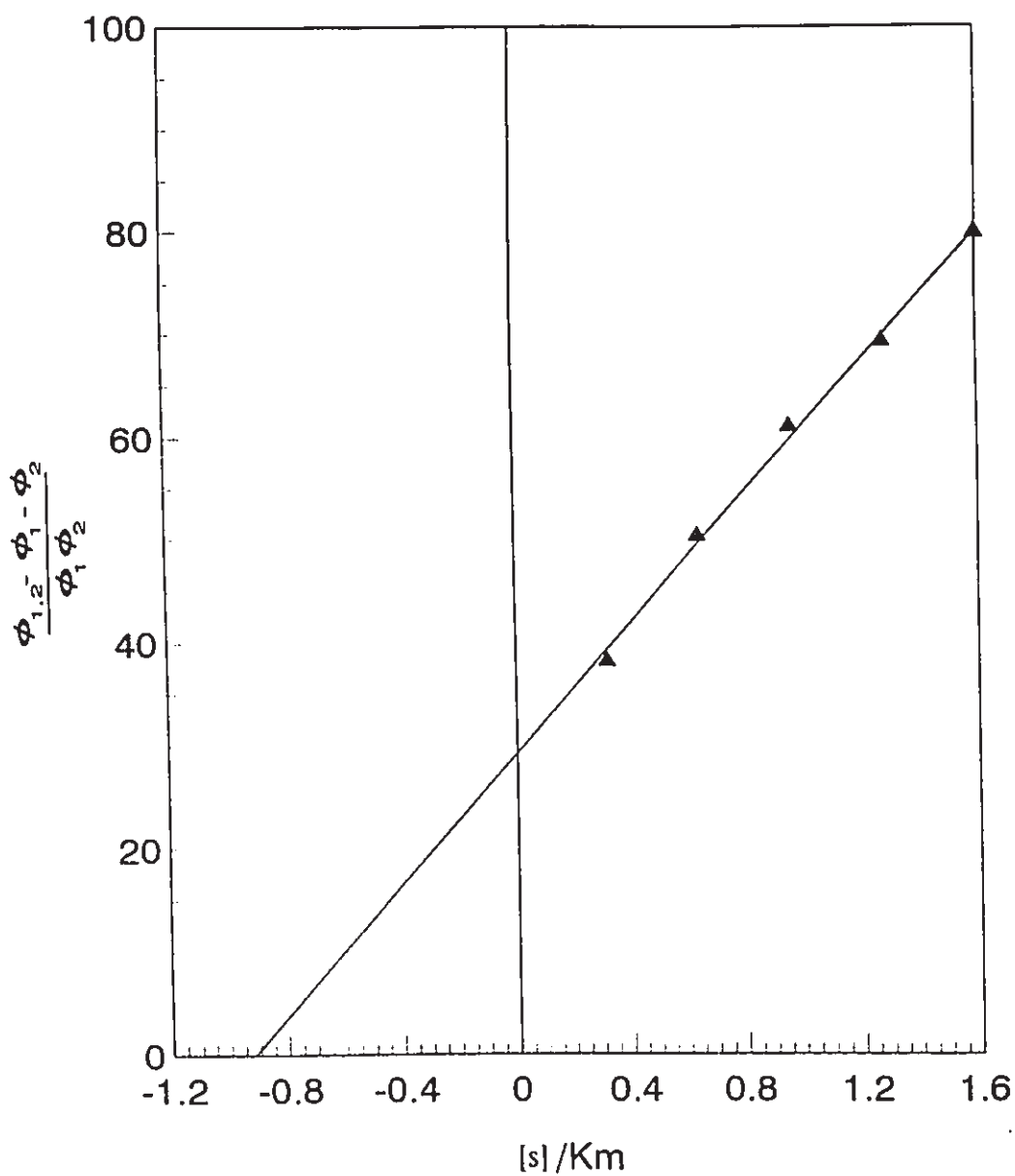


**Figure 15.** The same experimental values from figure 14 have been replotted using an alternative form of the combination plot as a diagnostic (equation (6)). The ordinate intercept of  $30 \pm 2$  and the slope value of  $28 \pm 3$  are reflective of the synergistic factor ( $1/\alpha$ ). The abscissa intercept of almost 1 ( $0.92 \pm .1$ ) indicates competitiveness is maintained by both inhibitors during the assay.

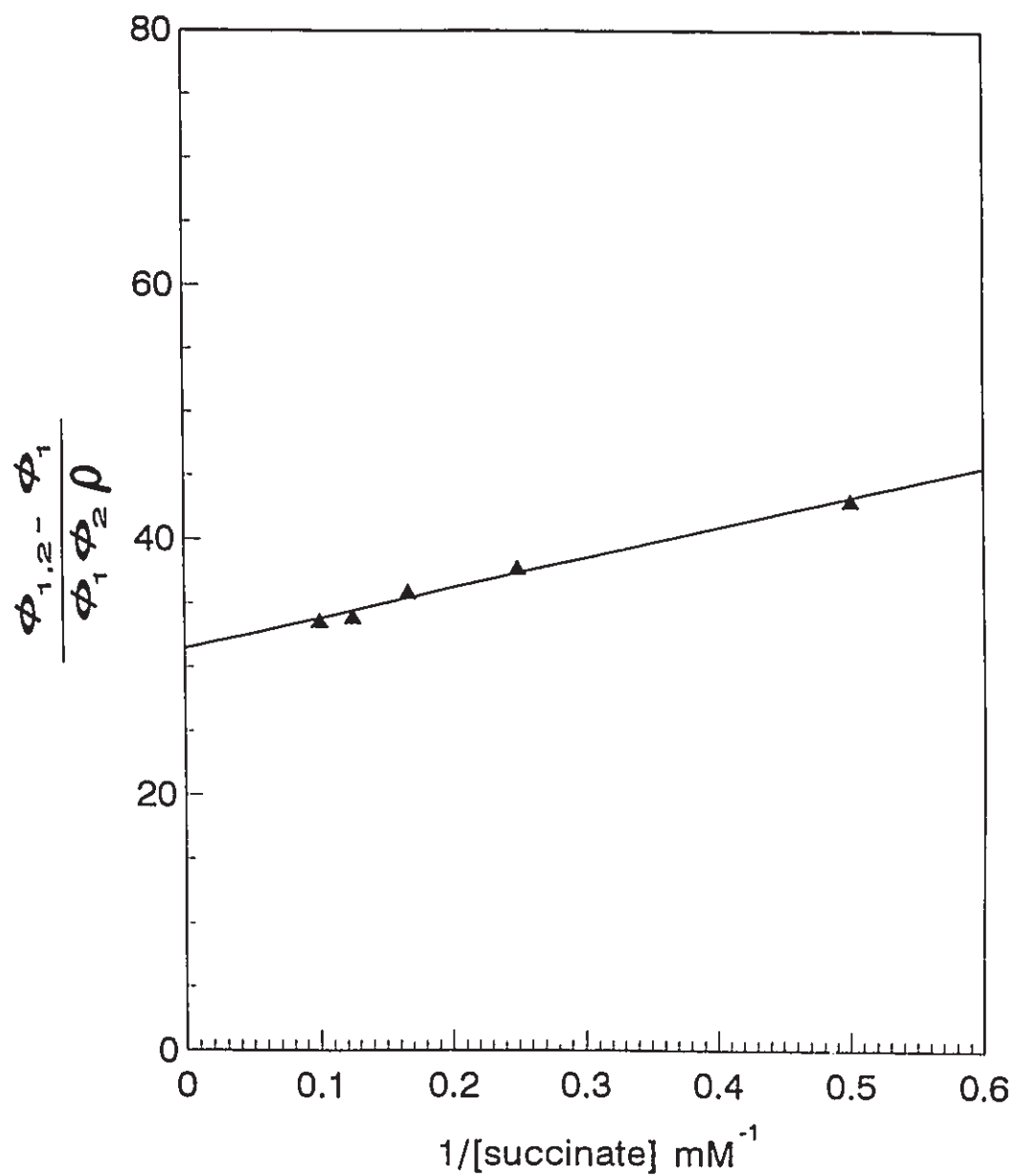


**Figure 16.** An alternative combination plot for the interaction between succinic acid and methylguanidine on carboxypeptidase-B. The ordinate intercept gives the  $1/\alpha$  value of 31 while the slope reflects the  $K_i$  ( $24 \pm 3$ ) of the inhibitor employed on the abscissa, succinic acid. The plot is based on equation (7).

To further confirm the convergence of both the combination and Yonetani-Theorell plots, data from the literature were retrieved and re-analyzed. Figure 17 is the replotted data (as retrieved by Chou and Talalay (1981)), for the analysis of the synergistic effects between ortho-phenanthroline and adenosine diphosphate (ADP) on horse liver alcohol dehydrogenase. The slope value ( $1/\alpha$ ) from the combination plot of 1.9, matches the  $\alpha$  value of 0.5 reported by the original authors (Yonetani and Theorell, 1964). It can be similarly observed that several data points are rendered redundant when the combination plot is used as previously noted (Figure 13).

Because the combination plot yields a slope which is a direct quantitative measure of the extent of interaction between two inhibitors, the plot predicts that if two inhibitors are mutually exclusive, they should have a slope of zero ie.  $1/\infty$ . Data also obtained by Yonetani and Theorell (1964) on the concurrent effects of ADP and ADP-ribose on horse liver alcohol dehydrogenase showed the two competitive inhibitors were mutually exclusive. As predicted by the combination plot, all the points as retrieved from the literature strikingly lie on the abscissa (Figure 18) ie. slope = 0, indicative of mutual exclusiveness and confirming the prediction.

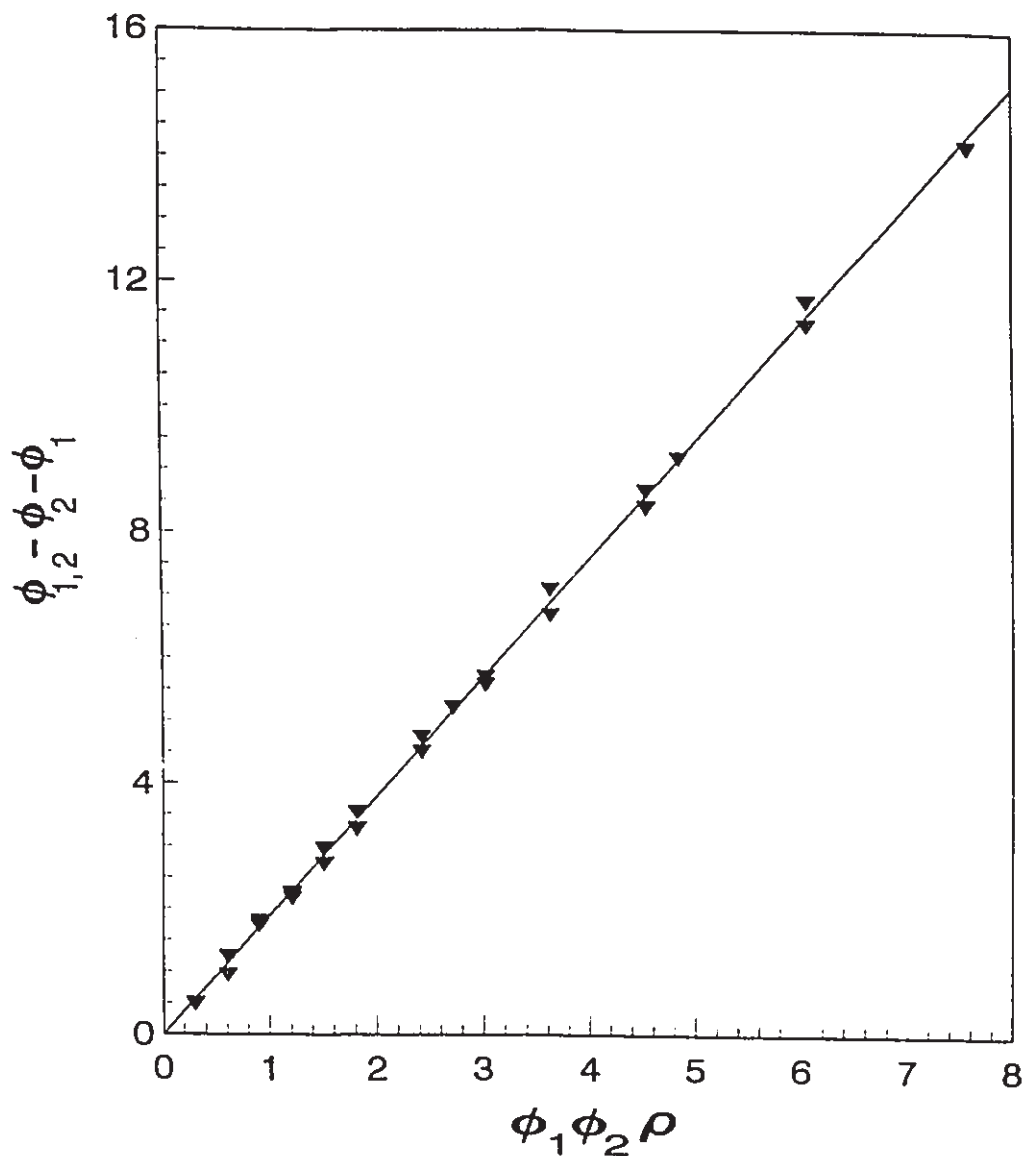


**Figure 17.** A replot of the retrieved data for the concurrent effects of ortho-phenanthroline and ADP on horse liver alcohol dehydrogenase (Yonetani and Theorell, 1964). The slope of  $1.9 \pm .1$  reflects the previously reported  $\alpha$  value of 0.5. (4.25, the  $\rho$  value used in constructing the plot was an average of four determinations (4.25, 4.09, 4.11 & 4.57) calculated respectively from the  $K_i$  &  $IC_{50}$  of ADP, O-phenanthroline, ADP-Ribose and from  $s$  &  $K_m$  of  $NAD^+$ ).

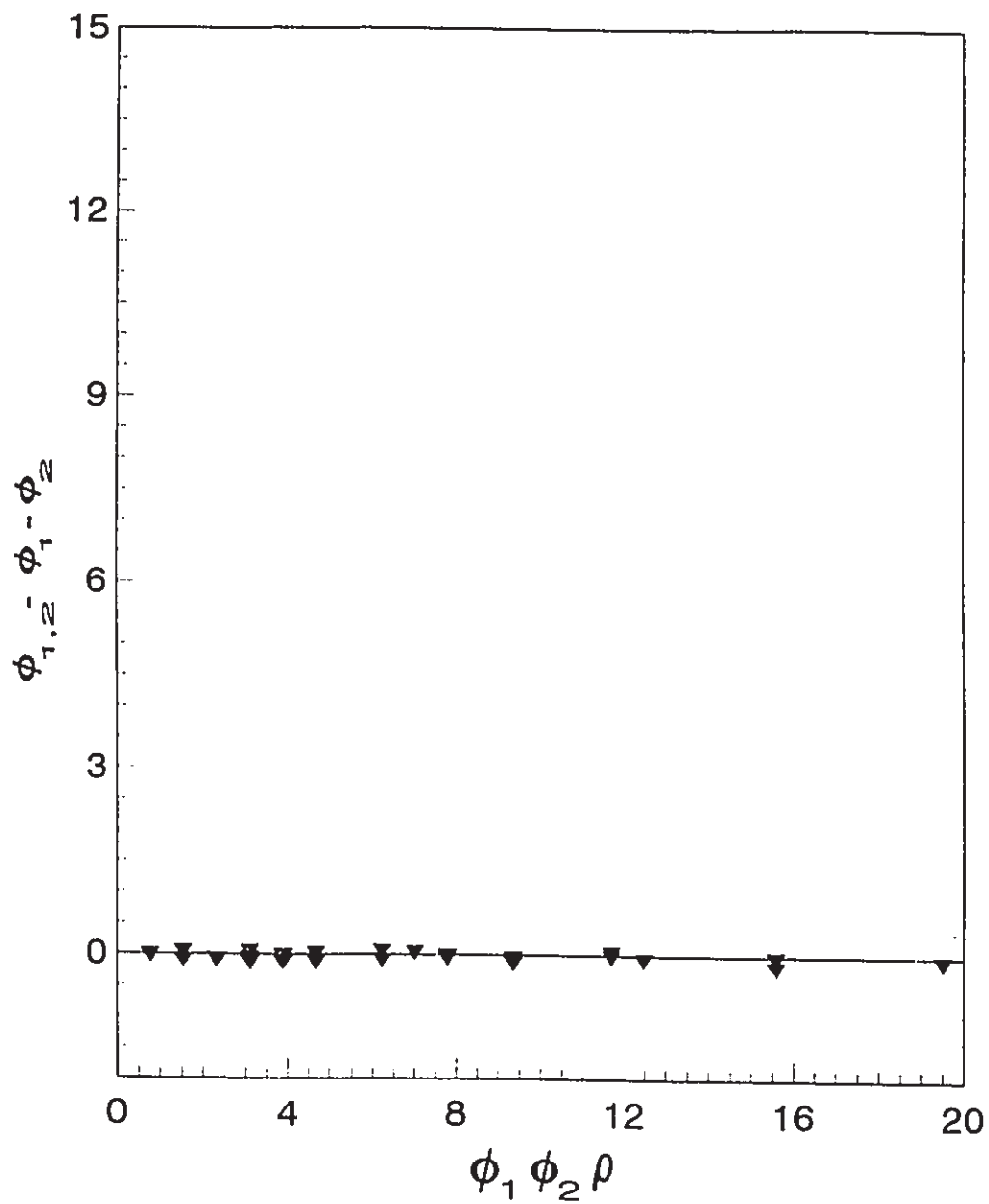


**Figure 18.** A replot of the retrieved data for the interaction between ADP and ADP-Ribose on horse liver alcohol dehydrogenase (Yonetani and Theorell, 1964). Mutual exclusiveness is indicated by all the data points lying on the abscissa. ( $\rho = 4.25$ , see figure 17 for how the value was obtained).

In addition to yielding an interaction constant between pairs of inhibitors, the combination plots may also be used to compare the extent of interaction between several pairs of inhibitors acting on the same enzyme as illustrated in figure 19. It is evident from the figure that while succinic acid interacts synergistically with methylguanidine, the acid exhibits mutually exclusive characteristics in the presence of  $\beta$ -mercaptoethanol. The slope of almost 1 for the interaction between  $\beta$ -mercaptoethanol and methylguanidine suggest their binding is independent of each other. Thus, through a visual inspection of the steepness of the slopes, the magnitude and order of positive or negative interactions of several pairs of inhibitors may be conveniently presented. The identification of positive and negative interactions between pairs of inhibitors for such comparative purposes can be enhanced by the introduction of a theoretical slope equal to unity. Hence, all lines upward of the theoretical depicts synergism while those beneath it are antagonistic with respect to their influence of the binding of each other on the enzyme. As presented in the figure, the interaction between methylguanidine and  $\beta$ -mercaptoethanol illustrates this point.



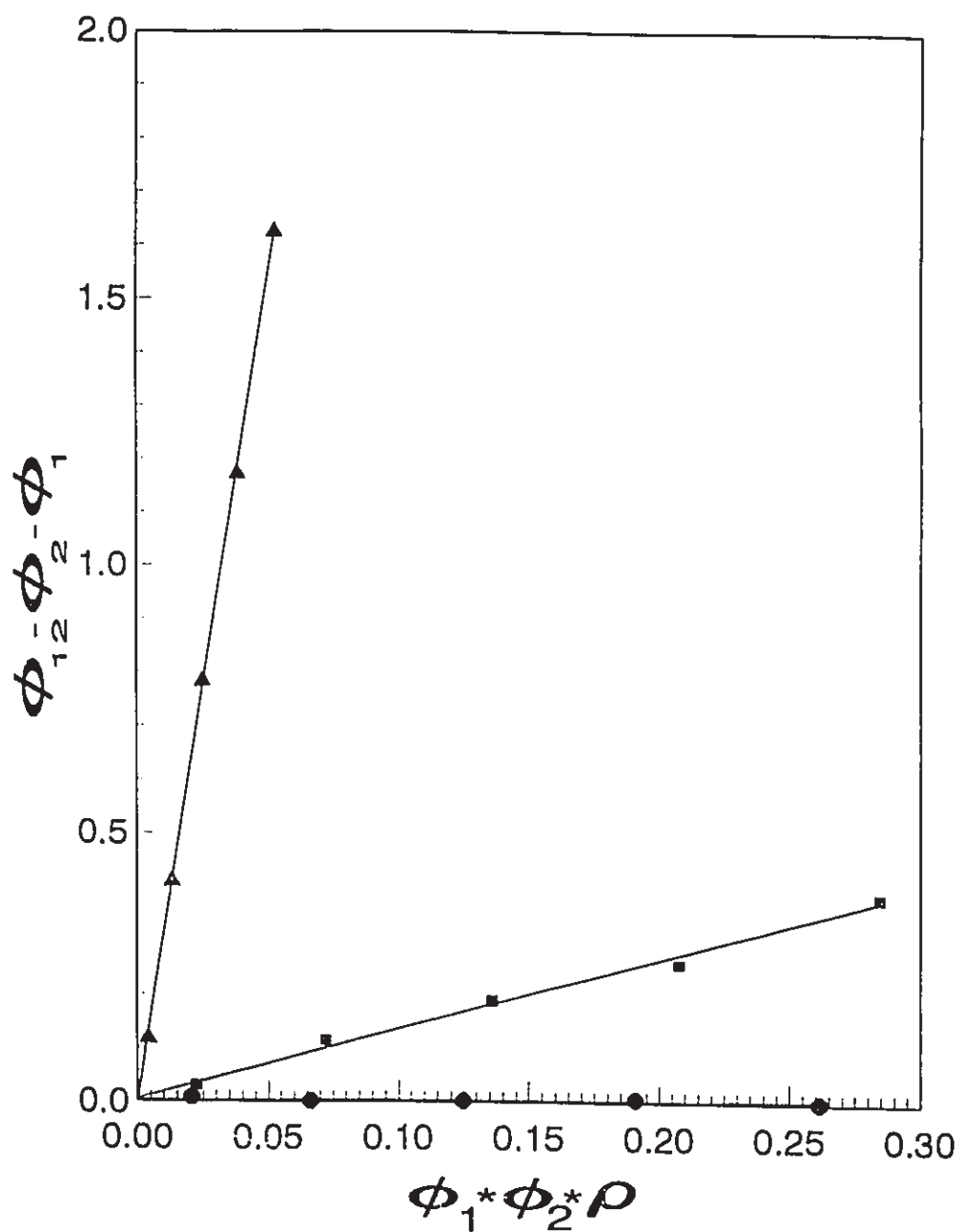


**Figure 19.** A representation of the concurrent effects of three different pairs of inhibitor interactions on carboxypeptidase-B. The pairs of inhibitors are as follows: ▲ succinate and methylguanidine ( $1/\alpha = 30 \pm 2$ ), ■ methylguanidine and  $\beta$ -mercaptoethanol ( $1/\alpha = 1.2 \pm .2$ ) and ●  $\beta$ -mercaptoethanol and succinate ( $1/\alpha \sim 0$ ).

#### 4.1.2.2 *Concurrent effects of three competitive inhibitors on carboxypeptidase-B.*

The applicability of the combination approach for the analysis of the concurrent effects of three purely competitive inhibitors was demonstrated by analyzing the effects of methylguanidine, methylsuccinic acid and  $\beta$ -mercaptoethanol on carboxypeptidase-B. As indicated by equation (13), the independent interaction constants,  $\alpha$ ,  $\beta$  and  $\gamma$  between each pair of the three inhibitors must be pre-established in order to determine the tripartite interaction constant,  $\tau$ . Previously shown in figure 19 is the interaction between methylguanidine and  $\beta$ -mercaptoethanol on carboxypeptidase-B. The synergistic factor of 1.2 indicates their binding is virtually independent of each other. The interaction between methylsuccinic acid and methylguanidine is also synergistic with their affinity for the enzyme increased by 25-fold when simultaneously present (see Table IX). The dissociation constant of methylsuccinic acid decreases by a factor of 2.6 when methylguanidine is present and *vice versa* (see Table XI). Hence  $1/\alpha$ ,  $1/\beta$  and  $1/\gamma$  are respectively 1.2, 25 and 2.6.

Figure 20 shows the concurrent effect of methylguanidine, methylsuccinic acid and  $\beta$ -mercaptoethanol on carboxypeptidase-B investigated with the aid of a combination plot. An overall interaction constant,  $\theta$ , of 0.014 ( $1/\theta = 70$ ) is obtained from the interactions of the three inhibitors. A tripartite interaction constant,  $\tau$ , of  $1.1 \pm .3$  ie  $(1.2*25*2.6/70)$  indicates that no additional synergistic effect is elicited upon the simultaneous application of the three inhibitors on the enzyme. A similar synergistic factor was obtained when the three inhibitors were assessed under a single substrate concentration of 0.8 mM using 9  $\phi$  values.

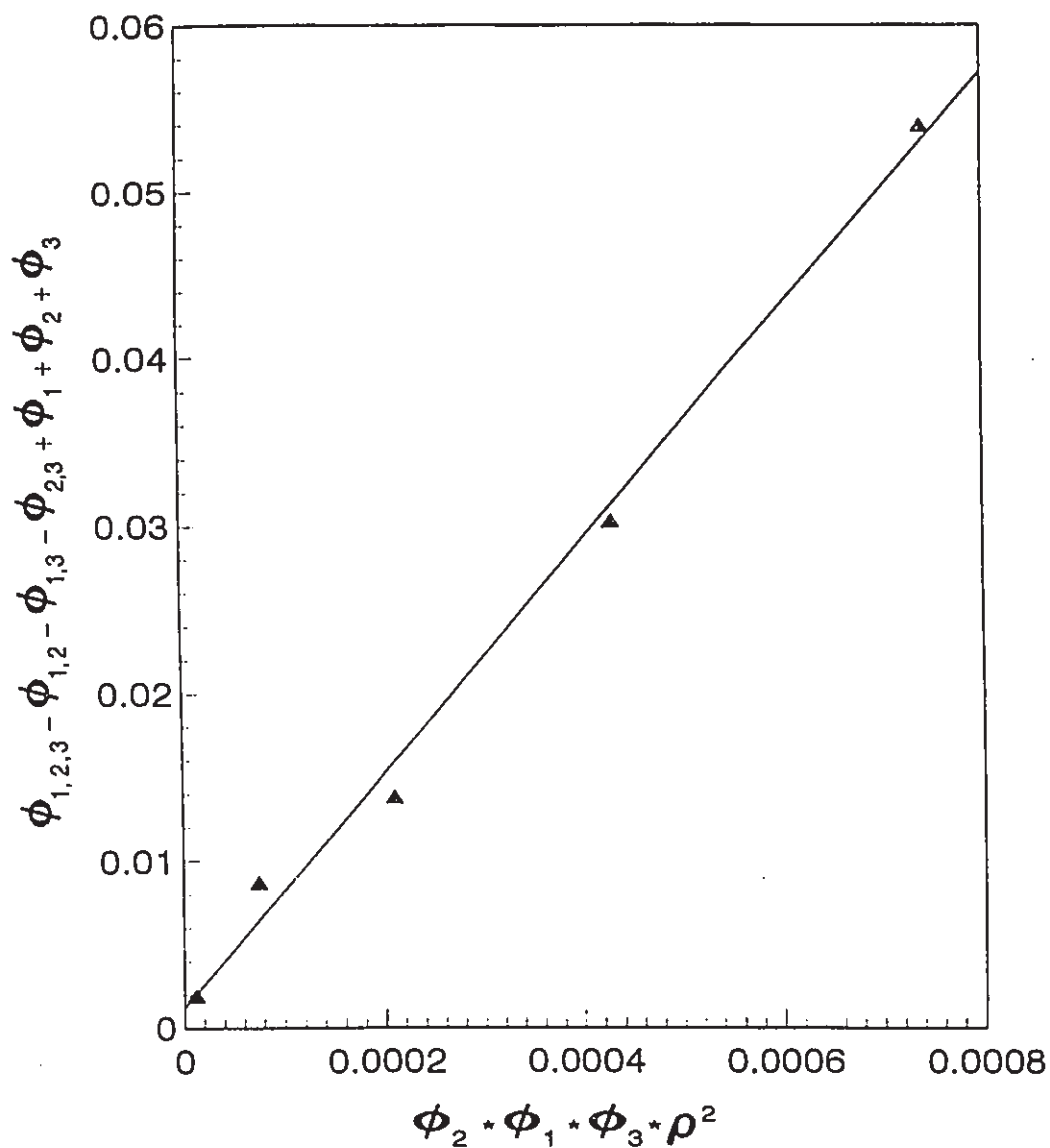


**Figure 20.** Concurrent effect of methylguanidine, methylsuccinic acid and  $\beta$ -mercaptoethanol on the activity of carboxypeptidase-B. The slope of 70 is equivalent to the overall synergistic factor ( $1/\theta$ ). A tripartite interaction constant,  $\tau$  of 1.1 is obtained from the relationship  $\theta/\alpha\beta\gamma=\tau$ . The assay was performed using five [s] of 0.4, 0.8, 1.2, 1.6 & 2.0 mM.

TABLE VI. Summary of equations, slopes and intercepts of combination plots for competitive inhibitors.

Intercepts			
Ordinate	Abscissa	Slope	equation
Plot of $\phi_{12}-\phi_1-\phi_2$ against $\phi_1\phi_2\rho$			
			$\phi_{1,2}-\phi_1-\phi_2-\phi_1\cdot\phi_2\cdot\rho\cdot\frac{1}{\alpha}$ (4)
0	0	$1/\alpha$	
Plot of $(\phi_{12}-\phi_1-\phi_2)/\phi_1\phi_2$ against $[s]/K_m$			
			$\frac{\phi_{1,2}-\phi_1-\phi_2}{\phi_1\phi_2} = \frac{1}{\alpha} \cdot \frac{[s]}{K_m} - \frac{1}{\alpha}$ (6)
$1/\alpha$	-1	$1/\alpha$	
Plot of $(\phi_{12}-\phi_1-\phi_2)/\phi_1\phi_2\rho$ against $1/[i_1]$			
			$\frac{\phi_{1,2}-\phi_1}{\phi_1\phi_2\rho} = \frac{1}{[i_1]} \cdot K_i + \frac{1}{\alpha}$ (7)
$1/\alpha$	$-1/\alpha K_i$	$K_i$	
Plot of $\phi_{123}-\phi_{12}-\phi_{13}-\phi_{23}+\phi_1+\phi_2+\phi_3$ against $\phi_1\phi_2\phi_3\rho^2$			
			$\phi_{123}-\phi_{12}-\phi_{13}-\phi_{23}+\phi_1+\phi_2+\phi_3-\phi_1\phi_2\phi_3\cdot\frac{\rho^2}{\theta}$ (14)
0	0	$1/\theta$	

## 4.2 DISCUSSION

Having recognized the merits of a truly quantitative plot, the combination plot, an improved graphical method for the analysis of enzyme-inhibitor interactions was developed. First and foremost, the plot is quantitative and yields a constant (the slope) which directly measures the extent and nature of interaction between inhibitors on an enzyme. As compared in figures 12 and 13, the synergistic factor ( $1/\alpha$ ) yielded by the combination plot directly matches the reciprocal value of the interaction constant ( $\alpha$ ) obtained with the Yonetani-Theorell plot. In order to confirm this unequivocally, it was necessary to re-analyze kinetic data from the literature (Figures 17 and 18); the result of figure 18, very convincingly, establishes mutual exclusivity of the inhibitors. In fact, this feature of the combination plot represents a major improvement on the Yonetani-Theorell plot and other methods. This is because, more often than not, experimental data points are not error-free, thus inasmuch as one would like to believe a family of lines are parallel (a condition for mutual exclusiveness for the Yonetani-Theorell plot for instance) there is always the probability that they do converge. The combination plot, unquestionably, solves this problem of discerning whether two inhibitors are mutually exclusive or not. In this plot, mutual exclusiveness is unambiguously established when the data points fall on the abscissa as clearly illustrated in figures 18 and 19.

The linear nature of the combination plot ensures its convenience and, more importantly, presents an inherent diagnostic advantage of alerting the experimenter of deviations from the norm. The approach judiciously substitutes a single straight line for a

family of lines in the determination of the interaction constant thus successfully departing from the long-standing tradition in enzymology of employing intercepting lines to determine kinetic constants. Although a version of the median-effect plot (Chou and Talalay, 1981) employs a single line, two other lines representing either of the inhibitors must also be present for comparative purposes. The plot then relies on the observation of a curvature in the line representing both inhibitors to establish synergism. This approach is therefore primarily qualitative and does not aptly describe the quantitative phenomenon. To quantitative synergism, the median-effect plot requires the determination of a Combination Index (CI) which requires a secondary replot of the data. The combination plots, on other hand, requires no replots making it more convenient.

The median-effect plot also suffers in some quantitative aspects with respect to simple enzymic systems. In an effort to achieve a broadly applicable method for the analysis of multi-inhibitor interactions in enzymic as well as complex biological systems, the use of kinetic constants are avoided with this approach. Thus, the Combination Index (CI), which is diagnostic of the type of interaction and calculated from the median-effect of the combination of inhibitors is not truly a constant, as the name suggests, and may vary with the extent and type of inhibition. The physical interpretation of CI may therefore be subject to some uncertainty. Furthermore, the concept of synergism as presented by the median-effect approach becomes unclear when related to simple enzymic systems in some cases. In whole cells and other complex biological systems, it is conceivable that two inhibitors, ligands or drugs may act synergistically while exhibiting mutual exclusive characteristics. For a single active site of an enzyme, the possibility of two or more reversible inhibitors

excluding each other and yet exhibiting synergistic characteristics is virtually non-existent. Thus, with respect to quantitative structure-activity relationships the median-effect approach has limited applicability.

Another merit associated with the linear nature of the combination plot is that it makes the maintenance of fixed proportions of both inhibitors unnecessary as required in the Yagi and Ozawa method (Yagi and Ozawa, 1960). Any combination of inhibitor concentration resulting in different  $\phi$  values can be employed for the analysis. Furthermore, in the isobol method (Loewe, 1957; Webb, 1963), for instance, it is a requirement that two inhibitor concentrations which give identical effects be established in the construction of an isobologram which can be very impractical and time-consuming. Such an approach necessarily precludes the analysis of a not-too-potent inhibitor or drug which becomes potent only in the presence of a synergistic or antagonistic effector. The application of combination plots circumvents these problems. The convenience of the combination plots is further underscored by the interchangeability between  $IC_{50}$  and  $K_i$ . For simple competitive systems,  $IC_{50}$ s may be more readily used for routine determinations, this is accommodated by the plot with no influence on the interaction constant. This is achieved by the introduction of the  $\rho$  factor which takes into account the effect of substrate concentration on the extent and type of inhibition.

Another redeeming feature of the combination plot is the ability to vary the substrate concentration within the same experimental setup as illustrated in figure 14. This flexibility becomes important in situations where anomalous substrate or inhibitor effects may be suspected; the combination plot readily provides a means of trouble-shooting. Several

alternative diagnostic plots may also be used with equal facility when both the substrate and inhibitor concentrations are being varied. Thus, it is now possible to ask whether inhibitors maintain their competitiveness when simultaneously bound. The application of combination plots in enzyme-inhibitor interactions should therefore guard against erroneous interpretation of kinetic data on the basis of unsuspecting substrate or inhibitor effects.

Qualitatively, the combination plot presents a clear and easy way of presenting the effects of several pairs of inhibitors on the same enzyme. This is clearly illustrated in figure 19 where a simple inspection of the different slopes reveals which pairs of inhibitors are synergistic, independent or antagonistic. The value which directly comes out of the Yonetani-Theorell analysis, arguably the most widely used method, presently, for the analysis of such inhibitor effects, is the apparent dissociation constant,  $\alpha K_i$ , thus a knowledge of the dissociation constant is required to fully appreciate its significance. In contrast, the combination plot explicitly reveals the positive or negative nature of the interaction between inhibitors through the value of the slope ( $1/\alpha$ )- the synergistic factor, thus clearly communicating the information. Like other kinetic methods, however, the combination plot is unable to distinguish between antagonism caused by steric hindrance and that caused by the masking of the binding site mediated through a conformational change in the enzyme.

Unlike previous methods with no obvious didactic value, the combination plot successfully provides a meaningful rationale for the phenomenon of synergism. Each  $\phi$  term physically represents the contribution of a particular enzyme-inhibitor species towards the observed rate (see Appendix II ). Thus, when the contribution of each enzyme-inhibitor



species is subtracted from the observed rate, the net effect of the ternary complex is obtained as a linear function of the normalized concentration of both inhibitors. Therefore, when the inhibitors are independent, a slope of 1 indicates no net contribution from the ternary complex in spite of its existence. When the inhibitors are mutually exclusive, because their concentrations have been normalized, the effect of one exactly matches that of the other yielding no observable slope. Mutual exclusiveness is therefore unerringly indicated by all data points lying on the abscissa.

The lack of suitable methods for the analysis of concurrent effects of three inhibitors can be inferred from the virtual absence of literature on structure-activity relationships of inhibitors employing such potentially useful approaches. The combination approach has been successfully extended for the analysis of such interactions for the first time. The plot was employed to analyze the concurrent effects of methylguanidine,  $\beta$ -mercaptoethanol and methylsuccinic acid on carboxypeptidase B. This work demonstrated the practicability of the combination approach. In the example studied, no extra synergism was evident when three pairs of synergistic inhibitors were analyzed concurrently. This result cannot, however, be generalized for the interactions of a triplet of inhibitors. It is conceivable that such studies would be most suited for the analyses of multi-inhibitor interactions in an enzyme with a rather extended active site displaying distinct specificities for subsites.

With the introduction and easy availability of computer curve-fitting software packages which allow for facile and direct application of the most complex of equations, graphical methods for the analysis of kinetic data are gradually being phased out. In certain cases, however, the obvious advantage with respect to the clarity of data presentation,

convenience and inherent didactic value associated with some graphical methods for the analysis of experimental kinetic data argue in favor of their application wherever and whenever necessary. The combination plots clearly fall in this category. The use of the plots for the analysis of concurrent effects of pairs or even triplets of inhibitors on an enzyme offers a lucid approach to the presentation of primary experimental data whereby a simple visual inspection or measure of the slope unambiguously communicates the underlying trend of the analysis even to the uninitiated. Furthermore, the plots are relatively easy-to-use and allow the rapid assessment of enzyme-inhibitor interactions. The plots are quantitative and can also be used for qualitative purposes. They are adaptable to different types of inhibition and can be easily extended for the analysis of interactions among a triplet of inhibitors. Because the use of fixed concentrations of inhibitors or the establishment of an iso-effective concentration is not a pre-requisite, poorly water-soluble inhibitors or less potent inhibitors can be analyzed if a more hydrophilic synergistic or antagonistic conjugate or probe is available.

Finally, the concept of combination plots could have broad application in the analysis of kinetic data in general. The plots simply construct a single straight line from a family of lines that would normally be obtained from such analysis using traditional approaches. Since several kinetic constants are obtained from families of lines, the principles described here should be applicable to other systems; for example the determination of the binding order of substrates in ping-pong kinetics (Segel, 1975).

## 5. INHIBITORS OF CARBOXYPEPTIDASES A AND B

### 5.1 RESULTS

Following the successful development of the combination plots, it was of considerable interest to use them to understand inhibitor interactions in an enzyme to fully appreciate their applicability. Together with similar approaches developed by Hunter and Downs (1945; see Figure 5) and Chan (1994; see Figure 6) for the determination of inhibition constants of a single inhibitor in unireactant enzymic systems, inhibitors of carboxypeptidases A and B were examined.

#### 5.1.1 Carboxylic acid inhibitors of carboxypeptidases A and B

Several carboxylic acid inhibitors of carboxypeptidase B were examined in an attempt to understand ligand interactions in this enzyme. 2-Ethyl-2-methylsuccinic acid turned out to be an unusually potent, reversible competitive inhibitor ( $K_i$   $3.4 \times 10^{-6}$  M) of the enzyme in view of its rather small size. Its mode of inhibition did not involve a probable sequestration of the essential zinc cation at the active site since a 72-hour incubation failed to reveal a time-dependent increase in its inhibitory potency. On the other hand, diluting the inhibitor concentration reduced its net inhibitory effect on the activity of the enzyme. Although numerous reports of inhibitors of carboxypeptidases A and B have been made (Byers and Wolfenden, 1973, 74; McKay and Plummer, 1978; Jacobsen and Bartlett, 1981; Ondetti *et al.*, 1979; Kaplan and Bartlett, 1991), disubstituted alkyl derivatives of dicarboxylic acids have not been reported.

Table VII. Carboxylic acid inhibitors of carboxypeptidase B<sup>a</sup>.

Carboxylic acid	K <sub>i</sub> (mM)	mode of inhibition
2-Ethyl-2-methylsuccinic acid <sup>b</sup>	0.0034	competitive
2,2-Dimethylsuccinic acid	0.028	competitive
Methylsuccinic acid <sup>b</sup>	4	competitive
Succinic acid <sup>c</sup>	28	competitive
meso 2,3-Dimethylsuccinic acid	44	competitive
Butyric acid	203	partial mixed
Succinamic acid	232	partial noncompetitive
Isobutyric acid	>200	partial mixed
Propionic acid	140	partial mixed
Pivalic acid	>200	-- <sup>d</sup>

<sup>a</sup>Assays were carried out as described under materials and methods. Maximum standard deviation in values is less than 20%.<sup>b</sup> A mixture of R & S stereoisomers were used thus the value given represents the upper limits of the inhibition constants. <sup>c</sup>Chan and Pfuetzner (1993) reported K<sub>i</sub> of 38 mM. <sup>d</sup>This compound acted as an activator under the assay conditions. 200 mM pivalic acid (3,3-dimethylpropionic acid) increased enzyme activity by 10%.

Structure-activity relationships of several carboxylic acids (Table VII) were therefore explored in an effort to elucidate the origins of the remarkable affinity of 2-ethyl-2-methylsuccinic acid for carboxypeptidase B. Decreasing the hydrophobic nature of the inhibitor by replacing the ethyl group with a methyl group decreased the affinity of the compound over 8-fold (Table VII). Elimination of the ethyl group reduced the potency of the compound by three orders of magnitude. A comparison of the  $K_i$ s of 2,2-dimethylsuccinic acid and methylsuccinic acid shows a reduction in potency of 140-fold with the removal of one of the methyl groups of the former. The weaker affinity of meso 2,3-dimethylsuccinic acid compared to succinic acid suggests that hydrophobicity alone does not adequately account for the observed potency and therefore specific structural features of the inhibitors are important. The absence of the dialkyl functional group leads to inhibitors with potencies three orders of magnitude lower. Thus, it appears the presence of a *gem*-dialkyl substitution on the parent succinic acid structure is a major contributing factor to the unusual potency of these inhibitors.

From table VII it is evident that removal of one of the carboxyl groups affects the specific binding of the inhibitor to the enzyme. Furthermore, the affinity of the monocarboxylic acids become substantially reduced. Thus, conversion of succinic acid into succinamic acid (a free carboxylic acid to an amide), resulted in a weaker inhibitor which exhibited non-linear binding characteristics. Substituting a methyl group for one of the carboxyl groups of succinic acid similarly resulted in an inhibitor, butyric acid, with hyperbolic binding characteristics and a much reduced affinity. Complete elimination of one of the carboxyl groups of the basic succinic acid structure also gave a weaker, hyperbolic

inhibitor, propionic acid. The hyperbolic binding characteristics of propionic acid was not repressed when assayed in the presence of either  $\beta$ -mercaptoethanol or methylguanidine, two competitive inhibitors of carboxypeptidase B which are expected not to bind to the cognate site(s) of propionic acid (Chan and Pfuetzner, 1993). Pivalic acid (3,3-dimethylpropionic acid) which corresponds to 2,2-dimethylsuccinic acid without the extra carboxyl moiety  $\alpha$  to the *gem*-dialkyl groups, surprisingly acted as an activator of the enzyme. The presence of the second carboxyl group therefore appears to properly anchor or orient the inhibitor within the active site through presumably the elimination of nonproductive binding resulting in a more potent inhibitor.

To ascertain whether the potency of the *gem*-dialkyl inhibitors were of a specific nature, the dicarboxylic acid inhibitors were also assessed on the closely related carboxypeptidase A (Table VIII). Binding potencies and characteristics followed trends previously observed for the mechanistically similar carboxypeptidase B with differences only in the magnitude of inhibitory potency. All the inhibitors showed higher potencies for carboxypeptidase A than for B. This observation was not unexpected in view of the greater preference for hydrophobic groups in this enzyme (Ondetti *et al.*, 1979; Zisapel and Sokolovsky, 1973). With a dissociation constant of  $1.1 \times 10^{-7}$  M for the *gem*-dialkyl inhibitor, 2-ethyl-2-methylsuccinic acid on carboxypeptidase A was surprisingly more potent than the well-known potent bi-product analogue, L-benzylsuccinic acid ( $K_i$   $4.5 \times 10^{-7}$  M) (Byers and Wolfenden, 1972, 1973). This observation clearly underscored the remarkable potency associated with the *gem*-dialkyl succinic acid derivatives.

TABLE VIII. Dissociation constants for dicarboxylic acid inhibitors on carboxypeptidase A<sup>a</sup>.

Dicarboxylic acid	K <sub>i</sub> (mM)
2-Ethyl-2-methylsuccinic acid	0.00011
2,2-Dimethylsuccinic acid	0.0016
Methylsuccinic acid	0.3
Succinic acid <sup>b</sup>	4
Meso 2,3-dimethylsuccinic acid	6.6
L - Benzylsuccinic acid	0.00045 <sup>c</sup>

<sup>a</sup>The maximum standard error in the determined dissociation constants was  $\pm 15\%$ . <sup>b</sup>K<sub>i</sub> = 28 mM (Chan and Pfuetzner, 1993); K<sub>i</sub> = 0.4 mM (Byers and Wolfenden, 1973). <sup>c</sup>Datum from Byers and Wolfenden (1973).

### 5.1.2 Interaction between two inhibitors: carboxypeptidase B

To further explore, kinetically, the nature of interaction of the *gem*-dialkyl inhibitors within the active site of carboxypeptidase B, the concurrent effect of pairs of inhibitors were examined. The independent dissociation constants of the zinc ligands and guanidine probes are given in table IX. All the inhibitors bound to the enzyme in a purely competitive fashion. As shown in table X, the interaction between the guanidine homologues and the succinic acid derivatives examined were all observed to be synergistic with the highest synergism observed for the interaction between guanidine and the respective dicarboxylic acids. The synergistic factor of 128 between guanidine and meso 2,3-dimethylsuccinic acid approximates the highest level previously observed in a zinc protease (Pfuetzner and Chan, 1988). It is intriguing that with the possible exception of meso 2,3-dimethylsuccinic acid, the interaction constants between the dicarboxylic acids and the guanidines were all not significantly different.

The fact that the dicarboxylic acid inhibitors are not transition-state or substrate analogues and supposedly do not resemble chemical intermediates generated during the catalytic process may have some bearing on the statistically similar synergistic factors. It is conceivable that the lack of very distinctive structural features among the inhibitors results in the similar responses. Alternatively, the observed synergism may result from a contribution of varying degrees of positive and negative interactions from the different inhibitors. Substitution of methylguanidine for guanidine resulted in a decrease in synergism for all the dicarboxylic acid inhibitors suggesting the lack of room in the presence of an extra methyl group. Contrary to expectation, this trend was not followed when a bulkier



TABLE IX. Zn ligands and Guanidine inhibitors of Carboxypeptidase B<sup>a</sup>.

Zn ligand		Guanidine homologue	
Compound	K <sub>i</sub> (mM)	Compound	K <sub>i</sub> (mM)
Formohydroxamic acid	80 ± 10	Guanidine	1 ± 0.1
Acetohydroxamic acid	150 ± 21	Methylguanidine	1.5 ± 0.2
β-mercaptoethanol	5 ± 1	Ethylguanidine	3.1 ± 0.4

<sup>a</sup>All the above compounds were previously shown by Chan and Pfuetzner (1993) to be competitive inhibitors of carboxypeptidase B with similar dissociation constants using Dixon plots (1953). The K<sub>i</sub>s reported here were obtained by the methods of Hunter and Downs (1945) and Chan (1994).

TABLE X. Synergistic factors ( $1/a$ ) for the concurrent effects between Carboxylic acids and Guanidine homologues on Carboxypeptidase B<sup>a</sup>.

Carboxylic acid	Guanidine homologues		
	Guanidine	Methylguanidine	Ethylguanidine
Succinic acid	78	30	61
Methylsuccinic acid	68	25	29
2,2-Dimethylsuccinic acid	85	18	82
Meso 2,3-dimethylsuccinic acid	128	29	106

<sup>a</sup>Synergistic factors were determined as described in text. Maximum error in synergistic factor determination is about 20 %.

ethylguanidine was subsequently employed. The anomalous binding mode of ethylguanidine was also evident when the effect of formohydroxamic acid on the binding of the guanidine homologues was examined (Table XI). While the interaction between guanidine and formohydroxamic acid dropped two-fold when methylguanidine served as the guanidine homologue, enhanced synergism was observed with the bulky but less potent ethylguanidine. The results indicate that ethylguanidine probably binds in an orientation different from the other guanidine homologues.

The marked difference in synergism between methylsuccinic acid and guanidine compared to succinic acid and methylguanidine (Table X) suggest that the methyl groups of the corresponding inhibitors presumably do not occupy the same locus. Whether the binding sites of these methyl groups are equivalent to or are different from the binding site of the *gem* dialkyl groups cannot be clearly established by these kinetic analyses.

The effect of the zinc ligands, formohydroxamic acid and  $\beta$ -mercaptoethanol, on the binding of the succinic acid derivatives is presented in table XII. As indicated, formohydroxamic acid reduced the affinity of the enzyme for succinic acid five-fold. This negative interaction retrogressed into mutual exclusiveness when  $\beta$ -mercaptoethanol substituted as the zinc ligand. Formohydroxamic acid also interfered with the binding of meso 2,3-dimethylsuccinic acid, however, unlike the scenario observed for succinic acid,  $\beta$ -mercaptoethanol reversed the negative interaction and synergized with meso 2,3-dimethylsuccinic acid increasing its affinity for the enzyme by a factor of three. The opposite effect of  $\beta$ -mercaptoethanol on the meso compound does not appear to be a result of an alternative binding mode since the zinc ligands are mutually exclusive on the enzyme.

TABLE XI. Synergistic factors ( $1/\alpha$ ) for the interaction between Formohydroxamic acid and Guanidine homologues on Carboxypeptidase B<sup>a</sup>.

Guanidine Homologue	synergistic factor ( $1/\alpha$ )
Guanidine	10 ± 2
Methylguanidine	6 ± 1
Ethylguanidine	18 ± 4

<sup>a</sup>Assays for the determination of synergistic factors were as described under materials and methods.

TABLE XII. Synergistic factors ( $I/a$ ) for the interaction between zinc ligands and Dicarboxylic acids on Carboxypeptidase B<sup>a</sup>.

Dicarboxylic acid	synergistic factor ( $I/a$ )	
	Formohydroxamic acid	$\beta$ -Mercaptoethanol
Succinic acid	$0.2 \pm 0.06$	<0.1
Meso 2,3-dimethylsuccinic acid	$0.5 \pm 0.1$	$3.1 \pm 0.6$
Methylsuccinic acid	$2.6 \pm 0.6$	$2.6 \pm 0.2$
2,2-Dimethylsuccinic acid	$2.1 \pm 0.5$	$5.5 \pm 0.5$

<sup>a</sup>Assays for the determination of synergistic factors were as described under materials and methods.

Subtle differences in binding can, however, influence the observed differences. Methylsuccinic acid and 2,2-dimethylsuccinic acid both interact synergistically to about the same extent with formohydroxamic acid. While this synergistic interaction is to a large extent maintained for methylsuccinic acid, it is doubled for 2,2-dimethylsuccinic acid with  $\beta$ -mercaptoethanol as the zinc ligand. Thus substitution of methyl groups on the methylene carbons of succinic acid appears not only to reduce interference in the presence of the zinc ligands but, in fact, promote synergism between the inhibitors.

### 5.1.3 Concurrent effect of three inhibitors

Chan and Pfuetzner (1993) previously observed synergism between pairs of inhibitors in carboxypeptidase B and suggested the existence of separate or overlapping binding sites for a zinc ligand, a basic compound and a carboxyl-containing inhibitor. In that study, however, a direct interaction between the carboxyl-recognition site and the zinc-ligand binding site was not investigated. Although, this has been accomplished in the current study, the data could still be interpreted in favor of alternate binding modes in regions of dual specificities. This problem was addressed by directly examining the concurrent effect of three purely competitive inhibitors of carboxypeptidase-B. The nature and extent of interaction between methylguanidine, methylsuccinic acid and  $\beta$ -mercaptoethanol was analyzed by extending the combination approach to accommodate the combinatorial effect of three inhibitors.

Figure 20 shows the concurrent effect of methylguanidine, methylsuccinic acid and  $\beta$ -mercaptoethanol on carboxypeptidase B investigated with the aid of a combination plot.

A tripartite interaction constant,  $\tau$ , of  $1.1 \pm 0.3$  indicated that no additional synergistic effect is elicited upon the simultaneous application of the three inhibitors. Substituting guanidine for methylguanidine did not significantly change the tripartite interaction constant ( $\tau = 0.8 \pm 0.3$ ). The result indicated that, in this particular case, synergism was simply cumulative and reflected what was observed when the inhibitors were used in pairs.

## 5.2 DISCUSSION

In an attempt to understand the nature of inhibitor interactions at the active site of carboxypeptidase B, a novel class of competitive inhibitors, the *gem*-dialkyl succinic acid derivatives has been found. 2-Ethyl-2-methylsuccinic acid turned out to be most effective with a  $K_i$  of  $3.4 \times 10^{-6}M$  which is remarkably potent for an inhibitor of its size. The basis of the high inhibitory potency associated with such a compound, if understood, could serve as a paradigm for the design of even more potent inhibitors for several related enzymes including pharmacologically important ones such as angiotensin-converting enzyme (Cushman *et al.*, 1977) which is also a zinc protease. This inhibitor was even more potent on the structurally and mechanistically related carboxypeptidase A ( $K_i$   $1.1 \times 10^{-7}M$ ). Elimination of both *gem*-dialkyl groups reduces inhibitory potency over 8000 fold and competitive inhibition is lost when one of the carboxyl moieties is removed. The activatory effect of pivalic acid, the hyperbolic binding characteristics of propionic and butyric acids together with the anomalous binding of ethylguanidine are consistent with multiple bind sites within the active site. Thus different sites possibly control the different kinetic effects

observed with the inhibitors. A similar conclusion was reached by Abramovich and co-workers (1973) by analyzing peptide substrates of this enzyme. A model for multiple binding sites in the related carboxypeptidase A has also been advanced by Vallee and co-workers (1970). Thus, through the use of inhibitor binding synergism, the existence of multiple binding modes can be confirmed for carboxypeptidase B.

The increased affinity associated with the presence of two carboxyl moieties on the succinic acid derivatives suggests the existence of two carboxyl recognition sites in carboxypeptidases A and B; this effect is well-known and has been variously addressed (Byers and Wolfenden, 1973; Ondetti *et al.*, 1979; McKay and Plummer, 1978; Jacobsen and Bartlett, 1981). The potential binding sites, the catalytically essential zinc atom and Arg-145 (carboxypeptidase A numbering system), are known from X-ray crystallographic analysis (Rees *et al.*, 1983; Schmid and Herriot, 1976). The crucial question in this case was how the presence of the *gem*-dialkyl inhibitors influenced the binding orientation of the carboxyl groups. Since the primary determinant of specificity in the carboxypeptidases is Arg-145, binding of one of the carboxyls could be expected; although the size of the inhibitors may result in a binding mode different from that of a typical substrate of the enzyme. That a carboxyl-recognition binding site was or overlapped the zinc-ligand binding site was explored by examining the concurrent effects of zinc ligands, formohydroxamic acid and  $\beta$ -mercaptoethanol on the one hand, and the dicarboxylic acids on the other. Although the binding of succinic acid and the zinc ligands seemed antagonistic or even mutually exclusive, the situation was different for the succinic acid derivatives (Table XII). The pattern of inhibitor binding synergism between the dicarboxylic acids and the zinc



ligands on carboxypeptidase B showed that the presence of the alkyl substitution reduces the negative interactions with the zinc ligands and may even result in a positive interaction. This observation will be more consonant with the carboxyl group  $\alpha$  to the alkyl substitutions binding closer to the zinc ligands. An inspection of the  $pK_a$  values of the dicarboxylic acid inhibitors show good correlation with synergism (Appendix III), thus an increase in  $pK_{a2}$  concomitant with a decrease in  $pK_{a1}$  appear to favor synergism. This will be consistent with the protonated form of the carboxylic acid being better accommodated in the vicinity of the zinc-ligand binding site rather than the carboxylate anion.

The significance of this synergism- $pK_a$  dependency is not entirely clear since both carboxyl groups would be expected to be primarily charged under the assay conditions (pH 7.5). However, if the xerophilic-shift mechanism of Chan and Pfuetzner (1993), is operative then one might expect such a correlation. The hypothesis explains the role of synergism in catalysis by proposing that upon the binding of one inhibitor to the enzyme, a conformational change in the protein ensues which increases the enzyme's affinity for the second inhibitor. Subsequently, when water is excluded from the active site upon the binding of both inhibitors, a shift in the  $pK$  of an essential ionizable residue at the active site is postulated to occur which converts the enzyme into a catalytically competent form. Such a mechanism could be envisioned to act analogously on the carboxylic acid inhibitors. This correlation is, therefore, what would be expected if the binding site of the second carboxyl group  $\alpha$  to the substituted carbon either overlaps the zinc ligand binding site or is in close proximity to it; since a higher  $pK$  through electron-donating inductive effect would be expected upon methyl substitution.

Alternatively, the phenomenon could be primarily due to the sheer presence of the alkyl groups which presumably interact favorably within a putative *gem*-dialkyl binding region thereby influencing the synergistic response. The active site of carboxypeptidase B contains a hydrophobic core at the bottom of which sits the specificity-determining Asp-255 which might contain such a site. Although  $pK_{a1}$  and  $pK_{a2}$  for meso 2,3-dimethylsuccinic acid are lower than those for succinic acid it interacts more positively with the zinc ligands than succinic acid. This greater positive interaction of meso 2,3-dimethylsuccinic acid with the zinc ligands suggests alkyl substitution may be the dominating influence since a more acidic inhibitor would be expected to interfere with the zinc ligands. This interpretation would be consistent with the decreasing interference or increasing synergism observed with alkyl substitution. Both mechanisms, however, could conceivably operate concurrently and may not necessarily be mutually exclusive.

The study on the effect of three competitive inhibitors of carboxypeptidase B clearly confirmed the existence of three binding sites for the three types of inhibitors analyzed. That a tripartite interaction constant of almost unity was observed is revealing. This intriguing observation indicates that in spite of the presence of the third inhibitor similar binding characteristics and interactions are presumably maintained between pairs of inhibitors under a situation where the active site could accommodate all three. The possibility that compensatory positive and negative interactions occur within the quaternary complex cannot, however, be totally discounted but is unlikely. The result clearly confirms that, minimally, there exist three separate or overlapping binding sites specific for a carboxylic acid, a zinc ligand and a basic inhibitor within the active site of carboxypeptidase-B which

was inferred from the investigations on pairs of inhibitors (Chan and Pfuetzner, 1993).

Since 2-ethyl-2-methylsuccinic acid is not a transition-state analogue and cannot be strictly classified as a product analogue, it is concluded that the tight binding of the inhibitor on the carboxypeptidases is a result of its opportunistic ability to interact favorably with the zinc proteases in some respects. Based on the tremendous affinity associated with the *gem*-dialkyl groups and perhaps their influence on  $pK_a$  values of the carboxyl groups coupled to the specificity contributed by the extra carboxyl group, it is suggested that 2-ethyl-2-methylsuccinic acid simultaneously interacts with the carboxyl-recognition site, presumably co-ordinates to the essential zinc atom while making extremely favorable van der Waals' contacts within the hydrophobic core of the active site ie. a putative "*gem*-dialkyl binding site" in the carboxypeptidases. It is hard to imagine how such a "small" inhibitor could derive the binding energy associated with its potency. Could the inhibitor be exploiting some as yet undefined aspect of the catalytic mechanism of the carboxypeptidases? The presence of a *gem*-dialkyl substituent apparently potentiates the inherent characteristics of an inhibitor. Thus pivalic acid acted as a better activator than propionic acid while 2,2-dimethylsuccinic acid was a more potent competitive inhibitor than succinic acid. It is interesting that the *gem*-dialkyl group would be located at the bond that would normally be susceptible to cleavage during a routine catalytic turnover assuming the carboxyl moiety  $\alpha$  to the substitution binds the zinc atom. It is also remembered from the work of Byers and Wolfenden (1973) that dicarboxylic acids longer or shorter than succinic acid are weaker inhibitors of carboxypeptidase A. The nature of these effects coupled with the unusual potency of the *gem*-dialkyl inhibitors thus hint at a potential role in catalysis. Exactly how

a *gem*-dialkyl group would marshal some aspect(s) of the catalytic apparatus in influencing these potentiating effects is intriguing. Further details regarding the possible role of these substituents in exerting the remarkable affinity on the carboxypeptidases would however, require structural analysis of the enzyme-inhibitor co-complex.

The binding orientation of these inhibitors cannot be predicted with any certainty based on the kinetic data. However, if the alternate-binding mode hypothesis advanced by Ondetti and co-workers (1979) to explain the lack of specificity of L-benzylsuccinic acid on these two enzymes is invoked, then one may speculate that the inhibitor would bind in an orientation identical to a normal substrate in carboxypeptidase A with the carboxyl group  $\alpha$  to the alkyl-substituted carbon binding within the carboxyl-recognition site (Arg-145). This orientation will then be reversed in carboxypeptidase B with the carboxyl group  $\alpha$  to the substituted carbon binding closer to the catalytically essential zinc atom.

## 6. APPENDICES

6.1 **APPENDIX I:** Kinetic equation describing effect of three mutually nonexclusive competitive inhibitors.

On the assumption that the inhibitors bind the enzyme reversibly and that binding neither involves covalent interactions nor appreciably deplete inhibitors or substrate, then the following equation is satisfied at equilibrium.

$$[E_T] = [E] + [ES] + [Ei_1] + [Ei_2] + [Ei_3] + [Ei_1i_2] + [Ei_1i_3] + [Ei_2i_3] + [Ei_1i_2i_3] \quad (16)$$

since  $v = k_{cat}[ES]$  and  $V_{max} = k_{cat}[E_T]$

$$\frac{v}{V_{max}} = \frac{[ES]}{[E] + [ES] + [Ei_1] + [Ei_2] + [Ei_3] + [Ei_1i_2] + [Ei_1i_3] + [Ei_2i_3] + [Ei_1i_2i_3]} \quad (17)$$

Substituting for the various enzyme-inhibitor complexes gives

$$\frac{v}{V_{max}} = \frac{\frac{[E][s]}{K_m}}{[E] + \frac{[E][s]}{K_m} + \frac{[E][i_1]}{K_{i_1}} + \frac{[E][i_2]}{K_{i_2}} + \frac{[E][i_3]}{K_{i_3}} + \frac{\frac{[E][s]}{K_m}}{\alpha K_{i_1}K_{i_2}} + \frac{\frac{[E][s]}{K_m}}{\beta K_{i_1}K_{i_3}} + \frac{\frac{[E][s]}{K_m}}{\gamma K_{i_2}K_{i_3}} + \frac{\frac{[E][s]}{K_m}}{\theta K_{i_1}K_{i_2}K_{i_3}}}$$

which can be simplified to give equation (19) (equivalent to equation (12)) describing the interaction between three linear competitive inhibitors acting concurrently on an enzyme

$$v = \frac{V_{\max} [s]}{K_m \left( 1 + \frac{[i_1]}{K_{i_1}} + \frac{[i_2]}{K_{i_2}} + \frac{[i_3]}{K_{i_3}} + \frac{[i_1][i_2]}{\alpha K_{i_1} K_{i_2}} + \frac{[i_1][i_3]}{\beta K_{i_1} K_{i_3}} + \frac{[i_2][i_3]}{\gamma K_{i_2} K_{i_3}} + \frac{[i_1][i_2][i_3]}{\theta K_{i_1} K_{i_2} K_{i_3}} \right) + [s]} \quad (19)$$

where the overall interaction constant,  $\theta = \tau \alpha \beta \gamma$

and  $\alpha$  is the interaction constant between inhibitors 1 and 2

$\beta$  " " " 1 and 3

$\gamma$  " " " 2 and 3

$\tau$  is the tripartite interaction constant resulting from the quaternary  $Ei_1i_2i_3$  complex.

6.2 APPENDIX II: Definition of  $\phi$ .

Assuming Michaelis-Menten kinetics for a competitively inhibited enzyme, the following species exist: E, ES & Ei

where

$$[E_T] = [E] + [Ei] + [ES] \quad (20)$$

on the assumption that rapid equilibrium conditions prevail, equation (20) can be simplified to

$$\frac{[E_T]}{[E]} - \frac{[i]}{K_i} = 1 + \frac{[S]}{K_m} \quad (21)$$

Introducing  $IC_{50}$  (see equation (5)) gives

$$\frac{[E_T]}{[E]} \cdot K_i - [i] = IC_{50} \quad (22)$$

since  $K_i = [E][i]/[Ei]$ , equation (22) can be transformed to

$$\frac{[Ei]}{[E_T] - [Ei]} = \frac{[Ei]}{[E] + [ES]} = \frac{[i]}{IC_{50}} = \phi \quad (23)$$

6.3 APPENDIX III: Ionization constants for dicarboxylic acid inhibitors of carboxypeptidases B<sup>a</sup>.

---

Inhibitor	pK <sub>a1</sub>	pK <sub>a2</sub>
Succinic acid	4.19	5.48
Methylsuccinic acid	4.13	5.64
2,2-Dimethylsuccinic acid	4.11	6.13
Meso 2,3-dimethylsuccinic acid	3.77	5.36

---

<sup>a</sup>Data from CRC Handbook of Biochemistry selected data for Molecular Biology (Edited by Sober, H. A. (1968) The Chemical Rubber Co. Cleveland, OH).



## 7. REFERENCES

- Abramovitz, N., Schechter, I., and Berger, A. (1967)** On the size of the active site in proteases II. Carboxypeptidase-A. *Biochem. Biophys. Res. Commun.* 29: 862-867.
- Aoyagi, T., Morishima, H., Nishazawa, R., Kunimoto, S., Takeuchi, T., Umezawa, H. and Ikzawa, H. (1972)** Biological activity of pepstatins, pepstatone A and partial peptides on pepsin, cathepsin D and renin. *J. Antibiot.* 25: 689-694.
- Auld, D.S., and Vallee, B.S. (1987)** In *Hydrolytic Enzymes* (A. Neuberger and K. Brocklehurst, Eds.,) pp. 201-255, Elsevier Science Publishers, New York, NY.
- Barrett, A.J. (1977)** *Proteinases in mammalian tissues and cells* (Ed. Barrett, A.J) North-Holland Publishing Co. Amsterdam. The Netherlands.
- Bendall, M.R., Cartwright, I.L., Clart, P.L., Lowe, G. and Nurse, D. (1977)** Inhibition of papain by N-acyl-aminoacetaldehydes and N-acyl-aminopropanones. *Eur. J. Biochem.* 79: 201-209.
- Billich, S., Knoop, M-T., Hansen, j., Strop, P., Sedlacek, J., Mertz, R., and Moelling, K. (1988).** Synthetic peptides as substrates and inhibitors of human immunodeficiency virus type 1 protease. *J. Biol. Chem* 263: 17905-17908.
- Blow, D.M. (1976)** Structure and mechanism of chymotrypsin. *Acct. Chem. Res.* 9: 145-152.
- Blow, D.M. Birktoft, J.J., and Hartley, B.S. (1969)** Role of a buried acidic group in the mechanism of action of chymotrypsin. *Nature* 221: 337-340.
- Blow, D.M. and Steitz, T.A. (1970)** X-ray diffraction studies of enzymes. *Annu. Rev. Biochem.* 39: 63-100.
- Blumenstein, J.J., Copeland, T.D., Oroszlan, S., and Michejda, C.J. (1989)** Synthetic non-peptide inhibitors of HIV protease. *Biochem. Biophys. Res. Commun.* 163: 980-987.
- Boger, J., Lohr, N.S., Ulm, E.H., Poe, M., Blaine, E.H., Fanelli, G.M., Lin, T.Y., Payne, L.S., Schorn, T.W., LaMont, B.I., Vassil, T.C., Stabilito, I.I., Veber, D.F., Rich, D.H., and Bopari, A.S. (1983)** Novel renin inhibitors containing the amino acid statine. *Nature* 303: 81-84.
- Bone, R., Vacca, J.P., Anderson, P.S., & Holloway, K.M. (1991)** X-ray crystal structure of the HIV protease complex with L-700,417, an inhibitor with pseudosymmetric C<sub>2</sub> symmetry. *J. Amer. Chem. Soc.* 113: 9382-9384.

- Breslow, R., and Wernick, D.** (1977) Unified picture of mechanisms of catalysis by carboxypeptidase A. *Proc. Natl. Acad. Sci. USA* 74: 1303-1307.
- Burbaum, J.J., Raines, R.T., Albery W.J., and Knowles, J.R.** (1989) Evolutionary optimization of the catalytic effectiveness of an enzyme. *Biochemistry* 28: 9293-9305.
- Byers, L.D., and Wolfenden, R.** (1972) A potent reversible inhibitor of carboxypeptidase A. *J. Biol. Chem.* 247: 606-608.
- Byers, L.D., and Wolfenden, R.** (1973) Binding of by-product analog benzylsuccinic acid by carboxypeptidase A. *Biochemistry* 12: 2070-2078.
- Cameron, C.E., Grinde, B., Jacques, P., Leis, J., Wlodawer, A. and Weber, I.T.** (1993) Comparison of the substrate-binding pockets of the Rous sarcoma virus and human immunodeficiency virus type 1 proteases. *J. Biol. Chem.* 268: 11711-11720.
- Chan, W.W-C** (1994) *Private communication.*
- Chan, W.W-C. and Pfuetzner, R.A.** (1993) General occurrence of binding synergism in zinc proteases and its possible significance. *Eur. J. Biochem.* 218: 529-534.
- Christianson, D.W. and Lipscomb, W.N.** (1989) Carboxypeptidase A. *Accts. Chem. Res.* 22:62-69.
- Chou, T.-C. and Talalay, P.** (1983) Analysis of combined drug effects: a new look at a very old problem. *TIPS* November, 450-454.
- Chou, T.-C. and Talalay, P.** (1981) Generalized equations for the analysis of inhibition of Michaelis-Menten and higher-order kinetic systems with two or more mutually exclusive and nonexclusive inhibitors. *Eur. J. Biochem.* 115: 207-216.
- Coleman, J.E. and Vallee, B.L.** (1960) Metallo-carboxypeptidases. *J. Biol. Chem.* 235: 390-395.
- Cushman, D.W., Cheun, H.S., Sabo, E.F., and Ondetti, M.A.** (1977) Design of potent competitive inhibitors of angiotensin-converting enzyme. Carboxyalkanoyl and mercaptoalkanoyl amino acids. *Biochemistry* 16: 5484-5490.
- Darke, P.L., Nutt, R.F., Brady, S.F., Garsky, V.M., Ciccarone, T.M., Leu, C-T., Lumma, P.K., Freidinger, R.M., Veber, D.M., and Sigal, I.S.,** (1988) HIV-1 protease specificity of peptide cleavage is sufficient for processing of *gag* and *pol* polyproteins. *Biochem. Biophys. Res. Commun.* 156: 297-303.
- Debouck, C.** (1992) The HIV-1 protease as a therapeutic target for AIDS. *AIDS Res.*

*Human Retro.* 8: 153-164.

**Debouck, C., Gorniak, J.G., Strickler, J.E., Meek, T.D., Metcalf, B.W. and Rosenberg, M.** (1987) Human immunodeficiency virus protease expressed in *Escherichia coli* exhibits autoprocessing and specific maturation of the gag precursor. *Proc. Natl. Acad. Sci. USA* 84: 8903-9006.

**DelMar, E.G., Largman, C., Brodrick, J.W. and Geokas, M.C.** (1979) A sensitive new substrate for chymotrypsin. *Anal. Biochem.* 99:316-320.

**DiGregorio, M., Pickering, D.S. and Chan, W.W.-C.** (1988) Multiple sites and synergism in the binding of inhibitors to microsomal aminopeptidase. *Biochemistry* 27: 3613-3617.

**Dixon, M.** (1952) The determination of enzyme inhibitor constants. *Biochem. J.* 55: 170-171.

**Dreyer, G.B., Boehm, J.C., Chenera, B., DesJarlais, R.L., Hassell, A. Meek, T.D., Tomaszek, T.A. and Lewis, M.** (1993) A symmetric inhibitor binds HIV-1 protease asymmetrically. *Biochemistry* 32: 937-947.

**Dreyer, G.B., Metcalf, B.W., Tomaszek, T.A. Jr., Carr, T.J., Chandler, A.C. III, Hyland, L., Fakhoury, S.A., Magaard, V.W., Moore, M.L., Strickler, J.E., Debouck, C. and Meek, T.D.** (1989) Inhibition of human immunodeficiency virus 1 protease *in vitro*: Rational design of substrate analogue inhibitors. *Proc. Natl. Acad. Sci. USA* 86: 9752-9756.

**Dunn, B.M. and Kay, J.** (1992) Substrate specificity and inhibitors of aspartic proteases. *Scand. J. Clin. Lab. Invest;* 52 (Suppl. 210): 23-30.

**Epps, D.E., Cheney, J., Schostarez, H., Sawyer, T.K., Prairie, M., Krueger, W.C. and Mandel, F.** (1990) Thermodynamics of the interaction of inhibitors with the binding site of recombinant human renin. *J. Med. Chem.* 33: 2080-2086.

**Erickson, J., Neidhart, D.J., VanDrie, J., Kempf, D.J., Wang, X.C., Norbeck, D.W., Plattner, J.J., Rittenhouse, J.W., Turon, M., Wideburg, N., Kohlbrenner, W.E., Simmer, R., Helfrich, R., Paul, D.A. and Knigge, M.** (1990) Design, activity, and 2.8 Å crystal structure of a C<sub>2</sub> symmetric inhibitor complexed to HIV-1 protease. *Science* 249: 527-533.

**Feder, J.** (1968) A spectrophotometric assay for neutral protease. *Biochem. Biophys. Res. Commun.* 32: 326-332.

**Fersht, A.** (1977) *Enzyme structure and mechanism*. 2nd Edition. W.H Freeman and Co. New York. NY.

**Fitzgerald, P.M.D., McKeever, B.M., VanMiddlesworth, J.F., Springer, J.P., Heimbach,**

J.C., Leu, C-T., Herber, W.K., Dixon, R.A.F. and Darke, P.L. (1990) Crystallographic analysis of a complex between human immunodeficiency virus type 1 protease and acetyl-pepstatin at 2.0Å resolution. *J. Biol. Chem.* 265: 14209-14219.

Folk, J.E., Piez, K.A., Carroll, W.R., and Gladner, J.A. (1960) Carboxypeptidase B. IV. Purification and characterization of the porcine enzyme. *J. Biol. Chem.* 235: 2272-2277.

Fruton, J.S. (1987) Aspartyl proteinases. In *Hydrolytic Enzymes* (A. Neuberger and K. Brocklehurst, Eds.,) pp. 1-37, Elsevier Science Publishers B.V.

Gacesa, P., and Hubble, J. (1987) *Enzyme Technology*. Open University Press. Milton Keynes. England.

Getman, D.P., DeCrescenzo, G.A., Heintz, R.M., Reed, K.L., Talley, J.J., Bryant, M.L., Clare, M., Houseman, K.A., Marr, J.J., Mueller, R.A., Vazquez, M.L., Shieh, H-S., Stallings, W.C., and Stegeman, R.A. (1993) Discovery of a novel class of potent HIV-1 protease inhibitors containing the (R)-(hydroxyethyl) urea isostere. *J. Med. Chem.* 36: 288-291.

Grant, S.K., Moore, M.L., Fakhoury, S.A., Tomaszek, T.A. jr, and Meek, T.D. (1992) Inactivation of HIV-1 protease by a tripeptidyl epoxide. *Bioorg. Med. Chem. Lett.* 2: 1441-1445.

Graves, M.C., Limm, J.J., Heimer, E.P., and Kramer, R.A. (1988) An 11 kDa form of human immunodeficiency virus protease expressed in *Escherichia coli* is sufficient for enzymatic activity. *Proc. Natl. Acad. Sci. USA* 85: 2449-2453.

Griffiths, J.T., Phylip, L.H., Konvalinka, J., Strop, P., Gustchina, A., Wlodawer, A., Davenport, R.J., Briggs, R., Dunn, B.M. and Kay, J. (1992) Different requirements for productive interaction between the active site of HIV-1 proteinase and substrates containing -hydrophobic\*hydrophobic- or -aromatic\*Pro- cleavage sites. *Biochemistry* 31: 5193-5200.

Grobelny, D., Wondrak, E.M., Galardy, R.E., and Oroszlan, S. (1990) Selective phosphinate transition-state analogue inhibitors of the protease of Human immunodeficiency virus. *Biochem. Biophys. Res. Commun.* 169: 1111-1116.

Guasch, A., Coll, M., Avilés, F.X., and Huber, R. (1992) Three-dimensional structure of porcine pancreatic procarboxypeptidase A. A comparison of the A and B zymogens and their determinants for inhibition and activation. *J. Mol. Biol.* 224:141-157.

Hansen, J., Billich, S., Schulze, T., Sukow, S., and Moelling, K. (1988) Partial purification of bacterially expressed HIV protease by means of monoclonal antibodies. *EMBO J.* 7: 1785-1791.

**Hanson, J.E., Kaplan, A.P., and Bartlett, P.A. (1989)** Phosphonate analogues of carboxypeptidase A substrates are potent transition-state analogue inhibitors. *Biochemistry* 28: 6294-6305.

**Hartley, B.S. (1960)** Proteolytic enzymes. *Annu. Rev. Biochem.* 29: 45-72.

**Hartley, B.S. and Kilby, B.A. (1954)** The hydrolysis of *p*-Nitrophenyl acetate by chymotrypsin and insulin. *Biochem. J.* 56:288-297.

**Hartsuck, J.A. and Tang, J. (1972)** The carboxylate ion in the active center of pepsin. *J. Biol. Chem.* 247:2575-2580.

**Hui, K.Y., Manetta, J.V., Gygi, T., Bowdon, B.J., Keith, K.A., Shannon, W.M., and Lai, M-H. T. (1991)** A rational approach in the search for potent inhibitors against HIV proteinase. *FASEB J.* 5: 2606-2610.

**Hunter, A. and Downs, C.E. (1945)** The inhibition of arginase by amino acids. *J. Biol. Chem.* 157: 427-446.

**Hyland, L., Moore, M.L., Shu, A.Y.L., Heys, J.R., and Meek, T.D. (1990)** A radiometric assay for HIV-1 protease. *Anal. Biochem.* 188: 408-415.

**Hyland, L., Tomaszek, T.A., and Meek, T.D. (1991(a))** Human immunodeficiency virus-1 protease. 2. Use of pH rate studies and solvent kinetic isotope effects to elucidate details of chemical mechanism. *Biochemistry* 30: 8454-8463.

**Hyland, L., Tomaszek, T.A., Roberts, G.D., Carrm S.A., Magaard, V.W., Bryan, H.L., Fakhoury, S.A., Moore, M.L., Minnich, M.D., Culp, J.S., DesJarlais, R.L., and Meek, T.D. (1991(b))** Human immunodeficiency virus-1 protease. 1. Initial velocity studies and kinetic characterization of reaction intermediates by <sup>18</sup>O isotope exchange. *Biochemistry* 30: 8441-8453.

**Jacobsen, N.E. and Bartlett, P.A. (1981)** A phosphoramidate dipeptide analogue as an inhibitor of carboxypeptidase A. *J. Amer. Chem. Soc.* 103:654-657.

**James, M.N.G. and Sielecki, A.R. (1986)** Molecular structure of an aspartic proteinase zymogen, porcine pepsinogen, at 1.8 Å resolution. *Nature* 319: 33-38.

**Jaskolski, M., Tomasselli, A.G., Sawyer, T.K., Staples, D.G., Heinrikson, R.L., Schneider, J., Kent, S.B.H. and Wlodawer, A. (1991)** Structure at 2.5Å resolution of chemically synthesized human immunodeficiency virus complexed with a hydroxyethylene-based inhibitor. *Biochemistry* 30: 1600-1609.

**Jencks, W. (1981)** On the attribution and additivity of binding energies. *Proc. Natl. Acad.*

*Sci. USA.* 78: 4046-4050.

**Jencks, W.P.** (1975) Binding energy, specificity and enzyme catalysis: the circe effect. *Adv. Enzymol. Relat. Areas Mol. Biol.* 43:219-410.

**Johnson, F.H., Eyring, H. and Kearns, W.** (1943) A quantitative theory of synergism and antagonism among diverse inhibitors, with special reference to sulfanilamide and urethane. *Arch. Biochem* 3: 1-31.

**Johnson, S.P., Veigl, M., Vanaman, T., and Leis, J.** (1983) Cyanogen bromide digestion of the avian myeloblastosis virus pp19 protein: Isolation of an amino-terminal peptide that binds to viral RNA. *J. Virol.* 45: 876-881.

**Jupp, R.A., Phylip, L.H., Mills, J.S., Le Grice, S.F.J. and Kay, J.** (1991) Mutating P<sub>2</sub> and P<sub>1</sub> residues at cleavage junctions in the HIV-1 po polyprotein. Effects on hydrolysis by HIV-1 protease. *FEBS Lett.* 283: 180-184.

**Kaplan, A.P. and Bartlett, P.A.** (1991) Synthesis and evaluation of an inhibitor of carboxypeptidase A with a K<sub>i</sub> value in the femtomolar range. *Biochemistry* 30: 8165-8170.

**Kauzmann, W. and Simpson, R.B.** (1953) The kinetics of protein denaturation III. The optical rotation of serum albumin,  $\beta$ -lactoglobulin, and pepsin in urea solutions. *J. Amer. Chem. Soc.* 75: 5154-5157.

**Kempf, D.J., Norbeck, D.W., Codacovi, L., Wang, X.C., Kohlbrenner, W.E., Wideburg, N.E., Paul, D.A., Knigge, M.F., Vasavanonda, S., Craig-Kennard, A., Saldivar, A., Rosenbrook, W, Jr., Clement, J.J., Plattner, J.J. and Erickson, J.** (1990) Structure-based C<sub>2</sub> symmetric inhibitors of HIV protease. *J. Med. Chem.* 33: 2687-2689.

**Kohl, N.E., Emini, E.A., Schleif, W.A., Davis, L.J., Heimbach, J.C., Dixon, R.A.F., Scolnick, E.M. and Sigal, I.S.** (1988) Active human immunodeficiency virus protease is required for viral infectivity. *Proc. Natl. Acad. Sci. USA* 85: 4686-4690.

**Konig, W.E. and Geiger, R.** (1970) A new method for synthesis of peptides: activation of carboxyl group with dicyclohexylcarbodiimide using 1-hydroxybenzotriazoles as additive. *Chem. Ber.* 103: 788-798.

**Konvalinka, J., Strop, P., Velek, J., Cerna, V., Kostka, V., Phylip, L.H., Richards, A.D., Dunn, B.M. and Kay, J.** (1990) Sub-site preferences of the aspartic proteinase from the human immunodeficiency virus, HIV-1. *FEBS Letts.* 268: 35-38.

**Koshland, D.E.** (1958) Application of a theory of enzyme specificity to protein synthesis. *Proc. Natl. Acad. Sci. USA* 44:98-104.



**Kotler, M., Danho, W., Katz, R.A., Leis, J., and Skalka, A.M. (1989)** Avian retroviral protease and cellular aspartic proteases are distinguished by activities on peptide substrates. *J. Biol. Chem.* 264: 3428-3435.

**Kotler, M., Katz, R.A., Danho, W., Leis, J. and Skalka, A.M. (1988)** Synthetic peptides as substrates and inhibitors of a retroviral protease. *Proc. Natl. Acad. Sci. USA* 85: 4185-4189.

**Kramer, R.A., Schaber, M.D., Skalka, A.M., Ganguly, K., Wong-Staal, F. and Reddy, E.P. (1986)** HTLV-III gag protein is processed in yeast cells by the virus pol-protease. *Science* 231: 1580-1584.

**Kraut, J. (1977)** Serine proteases: Structure and mechanisms of catalysis. *Annu. Rev. Biochem.* 46: 331-358.

**Lam, P.Y.S, Jadhav, P.K., Eyermann, C.J., Hodge, C.N., Ru, Y., Bacheler, L.T., Meek, J.L., Otto, M.J., Rayner, M.M., Wong, Y.N., Chang, C-H., Weber, P.C., Jackson, D.A., Sharpe, T.R., and Erickson-Vitanen, S. (1994)** Rational design of potent, bioavailable, nonpeptide cyclic ureas as HIV protease inhibitors. *Science* 263: 380-384.

**Lapatto, R., Blundell, T., Hemmings, A., Overington, J., Wilderspin, A., Wood, S., Merson, J. R., Whittle, P. J., Danley, D. E., Geoghegan, K. F., Hawrylik, S. J., Lee, E. L., Scheld, K. G., & Hobart, P. M. (1989)** X-ray analysis of HIV-1 proteinase at 2.7Å resolution confirms structural homology among retroviral enzymes. *Nature* 342: 299-302.

**Leatherbarrow, R. (1987)** *Enzfitter*. Elsevier Science Publishers, New York, NY.

**Leinhard, G.E. (1973)** Enzymatic catalysis and transition-state theory. *Science* 180: 149-154.

**Lineweaver, H., and Burk, D., (1934)** The determination of enzyme dissociation constants. *J. Amer. Chem. Soc.* 56: 658-666.

**Lingham, R.B., Hsu, A., Silverman, K.C., Bills, G.F., Dombrowski, A., Goldman, M.E., Darke, P.L., Huang, L., Koch, G., Ondeyka, J.G., and Goetz, M.A. (1992)** L-696,474, a novel cytochalasin as an inhibitor of HIV-1 protease III. Biological activity. *J. antibiot.* 45: 686-691.

**Lipscomb, W.N. (1983)** Structure and catalysis of enzymes. *Annu. Rev. Biochem.* 52: 17-34.

**Loewe, S. (1957)** Antagonisms and antagonists. *Pharmacol. Rev.* 9: 237-242.

**Lolis, E. and Petsko, G.A. (1990)** Transition-state analogues in protein crystallography:

Probes of the structural source of enzyme catalysis. *Annu. Rev. Biochem.* 59: 597-630.

**Lowe, G.** (1976) The cysteine proteinases. *Tetrahedron* 32: 291-302.

**Loewus, F.A., Westheimer, F.H., and Vennesland, B.** (1953) Enzymatic synthesis of the enantiomorphs of ethanol-1-d. *J. Amer. Chem. Soc.* 75: 5018-5023.

**Matrisian, L.M.** (1992) The matrix-degrading metalloproteases. *Bioessays* 14: 455-463.

**McKay, T.J and Plummer, T.H. jr.** (1978) By-product analogues for bovine carboxypeptidase B. *Biochemistry* 17: 401-405.

**McQuade, T.J., Tomasselli, A.G., Liu, L., Karacostas, V., Moss, B., Sawyer, T.K., Henrikson, R.L. and Tarpley, W.G.** (1990) A synthetic HIV-1 protease inhibitor with antiviral activity arrests HIV-like particle maturation. *Science* 247: 454-456.

**Meek, T.D., Dayton, B.D., Metcalf, B.W., Dreyer, G.B., Strickler, J.E., Gorniak, J.G., Rosenberg, M., Moore, M.L., Magaard, V.W. and DeBouck, C.** (1988) Human immunodeficiency virus 1 protease expressed in *Escherichia coli* behaves as a dimeric aspartic protease. *Proc. Natl. Acad. Sci. USA* 86: 1841-1845.

**Michaelis, L., and Menten, M.L.** (1913) Die kinetik der invertinwirkung. *Biochem. Z.* 49: 333-369.

**Miller, M., Schneider, J., Sathyanarayana, B.K., Toth, M.V., Marshall, G.R., Clawson, L., Selk, L., Kent, S.B.H., and Wlodawer, A.** (1989) Structure of complex of synthetic HIV-1 protease with a substrate-based inhibitor at 2.3Å resolution. *Science* 246: 1149-1152.

**Moore, M.L., Bryan, W.M., Fakhoury, S.A., Magaard, V.W., Huffman, W.F., Dayton, B.D., Meek, T.D., Hyland, L., Dreyer, G.B., Metcalf, B.W., Strickler, J.E., Gorniak, J.G. and DeBouck, C.** (1989) Peptide substrates and inhibitors of the HIV-1 protease. *Biochem. Biophys. Res. Commun.* 159: 420-425.

**Morrison, J.F., and Walsh, C.T.** (1988) The behavior and significance of slow-binding enzyme inhibitors. *Adv Enzymol. Relat. Areas Mol. Biol.* 61: 201-301.

**Navia, M.A., Fitzgerald, P.M.D., McKeever, B.M., Leu, C-T., Heimbach, J.C., Herber, W.K., Sigal, I.S., Darke, P.L. and Springer, J.P.** (1989) Three-dimensional structure of aspartyl protease from human immunodeficiency virus HIV-1. *Nature* 337: 615-620.

**Ondetti, M.A., Condon, M.E., Reid, J., Sabo, E.F., Cheung, H.S. and Cushman, D.W.** (1979) Design of potent and specific inhibitors of carboxypeptidase A and B. *Biochemistry* 18: 1427-1430.



- Ondetti, M.A.** and Cushman, D.W. (1982) Enzymes of the renin-angiotensin system and their inhibitors. *Annu. Rev. Biochem.* 51: 283-308.
- Pauling, L.** (1948) Nature of forces between large molecules of biological interest. *Nature* 161: 707-709.
- Pearl, L.H.** (1987) The catalytic mechanism of aspartic proteinases. *FEBS Letts.* 214: 8-12.
- Pearl, L.H.** and Taylor, W.R. (1989) A structural model for the retroviral proteases. *Nature* 329: 351-354.
- Plummer, T.H.,** and Kimmel, M.T. (1980) An improved spectrophotometric assay for human plasma carboxypeptidase N. *Anal. Biochem.* 108: 348-353.
- Pfeffer, S.R.** and Rothman, J.E. (1987) Biosynthetic protein transport by the endoplasmic reticulum and Golgi. *Annu. Rev. Biochem.* 56: 829-852.
- Pfuetzner, R.A.** and Chan, W.W.-C. (1988) Synergistic binding of ligands to angiotensin-converting enzyme. *J. Biol. Chem.* 263: 4056-4058.
- Pfuetzner, R.A.** and Chan, W.W.-C. (1993) Synergistic binding of hydrophobic probes and zinc ligands to thermolysin. *Eur. J. Biochem.* 218: 523-528.
- Polgar, L.** (1987) The mechanism of action of aspartic proteases involves "push-pull" catalysis. *FEBS Lett.* 219: 1-4.
- Poorman, R.A.,** Tomasselli, A.G., Heinrikson, R.L. and Kézdy, F.J. (1991) A cumulative specificity model for proteases from human immunodeficiency virus types 1 and 2, inferred from statistical analysis of an extended substrate data base. *J. Biol. Chem.* 266: 14554-14561.
- Rees, D.C.,** Lewis, M., and Lipscomb, W.N. (1983) Refined structure of carboxypeptidase A at 1.54 Å resolution. *J. Mol. Biol.* 168:367-387.
- Rich, D.H.,** Green, J., Toth, M.V., Marshall, G.R., and Kent S.B.H. (1990) Hydroxyethylamine analogues of the p17/p24 substrate cleavage site are tight-binding inhibitors of HIV protease. *J. Med. Chem.* 33: 1285-1288.
- Rich, D.H.** and Sun, E.T.O. (1980) Synthesis of analogues of the carboxyl protease inhibitor pepstatin. Effect of structure on inhibition of pepsin and renin. *J. Med. Chem.* 23: 27-33.
- Rich, D.H.,** Vara Prasad, J.V.N., Sun, C.-Q., Green, J., Mueller, R., Houseman, K., MacKenzie, D. and Malkovsky, M. (1992) New hydroxyethylamine HIV protease inhibitors

that suppress viral replication. *J. Med. Chem.* 35: 3803-3812.

**Richards, A.D.,** Phylip, L.H., Farmerie, W.G., Scarborough, P.E., Alvarez, A., Dunn, B.M., Hirel, P-H., Konvalinka, J., Strop, P., Pavlickova, L., Kostka, V., and Kay, J. (1990) Sensitive, soluble chromogenic substrates for HIV-1 proteinase *J. Biol. Chem.* 265: 7733-7736.

**Richards, A.D.,** Roberts, R., Dunn, B.M., Graves, M.C. and Kay, J. (1989) Effective blocking of HIV-1 proteinase activity by characteristic inhibitors of aspartic proteinases. *FEBS Letts.* 247: 113-117.

**Riordan, J.F.** (1973) Functional arginyl residues in carboxypeptidase A. Modification with butanedione. *Biochemistry* 12:3915-3923.

**Roberts, N.A.,** Martin, J.A., Kinchington, D., Broadhurst, A.V., Craig, J.C., Duncan, I.B., Galpin, S.A., Handa, B.K., Kay, J., Kröhn, A., Lambert, R.W., Merrett, J.H., Mills, J.S., Parkes, K.E.B., Redshaw, S., Ritchie, A.J., Taylor, D.L., Thomas, G.J. and Machin, P.J. (1990) Rational design of peptide-based HIV proteinase inhibitors. *Science* 248: 358-361.

**Schechter, I.** and Berger, A. (1967) On the size of the active site in proteases. *Biochem. Biophys. Res. Commun.* 27: 157-162.

**Schmid, M.F.,** and Herriot, J.R. (1976) Crystal structure of carboxypeptidase B at 2.8 Å. *J. Mol. Biol.* 103:175-190.

**Schneider, J.** and Kent, S.B.H. (1988) Enzymatic activity of a synthetic 99 residue protein corresponding to the putative HIV-1 protease. *Cell* 54: 363-368.

**Schoellman, G.,** and Shaw, E. (1963) Direct evidence of the presence of histidine in the active center of chymotrypsin. *Biochemistry* 2: 252-255

**Schramm, H.J.,** Billich, A., Jaeger, E., RÜcknagel, K-P., Arnold, G. & Schramm, W. (1993) The inhibition of HIV-1 protease by interface peptides. *Biochem. Biophys. Res. Commun.* 194: 595-600.

**Schramm, H. J.,** Nakashima, H., Schramm, W., Wakayama, H., & Yamamoto, N. (1991) HIV-1 reproduction is inhibited by peptides from the N- and C-termini of HIV-1 protease. *Biochem. Biophys. Res. Commun.* 179: 847-851.

**Segel, I.H.** (1975) *Enzyme kinetics.* Academic Press. New York. NY.

**Sham, H. L.,** Betebenner, D. A., Wideburg, N.E., Saldivar, A. C., Kohlbrenner, W. E., Vasavanonda, S., Kempf, D. J., Norbeck, D. W., Zhao, C., Clement, J. J, Erickson, J. E., Plattner, J. J. (1991) *Biochem. Biophys. Res. Commun.* 175: 914-919.

- Sheehan, J.C.** and Hess, G.P. (1955) A new method of forming peptide bonds. *J. Amer. Chem. Soc.* 77: 1067-1068
- Simpson, R.B.** and Kauzmann, W. (1953) The kinetics of protein denaturation. I. The behavior of the optical rotation of ovalbumin in urea solutions. *J. Amer. Chem. Soc.* 75: 5139-5152.
- Slater, E.C.** and Bonner, W.D. Jr. (1951) The effect of fluoride on the succinic oxidase system. *Biochem J.* 52: 185-196.
- Smith, R.A.,** Copp, L.J., Donnelly, S.L., Spencer, R.W., and Krantz, A. (1988) Inhibition of Cathepsin B by peptidyl aldehydes and ketones: Slow-binding behavior of a trifluoromethyl ketone. *Biochemistry* 27: 6568-6573.
- Stahl, E.** (1969) *Thin layer chromatography. A laboratory handbook.* Springer-Verlag Co. Berlin. Germany.
- Stroud, R.M.,** Kossiakoff, A.A. and Chambers, J.L. (1977) Mechanism of zymogen activation. *Annu. Rev. Biophys. Bioeng.* 6: 177-193.
- Stryer, L.** (1988) *Biochemistry.* 3rd Edition. W.H. Freeman and Co. New York, NY.
- Swain, A.L.,** Miller, M.M., Green, J., Rich, D.H., Schneider, J., Kent, S.B.H. and Wlodawer, A. (1990) X-ray crystallographic structure of a complex between a synthetic protease of human immunodeficiency virus 1 and a substrate-based hydroxyethylamine inhibitor. *Proc. Natl. Acad. Sci.* 87: 8805-8809.
- Szelke, M.,** Leckie, B., Hallet, A., Jones, D.M., Sueiras, J., Atrash, B., and Lever, A.F. (1982) Potent new inhibitors of human renin. *Nature* 299: 555-557.
- Takahashi, K.** and Chang, W-J. (1976) The structure and function of acid proteases. V. Comparative studies on the specific inhibition of acid proteases by diazoacetyl-DL-norleucine methyl ester, 1,2-epoxy-3-(*p*-nitrophenoxy)propane and pepstatin *J. Biochem.* 80: 497-506.
- Tang, J.** (1971) Specific and irreversible inactivation of pepsin by substrate-like epoxides. *J. Biol. Chem.* 246: 4510-4517.
- Titani, T.,** Ericsson, L.H., Walsh, K.A., and Neurath, H. (1975) Amino acid sequence of bovine carboxypeptidase B. *Proc. Natl. Acad. Sci. USA* 72: 1666-1670.
- Toh, H.,** Kikuno, R., Hayashida, H., Miyata, T., Kugimiya, W., Inouye, S., Yuki, S., and Saigo, K (1985) Close structural resemblance between putative polymerase of a drosophila

transposable genetic 17.6 and pol gene product of Moloney murine leukaemia virus. *EMBO J.* 4: 1267-1272.

Tomasselli, A. G., Olsen, M. K., Hui, J. O., Staples, D. J., Sawyer, T. K., Henrikson, R. L., & Tomich, C. S. (1990) Substrate analogue inhibition and active site titration of purified recombinant HIV-1 protease. *Biochemistry* 29: 264-269.

Umezawa, H., Aoyagi, T., Morishima, H., Matsuzaki, M., Hamada, H. and Takeuchi, T. (1970) Pepstatin, a new pepsin inhibitor produced by actinomycetes. *J. Antibiot.* 23: 259-262.

Vallee, B.L. and Auld, D.S. (1993) Zinc: Biological functions and coordination motifs. *Accts. Chem. Res.* 26: 543-551.

Vallee, B.L. and Galde, A. (1984) The metallobiochemistry of zinc enzymes. *Adv. Enzymol. Rel. Areas Mol. Biol.* 56: 284-430.

Vallee, B.L., Riordan, J.F., Bethune, J.L., Coombs, T.L., Auld, D.S. and Sokolovsky, M. (1968) A model for substrate binding and kinetics of carboxypeptidase A. *Biochemistry* 7: 3547-3556.

von Hickel, P. H. and Wong, K-Y. (1965) On the conformational stability of globular proteins. The effects of various electrolytes and non-electrolytes on the thermal ribonuclease transition. *J. Biol. Chem.* 240: 3909-3923.

Walsh, C.T. (1979) *Enzymatic Reaction Mechanisms*. W.H. Freeman and Co. San Francisco. CA.

Walsh, K. (1975) In *Proteases and Biological Control* (Eds. Reich, E., Rifkin, D. and Shaw, E.) Cold Spring Harbour Press. Long Island, NY.

Webb, J.L. (1963) *Enzyme and Metabolic inhibitors*. Vol. 1. General principles of inhibition. Academic press. New York. NY. pp 487-498.

Wlodawer, A. and Erickson, J.W. (1993) Structure-based inhibitors of HIV-1 protease. *Annu. Rev. Biochem.* 62: 543-585.

Wlodawer, A., Miller, M., Jaskolski, M., Sathyanarayana, B.K., Baldwin, E., Weber, I., Selk, L., Clawson, L., Schneider, J., & Kent, S.B.H. (1989) Conserved folding in retroviral proteases: crystal structure of a synthetic HIV-1 protease. *Science* 245: 616-621.

Wolfenden, R. (1972) Analog approaches to the structure of the transition state in enzyme reactions. *Accts. Chem. Res.* 5:10-18.

**Yagi, K. and Ozawa, T. (1959)** Complex formation of apo-enzyme coenzyme and substrate of D-amino acid oxidase. I. Kinetic analysis using indicators. *Biochim. Biophys. Acta.* 42: 381-387.

**Yasunaga, T., Sagata, N., and Ikawa, Y. (1986)** Protease gene structure and env gene variability of the AIDS virus. *FEBS Lett.* 199: 145-150.

**Yonetani, T. and Theorell, H. (1964)** Studies on liver alcohol dehydrogenase complexes. III. Multiple inhibition kinetics in the presence of two competitive inhibitors. *Arch. Biochem. Biophys.* 106: 243-251.

**Zisapel, N., Kurn-Abramovich, N., and Sokolovsky, M. (1973)** Basic and Non-basic substrates of carboxypeptidase B. *Eur. J. Biochem.* 35: 507-511.

**Zisapel, N., and Sokolovsky, M. (1975)** On the interaction of esters and peptides with carboxypeptidase B. *Eur. J. Biochem.* 54: 541-547.